

# Knot polynomials from 1-cocycles

Thomas Fiedler

March 6, 2022

*pour Séverine*

## Abstract

Let  $M_n$  be the topological moduli space of all parallel  $n$ -cables of long framed oriented knots in 3-space. We construct in a combinatorial way for each natural number  $n > 1$  a 1-cocycle  $R_n$  which represents a non trivial class in  $H^1(M_n; \mathbb{Z}[x_1, x_2, \dots, x_1^{-1}, x_2^{-1}, \dots])$ , where the number of variables  $x_i$  depends on  $n$ . To each generic point in  $M_n$  we associate in a canonical way an arc *scan* in  $M_n$ , such that  $R_n(\text{scan})$  is already a polynomial knot invariant. We show that  $R_3(\text{scan})$  detects the non-invertibility of the knot  $8_{17}$  in a very simple way and without using the knot group.

There are two well-known canonical loops in  $M_n$  for each parallel  $n$ -cable of a long framed knot  $K$ : Gramain's loop *rot* and the Fox-Hatcher loop *fh*. The calculation of  $R_n$  is of at most quartic complexity for these loops with respect to the number of crossings of  $K$  for each fixed  $n$ . It follows from results of Hatcher that  $K$  is not a torus knot if the rational function  $R_n(\text{fh}(K))/R_n(\text{rot}(K))$  is not constant for each  $n > 1$ .

$\oplus_n R_n$  is a natural candidate in order to separate all classes in  $H_1(M_1; \mathbb{Q}) \cong H_1(M_n; \mathbb{Q})$ , and in particular to distinguish all knot types  $\pi_0(M_1)$ .

1

---

<sup>1</sup>2000 *Mathematics Subject Classification*: 57M25 *Keywords*: polynomial valued 1-cocycles, non-invertibility of knots, global tetrahedron equations

# Contents

<b>1</b>	<b>Introduction</b>	<b>2</b>
<b>2</b>	<b>Main results</b>	<b>14</b>
2.1	The 1-cocycle $R_1$ in $M \setminus \Sigma_{trans-cusp}^{(2)}$ . . . . .	14
2.2	The 1-cocycle $R_n$ in $M$ for $n > 1$ . . . . .	21
<b>3</b>	<b>First applications, questions and conjectures</b>	<b>23</b>
3.1	Applications of the 1-cocycle $R_1$ in $M \setminus \Sigma_{trans-cusp}^{(2)}$ . Detecting the non-invertibility of string links with two components . . .	23
3.2	Applications of the 1-cocycle $R_n$ in $M$ for $n > 1$ . Detecting the non-invertibility of knots . . . . .	36
<b>4</b>	<b>Proof</b>	<b>48</b>
4.1	Generalities and reductions by using singularity theory . . . .	48
4.2	Reidemeister II moves in a cusp and in a flex . . . . .	55
4.3	Simultaneous Reidemeister moves . . . . .	56
4.4	Refined tetrahedron equation for string links . . . . .	59
4.5	Cube equations . . . . .	80
4.6	Moving cusps and scan-property . . . . .	93
4.7	Invariance of $R_n^i$ for $n > 1$ . . . . .	101

## 1 Introduction

This paper contains infinitely many new knot polynomials which

- can distinguish the orientations of knots
- can be calculated with a smaller degree of complexity than the Alexander polynomial
- can distinguish homology classes of loops in the space of all long knots
- carry topological and perhaps even geometrical information about knots
- distinguish perhaps all classical knots in 3-space.

They have their origin in a slight change of the subject: we study 1-parameter families of knots instead of individual knots.

The topological moduli space of a knot is the infinite dimensional space of all smooth knots isotopic to the given knot. Our philosophy is that *finite type invariants should be sufficient in general to separate all topological objects of a given kind if and only if each component of the topological moduli space of*

*these objects is a contractible space.* An example are braids. It is well known that the topological moduli space of each braid, seen as a tangle in the 3-ball, is a contractible space, and indeed e.g. Bar-Natan has proven that finite type invariants separate all braids [2]. (An exception to our philosophy are closed 2-braids. They are evidently distinguished by the unique finite type invariant of degree 1. However, in this case closed braids are isotopic if and only if the braids are already isotopic.) On the other hand the moduli spaces of closed braids in the solid torus (besides for the closed 1-braid) and of knots in the 3-sphere are never contractible spaces. Hatcher has proven e.g. that for the oriented trivial knot the moduli space deformation retracts onto the Grassmannian of oriented 2-planes in 4-space. It is not known whether finite type invariants can detect the non-invertibility of closed braids and of knots in 3-space, but it is known that quantum invariants can definitely not. Again, if we consider oriented tangles of two non-closed components in the 3-ball and such that the complement does not contain an incompressible torus then each component of the moduli space is a contractible space. And indeed Duzhin and Karev [13] have found a finite type invariant of degree 7, which can sometimes detect the non-invertibility of such a tangle (and it follows from results of Bar-Natan that there are no such invariants of degree smaller than 7, see [3], [1] ).

The topology of moduli spaces of knots and of long knots was much studied in [24], [7], [8], [9], [10]. In particular, there is a complete description of the homotopy type and of the homology groups (even with an additional structure of certain Gerstenhaber-Poisson algebras) for the space of long knots in  $\mathbb{R}^3$  (the same space, which was studied by Vassiliev using singularity theory) in the subsequent papers [24], [8], [9], [10]. Vassiliev [40] had constructed certain universally defined 0-dimensional cohomology classes. They give the finite type invariants of long knots (or equivalently of compact knots in the 3-sphere) when they are evaluated on the 0-dimensional homology classes of the disconnected space. It is known that all finite type knot invariants, also called Vassiliev-Goussarov invariants, have diagrammatic-combinatorial formulas, which allow the computation of the invariant from an arbitrary generic knot diagram [22]. Our goal is the construction of diagrammatic-combinatorial formulas for 1-dimensional cohomology classes of the space of long knots, which give knot invariants when they are applied to loops, represented by generic 1-parameter families of diagrams for long knots. It seems that the Teiblum-Turchin 1-cocycle  $v_3^1$  was the only known 1-cocycle for long knots which represents a non-trivial cohomology class and which has

(probably) an explicit diagrammatic-combinatorial formula for its computation. The Teiblum-Turchin 1-cocycle is an integer valued 1-cocycle of degree 3 in the sense of Vassiliev's theory [40]. Its reduction mod 2 had the first diagrammatic-combinatorial description of a 1-cocycle, see [41] and [39]. Sakai has defined a  $\mathbb{R}$  valued version of the Teiblum-Turchin 1-cocycle via configuration space integrals [37]. We have found a very complicated formula for an integer extension of  $v_3^1$  mod 2 in [16]. The most beautiful diagrammatic-combinatorial formula for an integer valued 1-cocycle for long knots which extends  $v_3^1$  mod 2 and which probably coincides with  $v_3^1$  was found by Mortier [32], [33]. Budney has defined another integer valued 1-cocycle on the space of long knots in [9], Propositions 6.1 and 6.3. But it is not clear at all how to calculate it from a loop of knot diagrams without already knowing the knot type and the homology class represented by the loop.

*The idea is now to construct polynomial valued 1-cocycles and to apply them to canonical loops in the components of the topological moduli space in order to obtain polynomial knot invariants.* Following this philosophy we had constructed integer valued finite type 1-cocycles for closed braids in [15]. In fact, these invariants have a completely evident deformation quantization to polynomial valued invariants, which are no longer of finite type but still calculable with polynomial complexity [18]. A refinement of these 1-cocycles, which uses in addition some local system by giving names to the crossings of the closed braids, can indeed detect sometimes the non-invertibility of a closed braid (that is the non-invertibility of the link in  $S^3$  which consists of the closed braid together with the closure of the braid axes), when it is applied to the loop generated by the rotation of the solid torus around its core, compare [15] or [18]. Since then we have tried to find such 1-cocycles for long knots in the 3-space.

It is well known that if a knot  $K$  in the 3-sphere is not a satellite then its topological moduli space is a  $K(\pi, 1)$  with  $\pi$  a finite group (in fact  $\pi = \text{Aut}(\pi_1(S^3 \setminus K), \partial)$ , where  $\partial$  is the peripheral system of the knot  $K$ , see [42], [26], [25]). Consequently, in this case there can't exist any non-trivial 1-cocycles with values in a torsion free module. However, it is well known that the components of the moduli space of knots in the 3-sphere are in a natural 1 – 1 correspondence with the components of the moduli space of long knots in 3-space. Hatcher has proven that for long knots in 3-space the situation is much better. There are always two canonical non-trivial loops in the component of the topological moduli space of a long knot  $K$  if it is not the trivial knot: Gramain's loop, denoted by  $\text{rot}(K)$ , and the Fox-Hatcher

loop, denoted by  $fh(K)$ . *Gramain's loop* is induced by the rotation of the 3-space around the long axis of the long knot [21]. *Fox-Hatcher's loop* is defined as follows: one puts a pearl (i.e. a small 3-ball  $B$ ) on the closure of the long framed knot  $K$  in the 3-sphere. The part of  $K$  in  $S^3 \setminus B$  is a long knot. Pushing  $B$  once along the knot with respecting the framing induces the Fox-Hatcher loop, see [24] and also [20]. The homology class of  $rot(K)$  does not depend on the framing of  $K$  and changing the framing of  $K$  adds multiples of  $rot(K)$  to  $fh(K)$ . Notice that the Fox-Hatcher loop has a canonical orientation induced by the orientation of the long knot. The same loops are still well defined and non-trivial for those  $n$ -string links which are  $n$ -cables of a framed non-trivial long knot. It follows from results of Hatcher [24] and Budney [10] that these two loops are linearly dependent in the rational homology if and only if the knot is a torus knot (compare also Lemma 1 in Section 3.2). Moreover, Hatcher has shown that the topological moduli space of a long hyperbolic knot deformation retracts onto a 2-dimensional torus. Hence it follows from Künneth's formula that it is sufficient to construct just 1-cocycles in this case.

Let us try to make it completely clear to the reader: the homology of the space of long knots depends very strongly on the component of the space. But luckily, each component contains two canonical 1-homology classes, namely the class represented by Gramain's loop and the class represented by the Fox-Hatcher loop (which are dependent or even trivial only in very particular cases). We can represent these loops by 1-parameter families of diagrams of long knots. We are now interested in those 1-cocycles of the space of long knots which are universally defined (i.e. independent of the component of the space) and which can be calculated from the 1-parameter family of diagrams alone.

We had constructed such a 1-cocycle for long knots with values in a module generated by singular long knots in [17]. Its construction is correct but the examples in [17] are wrong. We can prove now that this 1-cocycle is in reality a 1-coboundary and it is not interesting.

*The present paper contains the first polynomial valued 1-cocycle  $R_n$  for the topological moduli space of all oriented string links of  $n$  components for  $n > 1$ , and which is not a 1-coboundary, see Theorem 2 in Section 2.2.* It leads to the first knot polynomials which can detect the orientation of a classical knot by applying  $R_n$  to  $n$ -cables of a framed long knot, see Examples 4 and 5 in Section 3.2. An important point is that we do not make any explicit use of the knot group (thus avoiding the usual problems in group theory). Moreover,

our invariants are calculable with complexity of degree at most 4 for each fixed  $n$ , i.e. with  $O(c^4)$  operations or likewise in  $O(c^4)$  time with respect to the maximal number  $c$  of ordinary crossings of a diagram among all diagrams in the 1-parameter family which represents the loop in the space of long knots. However, for each fixed  $n > 1$  there are a priori  $n!(4^n - 3^n 2 + 2^n)$  new knot invariants from Gramain's loop and the same number of new invariants from the Fox-Hatcher loop. (An important point in order to get a complete calculable knot invariant would be, to find (if it exists) an upper bound  $U(c)$  for  $n$  as a function of the number of crossings  $c$  of the knot diagram, such that all our invariants do not contain new information for  $n \geq U(c)$  with respect to our invariants for  $n < U(c)$ .)

The goal of this paper is to construct these invariants, to calculate first examples and to give first applications. The development of the general theory of these invariants as well as perhaps a proof that they eventually distinguish all classical knots will probably be the subject of a long term research.

(Notice that our invariants can not be generalized for virtual knots in contrast to most other known knot invariants in dimension 3. This comes from the fact that each non-trivial loop contains necessarily forbidden moves. However,  $R_n(scan)$  could perhaps be generalized for welded knots because the scan-arc contains only one type of forbidden moves.)

**Definition 1** *We fix a orthogonal projection  $pr : \mathbb{C} \times \mathbb{R} \rightarrow \mathbb{C}$ . A long knot  $K$  is an oriented smoothly embedded copy of  $\mathbb{R}$  in  $\mathbb{C} \times \mathbb{R}$  which coincides with a fixed straight line (e.g. the real axis in  $\mathbb{C} \times 0$ ) outside a compact set. A (parallel)  $n$ -cable of a framed long knot is a  $n$ -component link with fixed endpoints where each component is parallel to the framed long knot with respect to the blackboard framing given by  $pr$ . A  $n$ -string link  $T$  is a  $n$ -component link with fixed endpoints where each component is parallel to a long knot in  $\mathbb{C} \times 0$  outside some compact set.*

It is convenient for calculations to represent a long knot  $K$  as a closed braid with just one strand opened to go to infinity.

*Let  $M$  be the topological moduli space of all oriented smooth string links in  $\mathbb{C} \times \mathbb{R}$  (in particular  $M_n \subset M$ ).*

It follows from Thom-Mather singularity theory that each component of the infinite dimensional space  $M$  has a natural *stratification with respect to  $pr$* :

$$M = \Sigma^{(0)} \cup \Sigma^{(1)} \cup \Sigma^{(2)} \cup \Sigma^{(3)} \cup \Sigma^{(4)} \dots$$

Here,  $\Sigma^{(i)}$  denotes the union of all strata of codimension  $i$ .

The strata of codimension 0 correspond to the usual generic *diagrams of knots*, i.e. all singularities in the projection are ordinary double points. So, our *discriminant* is the complement of  $\Sigma^{(0)}$  in  $M$ . Notice that this discriminant of non-generic diagrams is very different from Vassiliev's discriminant of singular knots [40].

The three types of strata of codimension 1 correspond to the *Reidemeister moves*, i.e. non generic diagrams which have exactly one ordinary triple point, denoted by  $\Sigma_{tri}^{(1)}$ , or one ordinary self-tangency, denoted by  $\Sigma_{tan}^{(1)}$ , or one ordinary cusp, denoted by  $\Sigma_{cusp}^{(1)}$ , in the projection  $pr$ . We call the triple point together with the under-over information (i.e. its embedded resolution) a *triple crossing*. We distinguish self-tangencies for which the orientation of the two tangents coincide, called  $\Sigma_{tan+}^{(1)}$ , from those for which the orientations of the tangents are opposite, called  $\Sigma_{tan-}^{(1)}$ .

**Proposition 1** *There are exactly six types of strata of codimension 2. They correspond to non generic diagrams which have exactly either*

- (1) *one ordinary quadruple point, denoted by  $\Sigma_{quad}^{(2)}$*
- (2) *one ordinary self-tangency with a transverse branch passing through the tangent point, denoted by  $\Sigma_{trans-self}^{(2)}$*
- (3) *one ordinary self-tangency in an ordinary flex ( $x = y^3$ ), denoted by  $\Sigma_{self-flex}^{(2)}$*
- (4) *two singularities of codimension 1 in disjoint small discs (this corresponds to the transverse intersection of two strata from  $\Sigma^{(1)}$ , i.e. two simultaneous Reidemeister moves at different places of the diagram)*
- (5) *one ordinary cusp ( $x^2 = y^3$ ) with a transverse branch passing through the cusp, denoted by  $\Sigma_{trans-cusp}^{(2)}$*
- (6) *one degenerate cusp, locally given by  $x^2 = y^5$ , denoted by  $\Sigma_{cusp-deg}^{(2)}$*

*We show these strata in Fig. 1.*

For a proof as well as for all other necessary preparations from singularity theory see [19] (and also [11] and references therein).

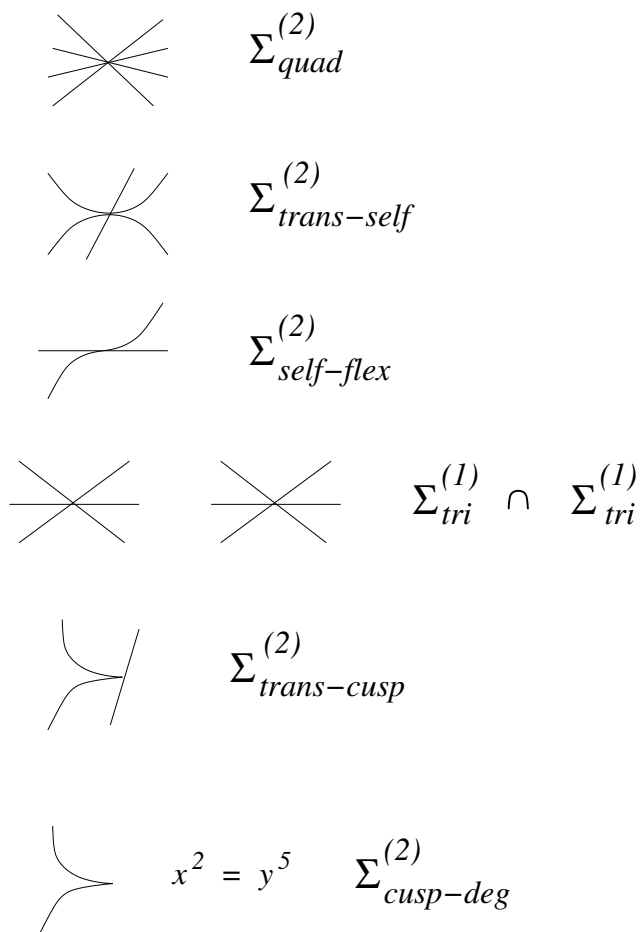


Figure 1: The strata of codimension 2 of the discriminant of non generic projections



Our strategy is the following: for an oriented generic loop or arc in  $M$  we associate some polynomial to the intersection with each stratum in  $\Sigma^{(1)}$ , i.e. to each Reidemeister move, and we sum up over all Reidemeister moves in the arc. We have to prove now that this sum is 0 for each meridian of strata in  $\Sigma^{(2)}$ . This is extremely complex but we use strata from  $\Sigma^{(3)}$  in order to reduce the proof to a few strata in  $\Sigma^{(2)}$ . It follows that our sum is invariant under generic homotopies of arcs (with fixed endpoints). But it takes its values in an abelian ring and hence it is a 1-cocycle.

The construction of  $R_n$  is now in two steps. First we construct a 1-cocycle  $R_1$  which represents a non-trivial class only in  $H^1(M \setminus \Sigma_{trans-cusp}^{(2)}; \mathbb{Z}[x, x^{-1}])$ , see Theorem 1 in Section 2.1. In order to make it a 1-cocycle without taking out  $\Sigma_{trans-cusp}^{(2)}$  we have to use cables. We refine  $R_1$  by using *admissible colorings of the 1-cocycle* coming from colorings of the components of the  $n$ -cable. The number of admissible colorings increases rapidly with  $n$ . Each admissible coloring  $i$  on  $R_1$  leads to a 1-cocycle  $R_n^i$  which represents an element now in  $H^1(M_n; \mathbb{Z}[x_i, x_i^{-1}])$  and  $R_n$  is the sum over all admissible colorings of  $R_1$ . We can apply  $R_n^i$  to the loops *rot* and *fh* in  $M_n$ . But let  $T$  be a tangle of  $n$  non-closed components in the 3-ball or equivalently a *string link* and such that there is no incompressible torus in its complement. Then of course  $[R_n] = 0$ . But it is remarkable that we can nevertheless extract non trivial information from the 1-cocycle  $R_n$ . Let us add a small positive curl (possibly linked with the other components of  $T$ ) to an arbitrary component of  $T$  near to the boundary  $\partial T$  of  $T$  at infinity.

**Definition 2** *The scan-arc  $scan(T)$  in  $M$  is the regular isotopy which makes the small curl big under the rest of  $T$  up to being near to infinity, compare Fig. 2.*

It turns out that  $R_n(scan(T))$  is an isotopy invariant of  $T$  for all  $n > 0$ . It can detect sometimes the orientation of a knot, at least starting from 3-cables of the long knot, and conjecturally  $R_1(scan(T))$  can detect sometimes with cubical complexity that a 2-component tangle  $T$  is not a 2-cable of any long knot (compare Section 3.1).

We could see the *scan-arc* in the following way. Given a framed knot in  $S^3$  we transform it first into a long knot. We add then a long longitude and we glue a meridian of the knot as a curl to the longitude. We push now the knot together with its longitude half way through the attached meridian and calculate  $R_n$  on this arc in the knot space. *Hence  $R_n(scan)$  is a combinatorial way to make explicit use of the peripheral system of a knot without*

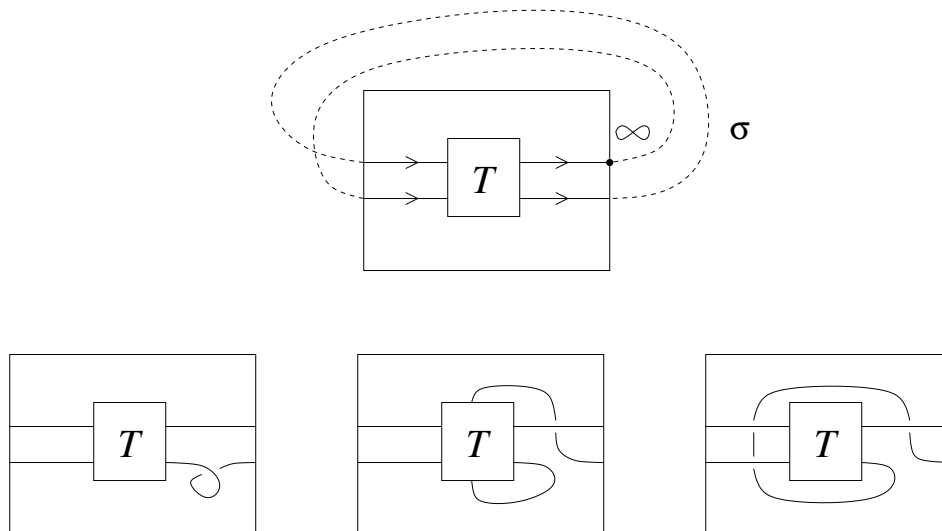


Figure 2: a scan-arc for a string link  $T$

*making explicit use of the knot group (compare [42] for the definition of the peripheral system and its application to knot theory).* This seems to be the reason that our invariant can detect the orientation of a knot in contrast to all other known knot invariants which make no explicit use of the knot group too: invariants of polynomial complexity as (the known) Vassiliev invariants, the Alexander polynomial, the Rozansky polynomials and invariants of exponential complexity as the Jones polynomial, the HOMFLYPT polynomial, the Kauffman polynomial and so on as well as their categorifications. Notice that even the A-polynomial, which uses representations of the knot group into  $SL(2, \mathbb{C})$ , does not distinguish the orientations of knots, compare e.g. [12].

The paper is organized as follows: in Section 2 we give a self-contained definition of  $R_n$  in its most compact form. The interested reader could already write a computer program and calculate lots of examples. The calculation of  $R_n$  is of complexity of degree 4 for the Fox-Hatcher loop (however the leading coefficient is already rather big for  $n = 2$ ) and it is of degree 3 for Gramain's loop and for the scan-arc with respect to the number of crossings of a long knot for fixed  $n$ . So, a priori it is even better than the Alexander polynomial (which can be calculated with complexity of degree 4, thanks to Dror Bar-Natan for the information) and it could be calculated for knots

with thousands of crossings.

In Section 3 we give first applications of  $R_n$  and we formulate conjectures and open questions.

Section 4 contains the proof that  $R_n$  is indeed a 1-cocycle. Showing that  $R_1 = 0$  for the meridians of  $\Sigma_{quad}^{(2)}$  is by far the hardest part. This corresponds to finding a new solution of the tetrahedron equation. Consider four oriented straight lines which form a braid and such that the intersection of their projection into  $\mathbb{C}$  consists of a single point. We call this an *ordinary quadruple crossing*. After a generic perturbation of the four lines we will see now exactly six ordinary crossings. We assume that all six crossings are positive and we call the corresponding quadruple crossing a *positive quadruple crossing*. Quadruple crossings form smooth strata of codimension 2 in the topological moduli space of lines in 3-space which is equipped with a fixed projection  $pr$ . Each generic point in such a stratum is adjacent to exactly eight smooth strata of codimension 1. Each of them corresponds to configurations of lines which have exactly one ordinary triple crossing besides the remaining ordinary crossings. We number the lines from 1 to 4 from the lowest to the highest (with respect to the projection  $pr$ ). The eight strata of triple crossings glue pairwise together to form four smooth strata which intersect pairwise transversally in the stratum of the quadruple crossing, see e.g. [19]. The strata of triple crossings are determined by the names of the three lines which give the triple crossing. For shorter writing we give them names from  $P_1$  to  $P_4$  and  $\bar{P}_1$  to  $\bar{P}_4$  for the corresponding stratum on the other side of the quadruple crossing. We show the intersection of a normal 2-disc of the stratum of codimension 2 of a positive quadruple crossing with the strata of codimension 1 in Fig. 24. The strata of codimension 1 have a natural coorientation, compare the next section. We could interpret the six ordinary crossings as the edges of a tetrahedron and the four triple crossings likewise as the vertices's or the 2-faces of the tetrahedron. For the classical tetrahedron equation one associates to each stratum  $P_i$  some operator (or some R-matrix) which depends only on the names of the three lines and to each stratum  $\bar{P}_i$  the inverse operator. The tetrahedron equation says now that if we go along the meridian then the product of these operators is equal to the identity. Notice, that in the literature, see e.g. [29], one considers planar configurations of lines. But this is of course equivalent to our situation because all crossings are positive and hence the lift of the lines into 3-space is determined by the planar picture. Moreover, each move of the lines in the plane which preserves the transversality lifts to an isotopy of the lines

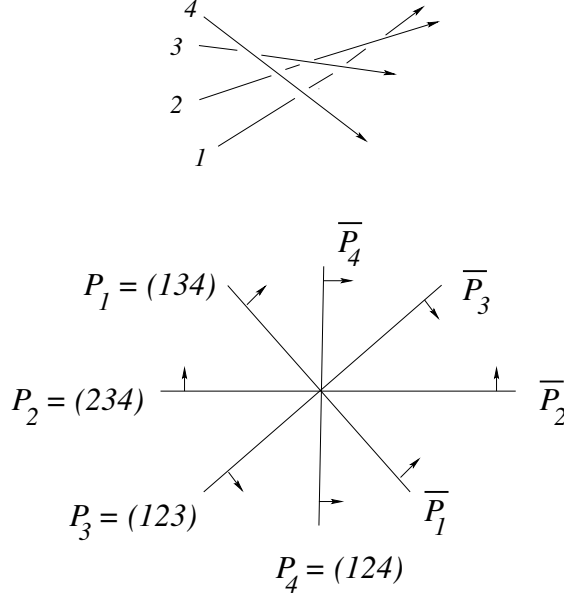


Figure 3: intersection of a normal 2-disc of a positive quadruple crossing with the strata of triple crossings

in 3-space. The tetrahedron equation has many solutions, the first one was found by Zamolodchikov, see e.g. [29].

However, the solutions of the classical tetrahedron equation are not well adapted in order to construct 1-cocycles for moduli spaces of knots. First of all there is no natural way to give names to the three branches of a triple crossing in an arbitrary knot isotopy besides in the case of closed braids. But it is not hard to see that in the case of braids Markov moves would make big trouble (see e.g. [5] for the definition of Markov moves and Markov's theorem). As well known, a Markov move leads only to a normalization factor in the construction of 0-cocycles, see e.g. [27]. However, the place in the diagram and the moment in the isotopy of a Markov move become important in the construction of 1-cocycles (as already indicated by the lack of control over the Markov moves in Markov's theorem). Secondly, a local solution of the tetrahedron equation is of no use for us because as already pointed out there are no integer polynomial valued 1-cocycles for knots in the 3-sphere. We have to replace them by long knots and we have to use the point at infinity on the knot. Therefore we have to consider *twenty four* different positive tetrahedron equations, corresponding to the six different abstract closures

of the four lines to a circle and to the four different choices of the point at infinity in each of the six cases. One easily sees that there are exactly *forty eight* local types of quadruple crossings (analog to the eight local types of triple crossings). Each of the six involved crossings appears in exactly four of the triple crossings. In order to obtain polynomial valued 1-cocycles instead of a integer valued one we have to keep track of the six crossings individually and we have to split the tetrahedron equation further into *six* equations: for each of the six crossings the contributions of the four corresponding strata of triple crossings have already to sum up to 0. Consequently, our tetrahedron equation splits into  $24 \times 48 \times 6 = 6912$  equations! Surprisingly, it has an interesting solution, which is constructed combinatorially by using relative finite type invariants of degrees 1 and 2 with respect to couples: a Reidemeister move of a knot diagram together with a crossing in the move. Our solution is *not local* in contrast to all other solutions which come from representation theory of the Yang-Baxter or the tetrahedron equation, i.e. the contribution of the move is not determined by the three lines alone but uses the whole Gauss diagram of the long knot.

We are conscious of the unusual technical complexity of the proof of Theorems 1 and 2. But there is no way to make the proof shorter. We see Theorems 1 and 2 as a combinatorial counterpart to a not yet existing analytical result in the same spirit as Reshetikhin-Turaevs combinatorial construction of the Jones polynomial for knots in 3-manifolds with respect to Witten's Feynmann integral construction of the same invariant. Unfortunately, our combinatorics is not yet standard, which adds to the difficulties for the reader. The long and complicated calculations of  $R_1(fh(3_1^+, w = 3)$ ,  $R_1(red - red, red - \infty)(scan(2 - cable(8_{17}), w = 0))$  and  $R_1(red - red, red - \infty)(scan(2 - cable(-8_{17}), w = 0))$  give all the expected results, see Section 3.1. This suggests that our formulas for the 1-cocycles should be correct. We give the calculation of Example 2 in Section 3.1 with many details. The example is too simple to make errors and can easily be checked by the reader. But it shows already that our invariants can detect the non-invertibility of 2-component string links, what the HOMFLYPT polynomial, the Kauffman polynomial and all finite type invariants of degree smaller than seven fail to do. We just say this to motivate the reader to spend perhaps some time and effort to understand the definition of our 1-cocycles and the proof of our theorems.

### Acknowledgments

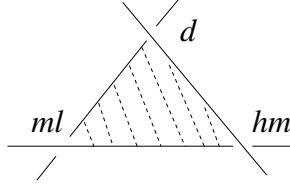


Figure 4: The names of the crossings in a R III-move

*I wish to thank Ryan Budney and Victor Turchin for patiently explaining to me the topology of moduli spaces of knots, and Hugh Morton for his observation that the graph in what has become the cube equations is indeed the 1-skeleton of a cube. I'm especially grateful to Dror Bar-Natan for first observing a telescoping effect which implies that all my previous 1-cocycles for long knots were actually 1-coboundaries. The present paper has grown out from trying to avoid this telescoping effect. Finally, let me mention that without Séverine, who has created all the figures, this paper wouldn't exist.*

## 2 Main results

### 2.1 The 1-cocycle $R_1$ in $M \setminus \Sigma_{trans-cusp}^{(2)}$

To each Reidemeister move of type III corresponds a diagram with a *triple crossing*  $p$ : three branches of the knot (the highest, middle and lowest with respect to the projection  $pr : \mathbb{C} \times \mathbb{R} \rightarrow \mathbb{C}$ ) have a common point in the projection into the plane. A small perturbation of the triple crossing leads to an ordinary diagram with three crossings near  $pr(p)$ .

**Definition 3** *We call the crossing between the highest and the lowest branch of the triple crossing  $p$  the distinguished crossing of  $p$  and we denote it by  $d$  ( $d$  stands for distinguished). The crossing between the highest branch and the middle branch is denoted by  $hm$  and that of the middle branch with the lowest is denoted by  $ml$ , compare Fig. 4.*

*Smoothing an arbitrary crossing  $c$  of a diagram  $D$  with respect to the orientation splits the closure of  $D$  into two oriented and ordered circles. We call  $D_c^+$  the component which goes from the under-cross to the over-cross at  $c$  and by  $D_c^-$  the remaining component, compare Fig. 5.*

*In a Reidemeister move of type II both new crossings are considered as*

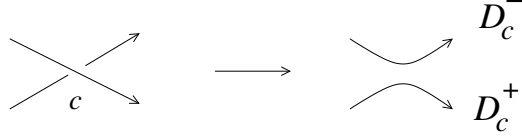


Figure 5: Two ordered knot diagrams associated to a crossing  $c$

*distinguished. We call the positive one  $d^+$  and the negative one  $d^-$  but we often identify them.*

A *Gauss diagram* of a long knot  $K$  is an oriented circle with oriented chords and a marked point corresponding to the point at  $\infty$ .

*String links are always oriented from the left to the right, i.e. near to infinity each component of  $T$  projects orientation preserving onto the oriented  $x$ -axis. We have to choose an abstract closure of  $T$  to a circle and we have to choose a point at infinity in the closure (we could see this as adding at infinity a pointed virtual permutation braid which represents in the symmetric group a  $n$ -cycle). We denote the closed diagram still by  $T$ .*

Our 1-cocycle will of course depend on these two choices. There exists an orientation preserving diffeomorphism from the oriented line to the closed oriented string link  $T$  such that each chord connects a pair of points which are mapped onto a crossing of  $pr(T)$  and infinity is mapped to the marked point. The chords are oriented from the preimage of the under crossing to the preimage of the over crossing (here we use the orientation of the  $\mathbb{R}$ -factor). The circle of a Gauss diagram in the plane is always equipped with the counter-clockwise orientation.

A *Gauss diagram formula* of degree  $k$  is an expression assigned to the diagram of a closed string link  $T$ , which is of the following form:

$$\sum_{\text{configurations}} \text{function}(\text{writhe of the crossings})$$

where the sum is taken over all possible choices of  $k$  (unordered) different crossings in the diagram such that the chords arising from these crossings in the diagram of  $T$  build a given sub-diagram with given marking. The marked sub-diagrams are called *configurations*, compare e.g. [35], [14], [18] and Figure 10. If the function is (as usual) the product of the writhes of the crossings in the configuration, then we will denote the sum shortly by the configuration itself. As usual, the writhe (or handedness) of a positive crossing is  $+1$  and the writhe of a negative crossing is  $-1$ .

**Definition 4** *An ordinary crossing  $c$  (i.e.  $pr(c)$  is an ordinary double point in the plane) in a diagram  $T$  (i.e. an arbitrary point in  $M$ ) is of (homological) type 1 if  $\infty \in D_c^+$  and is of (homological) type 0 otherwise, denoted by  $[c] = 1$  respectively  $[c] = 0$ .*

Let  $T$  be a generic diagram with a triple crossing or a self-tangency  $p$ , i.e.  $T \in \Sigma^{(1)} \setminus \Sigma^{(i)}$  for all  $i > 1$ , and let  $d$  be the distinguished crossing for  $p$ . In the case of a self-tangency, i.e.  $T \in \Sigma_{tan^+}^{(1)} \setminus \Sigma^{(i)}$  or  $T \in \Sigma_{tan^-}^{(1)} \setminus \Sigma^{(i)}$  we identify here the two distinguished crossings  $d^+$  and  $d^-$ .

**Definition 5** *Let  $c$  be a crossing of type 1. Then the linear weight  $W_1(c)$  is defined as the sum of the writhes  $w(r)$  of the crossings  $r$  in  $T$  which form one of the configurations shown in Fig. 6. These crossings  $r$ , which are of type 0 are called  $r$ -crossings of  $c$ .*

Notice that we do not multiply here  $W_1(c)$  by the writhe  $w(c)$ .

**Definition 6** *Let  $c$  be a crossing of type 0. Then the quadratic weight  $W_2(c)$  is defined by the Gauss diagram formula shown in Fig. 7. The crossings  $f$ , which are of type 1, are called  $f$ -crossings of  $c$ .*

The second (degenerate) configuration in Fig. 7 can of course not appear for a self-tangency but only for a triple crossing. So, the set of  $f$ -crossings is always defined with respect to a given crossing  $c$  of type 0. (Later the crossing  $c$  of type 0 will be exactly the crossings  $d$  or  $ml$  in Reidemeister moves of type II or III.) The  $f$ -crossings are exactly all crossings of type 1 and such that their foot (therefore they are called  $f$ -crossings) is in the open oriented arc in the circle from  $\infty$  to the head of  $c$  and their head is not equal to the foot of  $c$ . Each  $f$ -crossing defines a set of  $r$ -crossings as shown in Fig. 6, where we take for  $c$  a  $f$ -crossing.

**Definition 7** *We consider the Gauss diagrams for the three respectively two crossings which are involved in the Reidemeister move of type III respectively type II. The coorientation for a Reidemeister move of type II is the direction from no crossings to the diagram with two new crossings. For a Reidemeister III move the coorientation is the direction from two intersection points of the corresponding three arrows to one intersection point and of no intersection point of the three arrows to three intersection points, compare Fig. 8. (We*



$$W_I(c) = \begin{array}{c} \text{Diagram 1} \end{array} + \begin{array}{c} \text{Diagram 2} \end{array}$$

Diagram 1: A circle with a dot at the bottom. A vertical line segment labeled  $c$  goes from the dot to the top. Two diagonal lines labeled  $r$  go from the top to the left and right sides of the circle. A small arrow points down from the left side of the circle.

Diagram 2: A circle with a dot at the bottom. A vertical line segment labeled  $c$  goes from the dot to the top. Two diagonal lines labeled  $r$  go from the top to the left and right sides of the circle. A small arrow points down from the left side of the circle.

Figure 6: The linear weight  $W_I(c)$  for  $c$  of type 1

$$W_2(c) = \sum w(f) W_I(f) + \sum w(f) W_I(f)$$

$$\begin{array}{c} \text{Diagram 3} \end{array} \quad \begin{array}{c} \text{Diagram 4} \end{array}$$

Diagram 3: A circle with a dot at the bottom. A vertical line segment labeled  $c$  goes from the dot to the top. A diagonal line labeled  $f$  goes from the top to the right side of the circle. A small arrow points down from the left side of the circle.

Diagram 4: A circle with a dot at the bottom. A vertical line segment labeled  $c$  goes from the dot to the top. A diagonal line labeled  $f$  goes from the top to the right side of the circle. A small arrow points down from the left side of the circle.

$$+ \sum w(f) W_I(f) + \sum w(f) W_I(f)$$

$$\begin{array}{c} \text{Diagram 5} \end{array} \quad \begin{array}{c} \text{Diagram 6} \end{array}$$

Diagram 5: A circle with a dot at the bottom. A vertical line segment labeled  $c$  goes from the dot to the top. A horizontal line labeled  $f$  goes from the top to the left side of the circle. A small arrow points down from the left side of the circle.

Diagram 6: A circle with a dot at the bottom. A vertical line segment labeled  $c$  goes from the dot to the top. A diagonal line labeled  $f$  goes from the top to the right side of the circle. A small arrow points down from the left side of the circle.

Figure 7: The quadratic weight  $W_2(c)$  for  $c$  of type 0

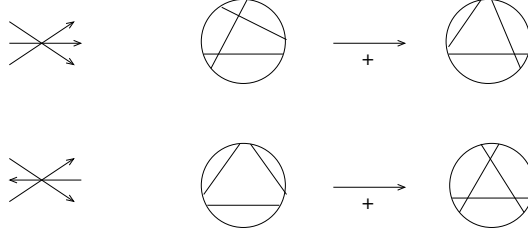


Figure 8: The coorientation for Reidemeister III-moves

will see later in the cube equations for  $\Sigma_{trans-self}^{(2)}$  that the two coorientations for triple crossings fit together for the strata of  $\Sigma_{tri}^{(1)}$  which come together in  $\Sigma_{trans-self}^{(2)}$ .) Evidently, our coorientation is completely determined by the corresponding planar curves and therefor we can draw just chords instead of arrows in Fig. 8. We call the side of the complement of  $\Sigma_{tri}^{(1)}$  in  $M$  into which points the coorientation, the positive side of  $\Sigma_{tri}^{(1)}$ .

We can ignore Reidemeister moves of type I because they will not contribute to our 1-cocycles.

Each transverse intersection point  $p$  of an oriented generic arc in  $M$  with  $\Sigma^{(1)}$  has now an intersection index  $+1$  or  $-1$ , called  $sign(p)$ , by comparing the orientation of the arc with the coorientation of  $\Sigma^{(1)}$ .

**Definition 8** The integer linking number  $l(c)$  of an ordinary crossing  $c$  is defined as the sum of the writhe of all crossings between  $D_c^+$  and  $D_c^-$  (hence in the case of a long knot it is twice the usual linking number of the oriented 2-component link).

**Definition 9** The linking number  $l(p)$  for  $p \in \Sigma_{tan-}^{(1)}$  is defined as  $l(d^+) = l(d^-)$  where  $d^+$  is the new positive crossing and  $d^-$  is the new negative crossing. The linking number  $l(p)$  for  $p \in \Sigma_{tan+}^{(1)}$  is defined as  $l(d^+) + 1 = l(d^-) - 1$  (in other words, only the arrows in the Gauss diagram which cut the double arrow  $d = d^+ = d^-$  contribute to  $l(p)$ ).

Let  $p \in \Sigma_{tri}^{(1)}$  and let  $c$  be an ordinary crossing from the triple crossing. Then the linking number  $l(c)$  is defined as  $l(c)$  taken on the positive side of  $\Sigma_{tri}^{(1)}$ . (For  $c = ml$  and  $c = hm$  the side of  $\Sigma_{tri}^{(1)}$  doesn't matter for  $l(c)$  but it changes by  $+2$  or  $-2$  for  $c = d$ .)

Notice, that all our weights  $W_1$  and  $W_2$  as well as the linking numbers  $l$  depend of course strongly on the chosen abstract closure to a circle of the string link  $T$ . The reader can easily become a bit familiar with our definitions by studying Example 2 in Section 3.1, where we give many details.

**Definition 10** *Let  $p \in \Sigma_{tri}^{(1)}$ . Then  $\eta(p) = 1$  if the homological type of the distinguished crossing  $[d] = 1$  and  $\eta(p) = -1$  if the homological type of the distinguished crossing  $[d] = 0$  (compare Definition 4 for the homological type).*

The following correction term is needed in the definition of  $R_1$ , it will disappear in the definition of  $R_n$  for  $n > 1$  in the case of a non-degenerate coloring (compare the next subsection).

**Definition 11** *Let  $p \in \Sigma_{tri}^{(1)}$ . Then  $\epsilon(p) = 1/2$  if  $[d] = 0$  and  $[hm] = 1$  and  $\epsilon(p) = 0$  otherwise.*

We are now ready to define  $R_1$ . There are  $8 \times 6 = 48$  different types of Reidemeister III moves for long knots and they contribute almost all in a different way to  $R_1$ . Luckily, we have managed to encode the contributions in a single formula.

**Definition 12** *(The 1-cocycle  $R_1$ )*

*Let  $s$  be an oriented generic smooth closed arc in  $M$  ( $s$  is in general position with respect to the stratification  $\Sigma^{(i)}$ , i.e. its endpoints are in  $\Sigma^{(0)}$ , it intersects  $\Sigma^{(1)}$  transversally in a finite number of points, called  $p$ , and it does not intersect  $\Sigma^{(i)}$  for  $i > 1$ ). We consider the crossings  $d$ ,  $ml$  and  $hm$  (compare Definition 3) for each  $p \in s \cap \Sigma_{tri}^{(1)}$  and we identify the two crossings  $d = d^+ = d^-$  for each  $p \in s \cap \Sigma_{tan}^{(1)}$ . Then  $R_1(s) \in \mathbb{Z}[x, x^{-1}]$  is defined by*

$$\begin{aligned}
R_1(s) = & \sum_{p \in \Sigma_{tri}^{(1)}, [d]=0} sign(p) 4l(d) x^{W_2(d) + \epsilon(p)w(hm)(w(ml)-w(d))} \\
& + \sum_{p \in \Sigma_{tri}^{(1)}, [ml]=0} sign(p) \eta(p) w(hm) (l(ml) - w(ml))^2 \times \\
& (x^{W_2(ml) + w(hm)W_1(hm) + \epsilon(p)w(hm)(w(ml)-w(d))} - x^{W_2(ml)}) \\
& + \sum_{p \in \Sigma_{tan-}^{(1)}, [d]=0} sign(p) 4l(d) x^{W_2(d)} \\
& + \sum_{p \in \Sigma_{tan+}^{(1)}, [d]=0} sign(p) 8l(d) x^{W_2(d)}
\end{aligned}$$

In other words, we associate to a Reidemeister move  $p$  of type III or type II some monomial if and only if the distinguished crossing  $d$  is of type 0 and we associate some binomial if and only if the crossing  $ml$  is of type 0. Notice that in the latter case we have to consider only Reidemeister III moves with  $[ml] = 0$  and  $[hm] = 1$ . Indeed, the binomial is 0 if  $[hm] = 0$  too because both  $W_1(hm) = 0$  and  $\epsilon(p) = 0$  (because  $W_1$  is only defined for crossings of type 1). But it can happen (namely exactly for the global type  $r_a$ , see Fig. 13 in Section 3.1) that  $d$  and  $ml$  contribute both for the same Reidemeister III move.

**Remark 1** *The main difference with our previous 1-cocycles [17] are the linking numbers  $l(d)$  and  $l(ml)$ . A fixed crossing of a diagram can contribute to  $R_1(s)$  in the arc  $s$  as a  $d$ -crossing and hence with linear coefficient  $4l(d)$ . Moving further in the arc  $s$  the same crossing could the next time contribute as a  $ml$ -crossing and hence with a quadratic coefficient  $(l(ml) - w(ml))^2$ . This makes a cancellation of monomials in the two contributions (the "telescoping effect") rather unlikely, because the linking number  $l$  of a crossing can only change by  $+2$  or  $-2$  when the crossing contributes as a  $d$ -crossing! But notice that it is of crucial importance that we associate to a crossing  $ml$  a binomial and not just a monomial. In fact, one of the monomials in the binomial corresponds to the weight  $W_2(ml)$  just before the RIII move and*

the other corresponds to the weight  $W_2(ml)$  just after the RIII move (the crossing  $hm$  becomes a  $f$ -crossing in exactly one of the two diagrams). Hence, by moving further on the arc  $s$  the weight of the crossing has changed now and can not cancel out with the previous contribution as a  $ml$ -crossing. It is this combinatorial structure of quadratic versus linear linking number and binomial versus monomial for the same crossing in different Reidemeister moves which makes the whole thing working!

But  $R_1$  is not a 1-cocycle in  $M$  because of the strata  $\Sigma_{trans-cusp}^{(2)}$ . In the unfolding of  $\Sigma_{trans-cusp}^{(2)}$  we see one crossing which appears from the cusp and exactly one triple crossing. Let  $\Sigma_{trans-cusp, cusp=[ml]=0, [d]=1}^{(2)}$  be the union of all strata of one ordinary cusp ( $x^2 = y^3$ ) with a transverse branch passing through the cusp in the projection, and such that in its unfolding the crossing which appears from the cusp becomes the crossing  $ml$  of type 0 in the triple crossing and the distinguished crossing  $d$  in the triple crossing is of type 1. This implies of course that the transverse branch moves *over* the cusp in the unfolding and hence intersections with strata of type  $\Sigma_{trans-cusp, cusp=[ml]=0, [d]=1}^{(2)}$  can not appear in  $scan(K_t)$  for any isotopy  $K_t, t \in [0, 1]$ , of a long knot  $K_0$ , because the branch moves *under* the rest of the knot, compare Section 4.6.

**Theorem 1**  $R_1$  represents a non-trivial cohomology class in

$H^1(M \setminus \Sigma_{trans-cusp, cusp=[ml]=0, [d]=1}^{(2)}; \mathbb{Z}[x, x^{-1}])$  for each choice of an abstract closure of  $T$  to a circle and for each choice of a point at infinity in  $\partial T$ . Moreover, for each generic point  $T$  in  $M$  (i.e.  $T \in \Sigma^{(0)}$ ) the Laurent polynomial  $R_1(scan(T))$  is an isotopy invariant of  $T$ .

## 2.2 The 1-cocycle $R_n$ in $M$ for $n > 1$

We consider  $R_1$ , which was defined in the previous subsection, and we take  $n > 1$ . Remember that we have chosen an abstract closure of  $T \in M$  to a circle and we have chosen a point at infinity in the closure. We start at the point at infinity and we go along the circle. This defines an ordering on the set of components of  $T : C_1, C_2, \dots, C_n$ , called the *coloring* of the components. Notice that we can obtain more colorings by identifying the colors of several components. A *coloring* of  $R_1$  is now a restriction in the definition of  $R_1$  to only those crossings  $d, ml, f$  and  $r$  with fixed colorings of the undercross and the overcross, denoted by undercross  $\rightarrow$  overcross:  $C_i \rightarrow C_j$ .

**Definition 13** *A coloring of  $R_1$  for  $n > 1$  by  $d$  in  $\Sigma_{tri}^{(1)}$  as well as in  $\Sigma_{tan}^{(1)}$  and  $ml$  in  $\Sigma_{tri}^{(1)}: C_{i_1} \rightarrow C_{i_2}$   
 $f: C_{i_2} \rightarrow C_{i_2}$  or  $C_{i_2} \rightarrow C_{i_3}$   
 $r: C_{i_3} \rightarrow C_{i_2}$  or  $C_{i_3} \rightarrow C_{i_3}$   
is called admissible if  
 $C_{i_1} \neq C_{i_2}$  and  $C_{i_2} \neq C_{i_3}$ .*

We enumerate for each fixed  $n$  the admissible colorings of  $R_1$  by natural numbers  $i$ .

**Definition 14** *(The 1-cocycle  $R_n^i$ )*

*The degenerate case:  $C_{i_1} = C_{i_3}$ .*

*Let  $i$  be a degenerate admissible coloring of  $R_1$ . Then  $R_n^i$  is defined as  $R_1$  but where only the crossings with prescribed colorings in  $i$  contribute and moreover  $[ml] = 0$  in a Reidemeister III move contributes only if the overcross of  $d$  in this move has the color  $C_{i_2}$  or  $C_{i_1} = C_{i_3}$ . We replace now the variable  $x$  in the values of  $R_n^i$  by the new variable  $x_i$ .*

*The non-degenerate case :  $C_{i_1} \neq C_{i_3}$ .*

*Let  $i$  be a non-degenerate admissible coloring of  $R_1$ . Then  $R_n^i$  is defined as  $R_1$  without the correction term  $\epsilon(p)w(hm)(w(ml) - w(d))$ , but where only the crossings with prescribed colorings in  $i$  contribute. ( If  $W_1(hm) = 0$  then  $[ml] = 0$  in a Reidemeister III move does not contribute because there is no correction term.  $W_1(hm) = 0$  automatically if the overcross of  $d$  in this move has not the color  $C_{i_2}$  or  $C_{i_3}$ .) We replace now the variable  $x$  in the values of  $R_n^i$  by the new variable  $x_i$ .*

*$R_n$  is defined as  $\sum_i R_n^i$  over all admissible colorings  $i$ .*

Notice that an admissible coloring for  $n = 2$  is evidently degenerate. We take always  $C_1 = \text{black}$  and  $C_2 = \text{red}$  (and hence  $\infty = \text{red-}\infty$  is always the end of the red component). Then  $R_2$  is just  $R_1$  with the admissible coloring  $C_{i_1} = \text{red}$  and  $C_{i_2} = \text{black}$ . Indeed, the other choice would lead to  $d$  and  $ml$  of homological type 1.

We consider the virtual closure  $\sigma_1\sigma_2$  and the colors  $C_1 = \text{black}$ ,  $C_2 = \text{green}$ ,  $C_3 = \text{red}$  for  $n = 3$ . We consider in this paper only the following non-degenerate admissible coloring, called 1, which turns out to contribute non-trivially to  $R_3$  in the case of  $\text{red-}\infty$ :  $C_{i_1} = \text{red}$ ,  $C_{i_2} = \text{black}$ ,  $C_{i_3} = \text{green}$ .

It is convenient for calculations (see the next section) to introduce *potential  $f$ -crossings* and *potential  $r$ -crossings*.

**Definition 15** *A crossing in a generic diagram is called a potential f-crossing for an admissible coloring if it is of (homological) type 1 and of (colored) type  $C_{i_2} \rightarrow C_{i_2}$  or  $C_{i_2} \rightarrow C_{i_3}$ . A crossing is called a potential r-crossing if it is of type 0 and of type  $C_{i_3} \rightarrow C_{i_2}$  or  $C_{i_3} \rightarrow C_{i_3}$ .*

The following theorem is the main result of this paper.

**Theorem 2**  *$R_n^i$  represents a cohomology class in  $H^1(M; \mathbb{Z}[x_i, x_i^{-1}])$  for each  $n > 1$  and for each admissible coloring  $i$ . The 1-cocycle  $R_n = \sum_i R_n^i$  is not always a 1-coboundary.*

*Moreover, for each generic point  $T$  in  $M$  the Laurent polynomial  $R_n^i(\text{scan}(T))$  is an isotopy invariant of  $T$ . It can be calculated with cubic complexity with respect to the number of crossings of  $T$  and it can sometimes detect the non-invertibility of a knot.*

**Remark 2** *All our definitions are very non-symmetric. In fact, if we apply our definitions to mirror images or to reversed orientations of knots then in general our 1-cocycles become new "dual" 1-cocycles.*

### 3 First applications, questions and conjectures

#### 3.1 Applications of the 1-cocycle $R_1$ in $M \setminus \Sigma_{trans-cusp}^{(2)}$ . Detecting the non-invertibility of string links with two components

Let  $K$  be a long knot up to regular isotopy (i.e. isotopy without Reidemeister moves of type I). Then Gramain's loop  $rot(K)$  has a nice representative: with a Reidemeister I move we add a small positive curl with negative Whitney index at the right end, then we perform the scan, we slide the knot along the curl, we perform an "over-scan" (i.e. the branch moves over the knot) and at the end we eliminate the small curl again with a Reidemeister I move (compare Fig. 9). If  $K$  and  $K'$  are regularly isotopic then evidently  $[rot(K)] = [rot(K')]$  in  $H_1(M \setminus \Sigma_{trans-cusp}^{(2)}; \mathbb{Z})$  for the above representatives, because no branch moves over the two cusps in any homotopy in  $M$ , which connects the two loops and which consists only of regular isotopies.

Let  $rot'(K)$  be the analogue loop with a small positive curl with positive Whitney index. The remaining possibilities of small curls are related to these two by Whitney tricks.

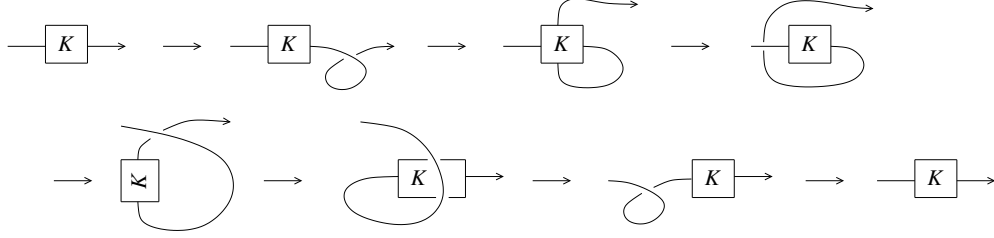


Figure 9: Nice realization of Gramain's loop

**Proposition 2** *Let  $K$  be a long knot and let  $v_2(K)$  be its Vassiliev invariant of degree 2 (normalized to be 1 on the trefoil).*

*Then  $R_1(\text{rot}(K)) = x^{v_2(K)} - 1$  and  $R_1(\text{rot}'(K))$  is identical 0 (i.e. no contributions of Reidemeister moves at all).*

*Proof.* Let  $K$  and  $K'$  be long knots and let  $K \sharp K'$  be the long knot which is their connected sum. Pushing  $K'$  through the positive curl at the right adds  $x^{v_2(K)} R_1(\text{rot}(K'))$  as contribution to  $R_1(\text{rot}(K \sharp K'))$ . Indeed, the knot  $K$  appears just after the point at infinity and hence each crossing of type 1 of  $K$  is a f-crossing for each crossing  $d$  or  $ml$  of  $K'$  which contributes to  $R_1(\text{rot}(K \sharp K'))$ . No crossing of  $K$  is ever a r-crossing for a crossing in  $K'$  and vice-versa. It follows now from the *Polyak-Viro Gauss diagram formulas for  $v_2(K)$* , compare [35] and Fig. 10, that  $K$  adds  $v_2(K)$  to each weight  $W_2$  and consequently, it adds the factor  $x^{v_2(K)}$  to each contribution to  $R_1(\text{rot}(K \sharp K'))$  of the crossings  $d$  and  $ml$  of  $K'$ .

Pushing now  $K$  through the positive curl adds only  $R_1(\text{rot}(K))$  to

$R_1(\text{rot}(K \sharp K'))$ . Indeed, the knot  $K'$  appears just before the point at infinity and hence no crossing of  $K'$  is ever a f-crossing for a crossing of type  $d$  or  $ml$  of  $K$  which contributes to  $R_1(\text{rot}(K \sharp K'))$ . It follows that

$R_1(\text{rot}(K \sharp K')) = x^{v_2(K)} R_1(\text{rot}(K')) + R_1(\text{rot}(K))$ . But the connected sum of long knots is commutative, i.e.  $K \sharp K'$  is even regularly isotopic to  $K' \sharp K$ . Consequently,  $R_1(\text{rot}(K \sharp K')) = x^{v_2(K')} R_1(\text{rot}(K)) + R_1(\text{rot}(K'))$  too. It follows that  $(x^{v_2(K)} - 1) R_1(\text{rot}(K')) = (x^{v_2(K')} - 1) R_1(\text{rot}(K))$  for a given knot  $K$  and an arbitrary knot  $K'$ . Hence, we have the alternative

*either  $R_1(\text{rot}(K)) = 0$  for each knot  $K$*   
*or  $R_1(\text{rot}(K)) = x^{v_2(K)} - 1$  for each knot  $K$ .*

A direct calculation for the positive trefoil shows that the second possibility is the right one.



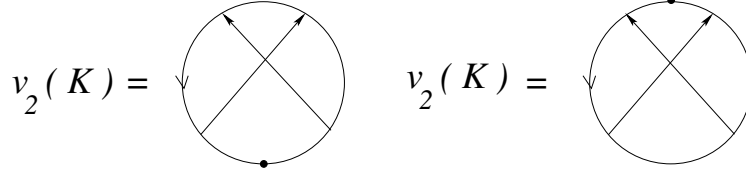


Figure 10: Polyak-Viro formulas for the Vassiliev invariant  $v_2$ . For each of the two configurations  $v_2(K)$  is the sum of the product of the writhe of all couples of crossings with the given configuration.

In the loop  $rot'(K)$  only triple crossings of type  $l_c$  could contribute to  $R_1(rot'(K))$  (because we have always  $[d] = 1$ ). But in the first passage of  $K$  the over-brunch goes over everything to  $\infty$  and hence  $W_1(hm) = 0$  and all contributions are 0. In the second passage all triple crossings are of type  $r_c$  or  $l_a$ , which do not contribute at all to  $R_1$ .

□

It follows from the proposition that  $dR_1(rot(K))/dx|_{x=1} = \alpha_3^1(rot(K)) = v_2(K)$ , where  $\alpha_3^1$  is the Mortier 1-cocycle. Notice that for  $x = 1$  the crossings  $ml$  do no longer contribute to  $R_1$ , as follows immediately from its definition.

One easily sees that the more interesting information of  $R_1(rot(K))$  is concentrated in  $R_1(scan(K))$ , because the "over-scan" part of the loop contributes only a constant to  $R_1$ . Indeed, in the "over-scan" part  $ml$  does never contribute and for each contribution of  $d$  the weight  $W_2(d) = 0$ , because there is never an undercross on the arc from  $\infty$  to the overcross of  $d$  and hence there are no f-crossings at all.

Let  $M_K^{reg} \subset M_K$  be the subspace of all *regular* long knots, i.e. long knots for which the projection  $pr$  into the plane is an immersion.  $R_1$  is evidently a 1-cocycle in  $M_K^{reg}$ . Thus, in order to calculate  $R_1(fh(K))$  it is sufficient to approximate the loop  $fh(K)$  in  $M_K$  by a loop in  $M_K^{reg}$ . It is easy to see that this can always be done by using Whitney tricks, see e.g. [14]. However, this approximation is a priori not unique. In order to have  $R_1(fh(K))$  as an invariant of framed knots, we need the following proposition.

**Proposition 3** *Let  $K$  be a hyperbolic knot or a torus knot and let  $in : M_K^{reg} \rightarrow M_K$  be the inclusion. Then  $R_1$  vanishes on the kernel of  $in_* : H_1(M_K^{reg}) \rightarrow H_1(M_K)$  for each component of  $M_K^{reg}$ .*

*Proof.*

Hatcher [24] has proven that if  $K$  is a hyperbolic knot or a torus knot then  $M_K$  deformation retracts onto a 2-dimensional torus respectively a circle. Consequently, in these cases  $\pi_1(M_K, *) = H_1(M_K)$ . Let  $\gamma(s) \subset M_K^{reg}$ ,  $s \in [0, 1]$ , be a generic loop with base point  $*$  which contracts in  $M_K$ . We try to contract it in  $M_K^{reg}$  to  $*$ . Let  $\gamma_t$ ,  $t \in [0, 1]$ , be a generic homotopy of  $\gamma_0 = \gamma$  to  $\gamma_1 = *$  in  $M_K$ .

We have only to study the following events in the 2-parameter family  $\gamma(s)_t$ ,  $s, t \in [0, 1]$ , (compare Proposition 1):

- (1)  $\gamma_t$  becomes tangential to  $\Sigma_{cusp}^{(1)} \subset M_K$ . In case (a) a cusp is born and dies immediately after and in case (b) a cusp dies and is immediately reborn.
- (2)  $\gamma_t$  passes through the transverse intersection of a stratum  $\Sigma_{cusp}^{(1)}$  with another stratum of  $\Sigma^{(1)}$
- (3)  $\gamma_t$  passes through  $\Sigma_{trans-cusp}^{(2)}$
- (4)  $\gamma_t$  passes through  $\Sigma_{cusp-deg}^{(2)}$

In (1a) we replace the birth and the following death of a cusp in  $\gamma_{t_0}$  by a Whitney trick and its inverse and we continue the homotopy  $\gamma_t \subset M_K^{reg}$ ,  $t > t_0$ . The effect are just two additional small curls on the diagrams for a small arc  $s$  in the loops  $\gamma_t$ ,  $t > t_0$ . We keep the small curls in the rest of the homotopy.

If  $\gamma_t$  touches  $\Sigma_{cusp}^{(1)}$  from the other side, i.e. in (1b), then we simply keep the corresponding small curl on the arc  $s$ .

In (2) there is no problem at all because we can make Whitney tricks simultaneously at different places of a diagram.

In (3) a branch moves over or under a cusp. But we can perform a Whitney trick which creates or eliminates the cusp simultaneously with moving the brunch over or under the Whitney trick.

In (4) a Reidemeister II move is replaced by the birth or the death of two cusps with different writhe and different Whitney index. We can replace this by a single Whitney trick, which is followed by sliding one of the two curls once over the other in order to obtain the diagram which allows the Reidemeister II move.

We end up with a diagram  $*'$  which is regularly isotopic to  $*$ , but which differs from  $*$  by lots of small curls on it. But because  $*'$  and  $*$  are regularly

isotopic the sum of the writhe's of the small curls as well as the sum of their Whitney indices vanishes. This implies that we can eliminate them two by two with Whitney tricks. This approximation of the homotopy  $\gamma_t$  by a homotopy in  $M_K^{reg}$  is unique up to adding loops in  $M_K^{reg}$  which consist of sliding small curls through small curls (but we use here that no small curl can slide over  $\infty$ ). These loops are evidently contractible in  $M_K$ , but our method does not show that they are contractible in  $M_K^{reg}$ , because we are not allowed to contract small curls (as in (1b)). However, each such loop is just a combination of loops  $rot(U)$  or  $rot'(U)$  as studied in Proposition 2. Here  $U$  is the unknot, given by a connected sum of curls, which is somewhere on  $K$ . But  $K$  is not involved in the rotations  $rot$  and  $rot'$  of the unknot part. It follows now from the proof of Proposition 2 that  $R_1(rot(U))$  is of the form  $(x^0 - 1)x^m = 0$  and that  $R_1(rot'(U))$  is identical 0.

□

(In fact, one can prove that e.g. the loop  $rot(U)$ , which is obtained by exchanging two positive curls with the same negative Whitney index, is not contractible in  $M_U^{reg}$  by using the techniques of *trace graphs* developed in [19]. The trace graph of a loop of long knots is an oriented singular link in the solid torus. All its singularities are ordinary triple points. The parity of the number of non-contractible components of any resolution of the trace graph in the solid torus is an invariant of the homotopy class of the loop in  $M_U^{reg}$ , compare [19]. The trace graph of the constant loop is just the standard closure of the trivial  $n$ -braid, where  $n$  is the number of crossings of the knot, hence  $n = 2$  in our case. On the other hand, one easily sees that any resolution of the trace graph of  $rot(U)$  has only one component, because the two crossings are interchanged.

This implies that the kernel of  $in_* : H_1(M_K^{reg}) \rightarrow H_1(M_K)$  is never trivial.)

*However, it follows that  $R_1(fh(K))$  is well-defined for hyperbolic knots and torus knots because it does not depend on the chosen approximation of  $fh(K)$  by a loop in  $M_K^{reg}$ .*

It seems to us that  $R_1$  in  $M_K^{reg}$  is a *deformation quantization* of the Teiblum-Turchin or Mortier 1-cocycle, i.e. if we set  $x = 1 + q$  and develop the invariant in  $q$  then the coefficient of the linear term is equal to the value of the Teiblum-Turchin or Mortier 1-cocycle. A calculation of Mortier [32] would suggest that  $dR_1(fh(K))/dx|_{x=1} = \alpha_3^1(fh(K)) = 6v_3(K) - w(K)v_2(K)$ . (Here,  $w(K)$  is the writhe of the framed knot  $K$  and  $v_3(K)$  is the unique Vassiliev invariant of degree 3 normalized to be 1 on  $3_1^+$  and -1 on  $3_1^-$ .) We have

calculated that  $R_1(fh(3_1^+, w = 3)) = 3x - 3$  and that  $R_1(fh(4_1, w = 0)) = 0$ , which fits with Mortier's calculation.

The proposition shows also that already  $R_1(rot(K))$  is *not* multiplicative for the connected sum of two knots.

Morally, Proposition 2 tells us that for long knots we have to add long longitudes in order to get something really interesting. On one hand we want a 1-cocycle for the whole space  $M_T$  without taking out any strata in  $\Sigma^{(2)}$  and on the other hand, adding a local knot on a component of the string link  $T$  should not lead to a formula which already calculates the invariant as in Proposition 2.

**Remark 3** *We will achieve both goals with  $R_n$  for  $n > 1$  because by definition the colors of the foot and of the head are always different for the crossings  $d$ ,  $ml$  and there are no  $f$ -crossings of type  $C_{i_3} \rightarrow C_{i_3}$  and no  $r$ -crossings of type  $C_{i_2} \rightarrow C_{i_2}$ . There can be  $f$ -crossings  $C_{i_2} \rightarrow C_{i_2}$  and  $r$ -crossings  $C_{i_3} \rightarrow C_{i_3}$  but  $C_{i_2} \neq C_{i_3}$ . It follows immediately that the crossing  $ml$  in  $\Sigma_{trans-cusp, cusp=[ml]=0, [d]=1}^{(2)}$  does never contribute (because  $ml$  is just the crossing of the small curl) and that there are no contributions to  $W_2$  by crossings only in a local knot on a component. Consequently, adding a local knot  $K$  to a component of the string link does not lead to just a multiplication of the invariant by  $x^{v_2(K)}$ .*

Let us replace now the framed knot  $K$  by its parallel 2-cable determined by the framing, which we denote by  $2 - cable(K), w(K)$ . Here as usual the framing is encoded in the writhe  $w(K)$  of the diagram, i.e. the algebraic number of crossings with respect to the fixed projection  $pr$ . It turns out that there is a first splitting of  $R_1$  into several 1-cocycles (compare Section 4.4): we take into account only the crossings  $d$  and  $ml$  which are in addition of a given colored type e.g.  $red \rightarrow red$  or  $red \rightarrow black$ .

*We take always  $red - \infty$  as the end of the red component and  $black - \infty$  as the end of the black component.*

The corresponding 1-cocycles are denoted by  $R_1(red - red, red - \infty)$ ,  $R_1(red - red, black - \infty)$ ,  $R_1(red - black, red - \infty)$  and so on. These splittings do not yet correspond to admissible colorings because we do not care about the colors for the  $f$ - and the  $r$ -crossings.

We have calculated the following examples, where we use the standard notations for knots from the *knot atlas*. Let the knot  $8_{17}$  be the standard

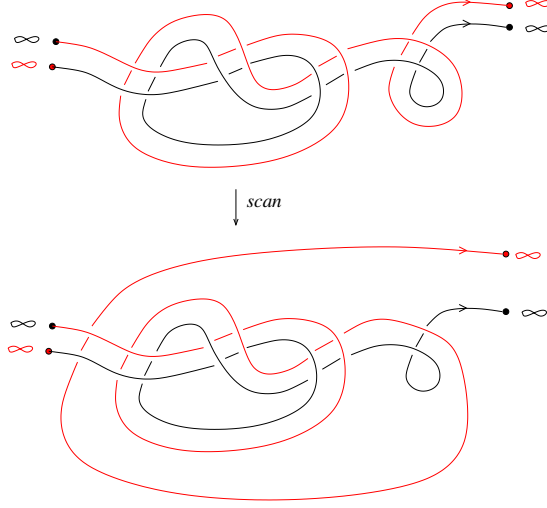


Figure 11: scan of the 2-cable of the positive trefoil

closure of the 3-braid  $\sigma_2\sigma_2\sigma_1^{-1}\sigma_2\sigma_1^{-1}\sigma_2\sigma_1^{-1}\sigma_1^{-1}$  oriented as usually from the left to the right.

We show the arc  $\text{scan}(2 - \text{cable}(3_1^+), w = 3)$  in Fig. 11 as an example.

**Example 1**

$$R_1(\text{red} - \text{red}, \text{red} - \infty)(\text{scan}(2 - \text{cable}(3_1^+), w = 3)) = x^{14} - 49x^{13}$$

$$R_1(\text{red} - \text{black}, \text{red} - \infty)(\text{scan}(2 - \text{cable}(3_1^+), w = 3)) = -8x^6 + 36x^{12}$$

$$R_1(\text{red} - \text{red}, \text{black} - \infty)(\text{scan}(2 - \text{cable}(3_1^+), w = 3)) = x^9 - 49$$

$$R_1(\text{red} - \text{red}, \text{red} - \infty)(\text{scan}(2 - \text{cable}(4_1), w = 0)) = x^{-1} - 1$$

$$R_1(\text{red} - \text{red}, \text{red} - \infty)(\text{scan}(2 - \text{cable}(8_{17}), w = 0)) = x^{-1} - 1$$

$$R_1(\text{red} - \text{red}, \text{red} - \infty)(\text{scan}(2 - \text{cable}(-8_{17}), w = 0)) = x^{-1} - 1$$

It is easy to see that  $R_1(\text{red} - \text{black}, \text{black} - \infty)(\text{scan}(2 - \text{cable}(K))) = 0$  as well as  $R_1(\text{black} - \text{black}, \text{black} - \infty)(\text{scan}(2 - \text{cable}(K))) = 0$  for each knot  $K$  because no crossing at all can contribute for a moving red arc under the rest of the knot.

**Conjecture 1** (*Fewnomials*)

The values of the 1-cocycles  $R_1(\text{red} - \text{red}, \text{red} - \infty)(\text{scan}(2 - \text{cable}(K, w)))$ ,  $R_1(\text{red} - \text{red}, \text{black} - \infty)(\text{scan}(2 - \text{cable}(K, w)))$  and  $R_1(\text{red} - \text{red}, \text{black} -$

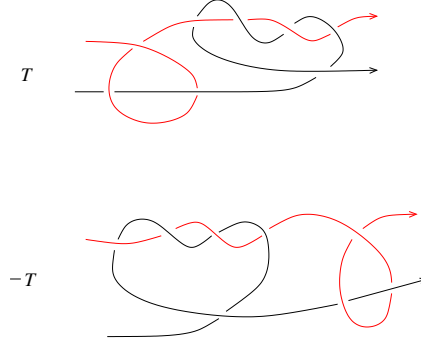


Figure 12: The 2-tangle  $T$  and its inverse

$\infty)(\text{scan}(2 - \text{cable}(K, w)))$  are completely determined by the Vassiliev invariants  $w(K)$  of degree 1 for (framed) knots and  $v_2(K)$  of degree 2 and each value is at most a binomial.

It seems likely that e.g. if  $w(K) = 0$  then always

$$R_1(\text{red} - \text{red}, \text{red} - \infty)(\text{scan}(2 - \text{cable}(K, w = 0))) = x^{v_2(K)} - 1,$$

but we have no proof for this. (Notice that  $R_1(\text{red} - \text{red}, \text{red} - \infty)(\text{scan}(2 - \text{cable}(K, w)))$  could be 0 for  $w(K) = 0$  and  $v_2(K) = 0$  and it could be a monomial for  $w(K) \neq 0$  and  $v_2(K) = 0$ .)

The above conjecture looks like bad news:  $R_1(\text{scan})$  is not interesting for 2-cables of long knots neither. However, it turns out to be extremely interesting for 2-tangles other than 2-cables.

**Example 2** Let  $T$  be the 2-tangle shown in Fig. 12 and let  $-T$  be its inverse. Each of the components is a long trivial knot. We add to each of the two tangles a crossing  $\sigma_1$  at the right end. Then

$$R_1(\text{black} - \text{black}, \text{red} - \infty)(\text{scan}(T\sigma_1)) = -49 + x^{-1}$$

$$R_1(\text{black} - \text{black}, \text{red} - \infty)(\text{scan}(-T\sigma_1)) = -49 - 39x^{-1} + 40x^{-2}$$

Notice that the two Laurent polynomials have the same value at  $x = 1$ .

For the convenience of the reader and in order to get a bit familiar with the new invariants we give the calculation of  $R_1(\text{black} - \text{black}, \text{red} - \infty)(\text{scan}(-T\sigma_1))$  in some detail below.

There are exactly six different *global types* of triple crossings with a point at infinity. For shorter writing we give names to them and show them in

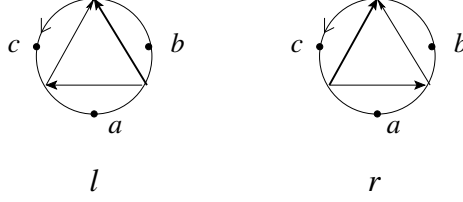


Figure 13: The six global types of triple crossings

Fig. 13. (Here "r" indicates that the crossing between the middle and the lowest branch goes to the right and "l" indicates that it goes to the left.) It follows from the definitions that  $d$  can contribute only for the triple crossings of the types  $r_a, r_b, l_b$ . The crossing  $ml$  can contribute only for the types  $r_a$  and  $l_c$ .

The abstract closure of  $T\sigma_1$  and  $-T\sigma_1$  to a circle is now by the trivial 2-braid because we have already added a  $\sigma_1$ . The arc of the diagram which moves under the tangle in *scan* is now black.

There are exactly 10 Reidemeister moves which can contribute to  $R_1(\text{black-black}, \text{red} - \infty)(\text{scan}(-T\sigma_1))$ . We give numbers to them in Fig. 14. We show the corresponding Gauss diagrams together with the calculation of the contributions to  $R_1$  in Fig. 15 and Fig. 16. We draw the crossing  $d$  always by a bold arrow for better visualizing the global type of the move.

The calculation gives now:

- move 1:  $+l_c$ ,  $w(ml) = w(d)$ ,  $W_1(hm) = 0$ , no contribution
- move 2:  $+r_b$ ,  $l(d) = -2$ ,  $W_2(d) = -1$ , contribution  $4(-2)x^{-1}$
- move 3:  $-l_c$ ,  $\eta = -1$ ,  $\epsilon = 0$ ,  $w(ml) = 1$ ,  $w(hm) = -1$ ,  $l(ml) = -2$ ,  $W_1(hm) = 1$ ,  $W_2(ml) = 0$ , contribution  $(-3)^2(x^{-1} - 1)$
- move 4:  $+tan^+$ ,  $l(d) = -5$ ,  $W_2(d) = -1$ , contribution  $8(-5)x^{-1}$
- move 5:  $+r_b$ ,  $l(d) = -2$ ,  $W_2(d) = -2$ , contribution  $4(-2)x^{-2}$
- move 6:  $-r_a$ ,  $w(ml) = w(d) = 1$ ,  $l(d) = -2$ ,  $W_2(d) = 0$ , contribution  $-4(-2)x^0$ ,  $w(hm) = 1$ ,  $\eta = -1$ ,  $l(ml) = -6$ ,  $W_1(hm) = -2$ ,  $W_2(ml) = 0$ , contribution  $(-7)^2(x^{-2} - 1)$
- move 7:  $+l_c$ ,  $w(ml) = w(hm) = -1$ ,  $l(ml) = -2$ ,  $W_1(hm) = -1$ ,  $W_2(ml) = -2$ , contribution  $(-1)^2(x^{-1} - x^{-2})$
- move 8:  $+r_b$ ,  $l(d) = 0$ , no contribution
- move 9:  $+l_c$ ,  $w(ml) = w(hm) = -1$ ,  $l(ml) = 0$ ,  $W_1(hm) = -1$ ,  $W_2(ml) = -1$ , contribution  $(+1)^2(1 - x^{-1})$
- move 10:  $-tan^-$ ,  $l(d) = 0$ , no contribution.

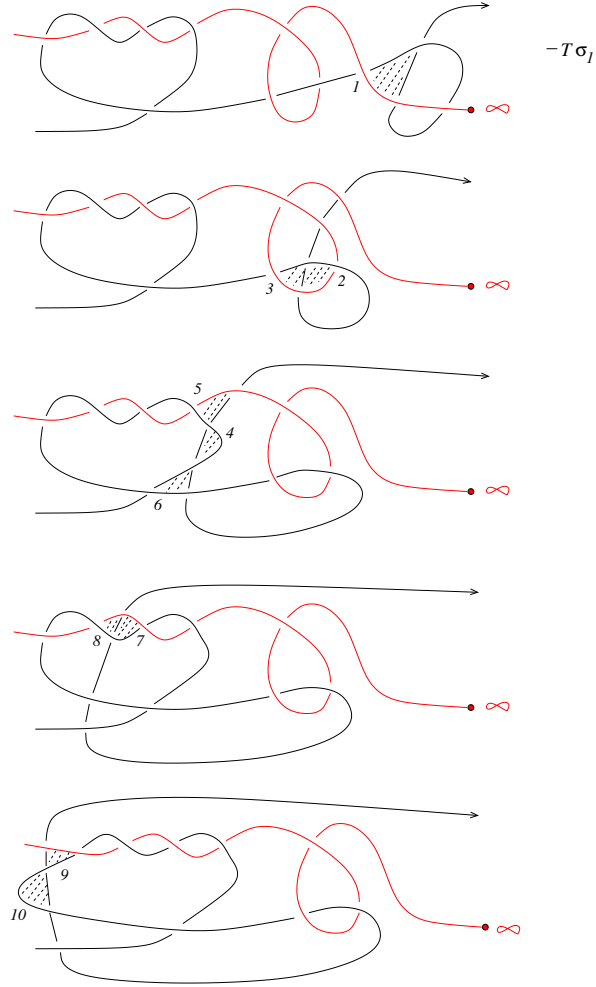
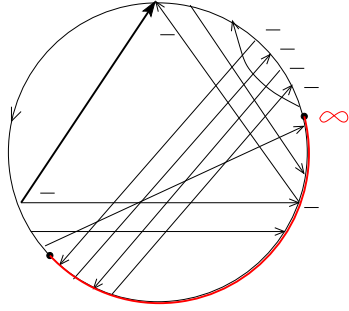


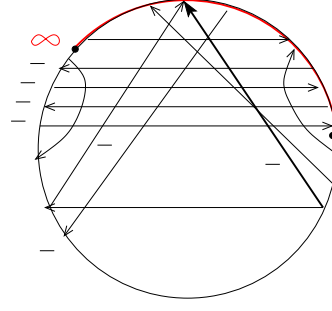
Figure 14: The Reidemeister moves in  $\text{scan}(-T\sigma_1)$



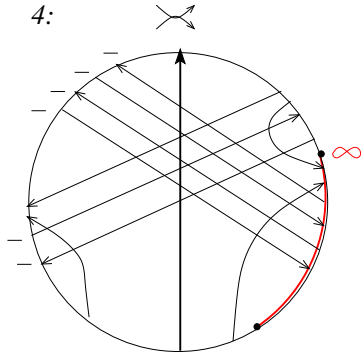
2:



3:



4:



5:

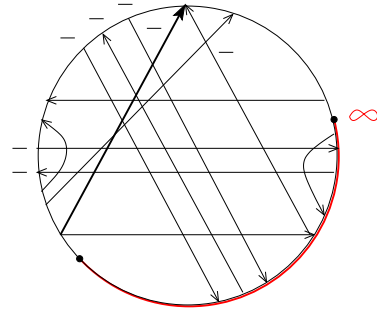


Figure 15: The Gauss diagrams for the moves in  $scan(-T\sigma_1)$

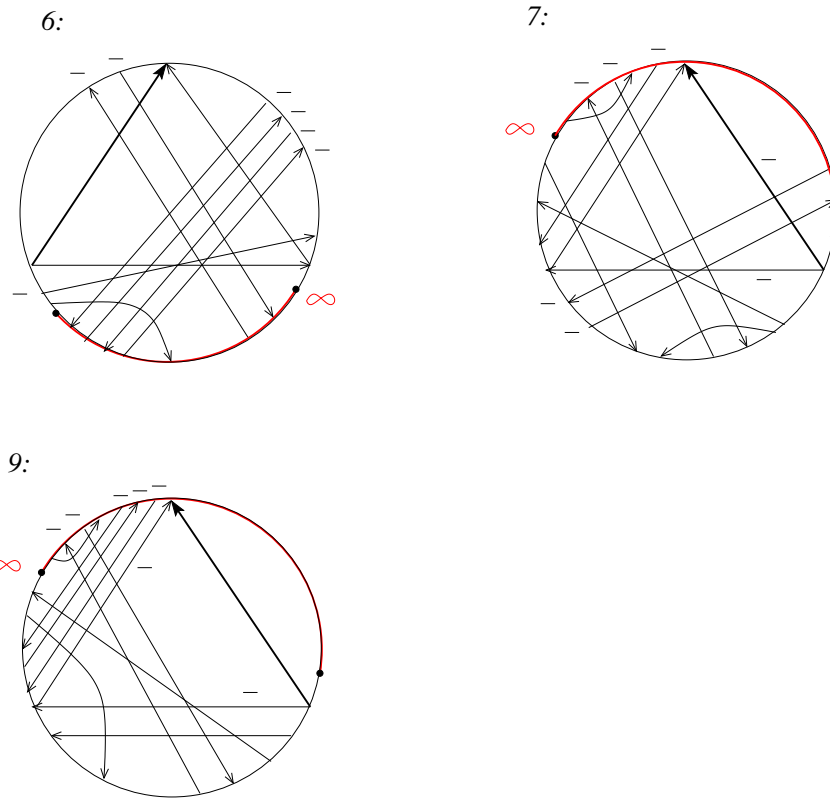


Figure 16: The remaining Gauss diagrams for the moves in  $scan(-T\sigma_1)$

Consequently,  $R_1(\text{black-black}, \text{red}-\infty)(\text{scan}(-T\sigma_1)) = -8x^{-1} + 9(x^{-1} - 1) - 40x^{-1} - 8x^{-2} + 8 + 49(x^{-2} - 1) + (x^{-1} - x^{-2}) + (1 - x^{-1}) = -49 - 39x^{-1} + 40x^{-2}$ .

It turns out that for  $R_1(\text{black} - \text{black}, \text{red} - \infty)(\text{scan}(T\sigma_1))$  no Reidemeister move at all contributes with a term of degree  $-2$ .

**Corollary 1**  *$R_1(\text{scan})$  distinguishes the above tangle  $T$  from its inverse  $-T$  as an invariant which can be calculated with cubic complexity with respect to the number of crossings.*

*Proof.* Evidently, if  $T\sigma_1$  is not isotopic to  $-T\sigma_1$  then  $T$  is not isotopic to  $-T$ . The calculation of the invariant  $R_1(\text{scan})$  is of complexity of degree at most 3 with respect to the number of crossings of the tangle. Indeed, the number of Seifert circles  $s$  (i.e. the number of circles in the plan which are obtained by smoothing all double points of  $pr(T)$  with respect to the orientation) is not bigger than the number of crossings  $c$ . We can assume that the moving arc in  $\text{scan}$  has at each moment at most  $2s$  new crossings. Each crossing contributes at most once in a RIII-move and it is easy to see that we can change the diagram by an isotopy so that there are at most  $2c$  RII-moves in  $\text{scan}$ . For each of the Reidemeister moves we have to calculate a weight of at most quadratic complexity with respect to  $c + 2s$  (namely  $W_2(d)$ ). Consequently, the whole  $R_1(\text{scan})$  is at most of cubic complexity with respect to the number of crossings  $c$ .

□

As already mentioned in the Introduction Bar-Natan has shown that there is no finite type invariant of degree smaller than 7 which can distinguish a 2-component string link from its inverse. It is easy to see that  $T$  and  $-T$  can not be distinguished by the HOMFLYPT, Kauffman and Kuperberg invariants in the corresponding skein modules for 2-tangles in the 3-ball, because the corresponding skein modules are commutative and the skein relations and generators of the skein modules are invariant under orientation change of the 2-tangles, see e.g. [4], [36], [38]. It seems to be not known whether there is a primitive finite type invariant of degree at least 7, but which can nevertheless be calculated with complexity of degree 3. If there is no such invariant then it would follow that  $R_1(\text{scan})$  for a general string link  $T$  is not determined by any finite type invariants of  $T$  and in particular it is not determined by any quantum invariants (which can be decomposed into infinite series of finite type invariants).

The value in the example of  $R_1(\text{black} - \text{black}, \text{black} - \infty)(\text{scan}(-T\sigma_1))$  is a *trinomial*. If the Viewnomial conjecture is true this would imply that  $-T\sigma_1$  is not a 2-cable of any long knot.

*So, it seems likely that  $R_1(\text{scan})$  can detect sometimes with cubic complexity with respect to the number of crossings that a 2-component string link is not a 2-cable of any long knot.* (Sometimes the Alexander polynomial can detect this too, but with complexity of degree 4. It is not easy to establish this in general. One has to find the JSJ-decomposition of the complement of the string link in the 3-ball. If  $T$  is a 2-cable of a non-trivial long knot then there is an incompressible embedded torus  $T^2$  in  $D^3 \setminus T$  and which intersects  $\partial D^3$  in a cylinder  $C$ .  $T^2 \setminus C$  bounds a properly embedded solid cylinder in  $D^3$  with the tangle  $T$  inside it. The tangle in this solid cylinder has to be a 2-braid. This is the case if and only if the fundamental group of the complement of  $T$  in the solid cylinder is the free group  $F_2$ .)

### 3.2 Applications of the 1-cocycle $R_n$ in $M$ for $n > 1$ . Detecting the non-invertibility of knots

Let us consider now  $R_n$ . Gramain's loop is still defined in the same way for  $M_n$ , but at the end we have just to push a full twist of the  $n$ -strands back through the knot.

As already mentioned in the previous section there is only  $R_2$  which is interesting for  $n = 2$ .

#### Example 3

$$\begin{aligned} R_2(\text{rot}(2 - \text{cable}(3_1^+), w = 3)) &= 36x^{12} - 72x^{10} + 56x^8 + 20x^5 - 20x^2 - 20 \\ R_2(\text{scan}(2 - \text{cable}(3_1^+), w = 3)) &= 36x^{11} + 20x^8 \end{aligned}$$

*$R_2$  is the first non-trivial polynomial valued 1-cocycle for long knots.  $R_2(\text{rot}(2 - \text{cable}(3_1^+), w = 3))$  and  $R_2(\text{scan}(2 - \text{cable}(3_1^+), w = 3))$  are new polynomial invariants of the positive trefoil and which do not come from representation theory neither from generating functions of categorifications of known polynomial invariants! They can be calculated with cubic complexity with respect to the number of crossings and  $R_2$  can distinguish the homology classes of loops in  $M_2$ .*

Notice that  $R_2(\text{rot}(2 - \text{cable}(3_1^+), w = 3))$  vanishes at  $x = 1$  (in fact, it is not very difficult to prove that this is the case for each knot). It is clear that  $R_2$  depends strongly on the framing  $w(K)$  because the string links

$2\text{-cable}(K), w(K)$  are not isotopic for different  $w(K)$ , but concrete examples have to be calculated with a computer.

The Fox-Hatcher loop has a nice combinatorial realization too: we go on  $K$  from  $\infty$  to the first crossing. If we arrive at an under-cross then we move the branch of the over-cross over the rest of the knot up to the end of  $K$ . If we arrive at an over-cross then we move the branch of the under-cross under the rest of the knot up to its end. We continue the process up to the moment when we obtain a diagram which is isotopic to our initial diagram of  $K$ , compare [24]. We can of course consider the analog loop for cables of long framed knots in  $M_n$ . It follows that the complexity of  $R_n(fh(n\text{-cable}(K), w))$  is of degree 4 with respect to the number of crossings for each fixed  $n$ . Indeed, by moving an arc over or under the rest of the diagram each of the  $c$  crossings contributes at most with a weight of degree 2 and we have to move at most  $2c$  arcs in the loop. Unfortunately, even for the 2-cable of  $4_1$  the calculation by hand is already too complicated. However, the example  $2\text{-cable}(3_1^+), w = 3$  shows that  $R_n(fh(n\text{-cable}(K), w))$  is not always trivial too.

Let  $K$  be a non-trivial long knot and  $M_K$  its component in the moduli space. There is a well known action of the braid group  $B_n$  on  $M_K^n$ , see [21] and also [10], where  $M_K^n$  denotes the moduli space of the connected sum of  $n$  copies of the knot  $K$ . The generator  $\sigma_i$  acts by pushing the  $i$ -th copy of  $K$  through the  $i + 1$ -th copy of  $K$  and the inverse  $\sigma_i^{-1}$  acts by pushing the  $i + 1$ -th copy back through the  $i$ -th. The same action is still well defined for cables of framed knots. In particular,  $R_2(\beta)$  is another polynomial knot invariant of  $K$  for each  $\beta \in B_n$  when we apply  $R_2$  to the 2-cable of the connected sum of long framed non-trivial knots  $K$ . Its calculation is of quartic complexity with respect to the numbers of crossings of  $K$  for each fixed braid  $\beta$ . Unfortunately, it is too difficult to calculate examples by hand.

**Question 1** *Is  $R_2(\beta)$  non-trivial for non-trivial braids?*

We could also define a polynomial valued bilinear form on  $H_0(M_2)^2$  by evaluating  $R_2$  on the loop which consists of pushing the 2-cable of a long framed knot  $K_1$  through the 2-cable of a long framed knot  $K_2$  and then pushing the 2-cable of  $K_2$  through the 2-cable of  $K_1$ . But again, without a computer program we do not know yet whether it is trivial or not.

Let  $R_3^1$  be the 1-cocycle corresponding to the admissible coloring 1, with virtual closure  $\sigma_1\sigma_2$  and red- $\infty$ , which has been introduced in the previous

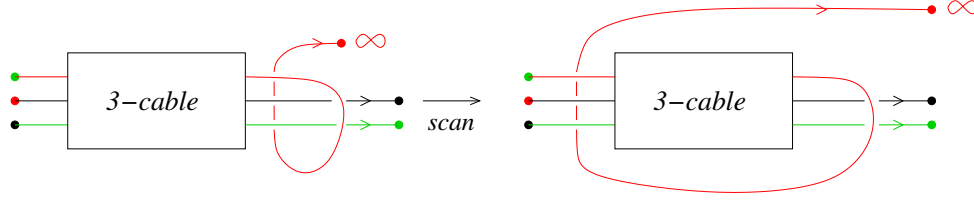


Figure 17: The scan of the 3-cable of the knot  $8_{17}$

section. We consider *scan* with the red arc, see Fig. 17. The calculation by hand of  $R_3^1(\text{scan})$  is rather laborious. Therefore we have calculated only the terms of the lowest degree in  $x_1$ , but which are already sufficient in order to distinguish  $8_{17}$  from  $-8_{17}$ .

**Example 4**  $R_3^1(\text{scan}(3 - \text{cable}(8_{17}), w = 0)) = \text{terms of degree 0 and -1}$   
 $R_3^1(\text{scan}(3 - \text{cable}(-8_{17}), w = 0)) = (\text{term of degree -1}) + 8x_1^{-2}$

This example shows that the degree of a given invariant  $R_n^i(\text{scan})$  can even define an ordering of a knot and its inverse.

Because of the great importance of the example we give the calculation below in some detail .

Remember that d-or ml-crossings have to be of the type *red*  $\rightarrow$  *black* in order to contribute to  $R_3^1$  and that in addition the crossing *ml* only contributes if the overcross of the crossing *d* in the R III move is *green* or *black*. f-crossings have to be of type *black*  $\rightarrow$  *black* or *black*  $\rightarrow$  *green*. r-crossings have to be of the type *green*  $\rightarrow$  *green* or *green*  $\rightarrow$  *black*.

The  $(3 - \text{cable}(8_{17}), w = 0)$  is shown in Fig. 18 together with the ordered potential f-crossings  $\{1, \dots, 11\}$ , compare Definition 15. We show the Gauss diagram of the potential f- and r-crossings in Fig. 19. (For better visualizing the r-crossings are drawn in green.) We observe that the weight  $W_1(f)$  of a f-crossing can only change in a R III move of type  $l_a$ , compare Fig. 13, with a black lowest branch in the move. But this can not happen in the scan-arc because the lowest branch is always red. There can't appear new f-crossings from R II moves in the scan-arc for the same reason. It follows that all the weights  $W_1(f)$  are constant in the scan-arc. The calculation of  $w(q)W_1(q)$  for each potential f-crossing  $q \in \{1, \dots, 11\}$  gives now the sequence:

0, -1, 2, -2, 1, -1, 1, 0, 0, 0, -1. Going from red- $\infty$  along the black component we always come first to the undercross of a potential f-crossing. Con-

sequently, the weights  $W_2(d)$ ,  $W_2(ml)$  and  $W_2(ml) + w(hm)W_1(hm)$  are always of the form  $W(0) = 0$  or  $W(k) = w(1)W_1(1) + w(2)W_1(2) + \dots + w(k)W_1(k)$  for some  $k \in \{1, \dots, 11\}$ . An easy calculation gives now

$W(1) = 0, W(2) = -1, W(3) = 1, W(4) = -1, W(5) = 0, W(6) = -1, W(7) = 0, W(8) = 0, W(9) = 0, W(10) = 0, W(11) = -1$ . The R II moves contribute to  $x_1^0$  (from  $W(8)$ ) respectively  $x_1^{-1}$  (from  $W(6)$ ). Consequently, there are no contributions of degree strictly smaller than  $-1$  at all and the maximal possible degree of  $x_1$  is 1. This happens exactly for  $ml$  in the R III moves with the crossing  $hm = 3$  and  $hm = 4$ . But one easily sees that their contributions cancel out together.

The  $(3\text{-cable}(-8_{17}), w = 0)$  is shown in Fig. 20 together with the ordered potential f-crossings  $\{1, \dots, 11\}$ . We show the Gauss diagram of the potential f- and r-crossings in Fig. 21. The calculation of  $w(q)W_1(q)$  for each potential f-crossing  $q \in \{1, \dots, 11\}$  gives now the sequence:

$2, -4, 2, -1, 1, -1, 0, 0, 0, -1, 0$ . This time we have

$W(1) = 2, W(2) = -2, W(3) = 0, W(4) = -1, W(5) = 0, W(6) = -1, W(7) = -1, W(8) = -1, W(9) = -1, W(10) = -2, W(11) = -2$ .

The R II moves contribute to  $x_1^{-1}$  (from  $W(4)$ ) respectively  $x_1^{-1}$  (from  $W(8)$ ). Considerations analogue to those for  $8_{17}$  show that the contributions with  $x_1^0$  and the contributions with  $x_1^2$  both cancel out. A somewhat longer calculation shows now that  $8x_1^{-2}$  stays as the term of degree  $-2$ .

□

But the invariant  $R_3^1(\text{scan}(3\text{-cable}(K), w))$  can still be refined in the following way: let  $t$  be an even natural number and let us add  $t/2$  full-twists at the very end of the 3-cable of  $K$  but only *between the red and the black branch*, see Fig. 22. The  $t$  new crossings are never d-crossings or  $ml$ -crossings because they are never involved in Reidemeister moves in the scan-arc. They are never f-crossings or r-crossings because they don't have the right colors. In Fig. 23 we show the Gauss diagram of the  $t$  new crossings together with the only possibilities for crossings of type  $d$  and  $ml$  which contribute. It follows that for each of them the linking number  $l$  becomes  $l + t$ . Consequently, the invariant is now of the form

$$R_3^1(\text{scan}(3\text{-cable}(K), w, t)) = t^2 P_2(x_1) + t P_1(x_1) + R_3^1(\text{scan}(3\text{-cable}(K), w)),$$

where  $P_2(x_1)$  and  $P_1(x_1)$  are some new Laurent polynomials. Notice that  $P_2(x_1)$  is completely determined by the contributions of the crossings of type  $ml$  alone and that we don't even have to calculate the linking numbers  $l(ml)$ , compare Definitions 12 and 14. We use the  $t^2$ -part of the invariant to distinguish  $8_{17}$  from  $-8_{17}$  even faster.

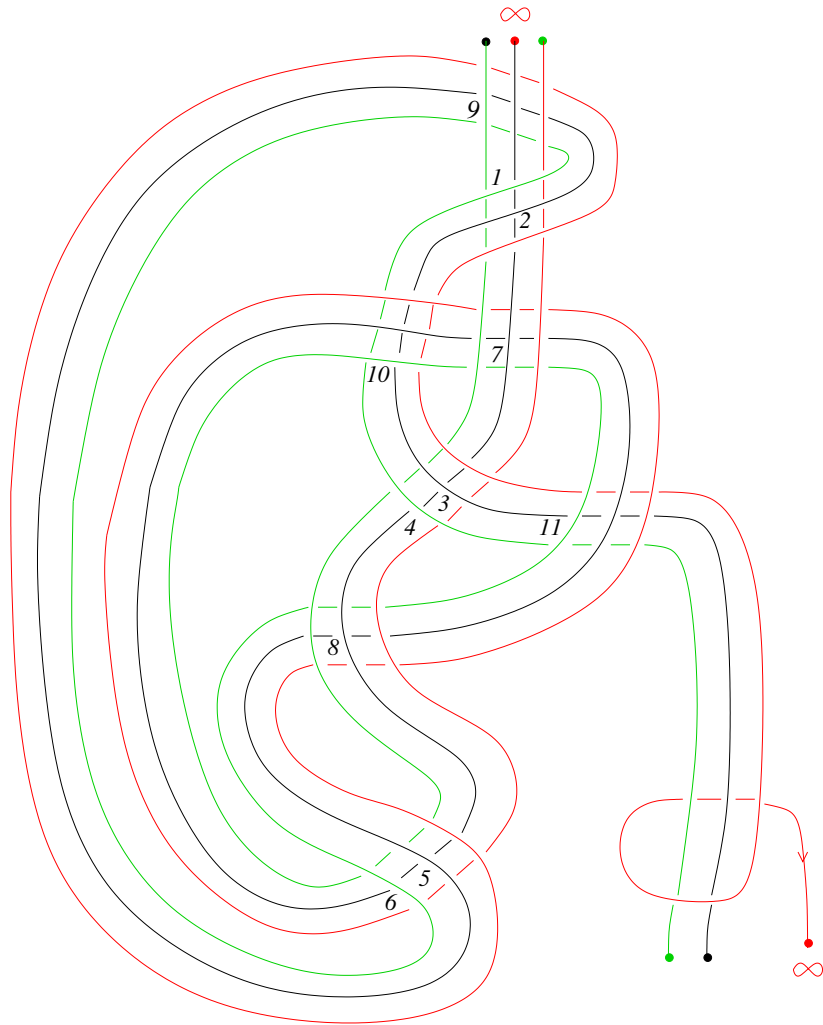


Figure 18: The potential f- and r-crossings for the 3-cable of  $8_{17}$



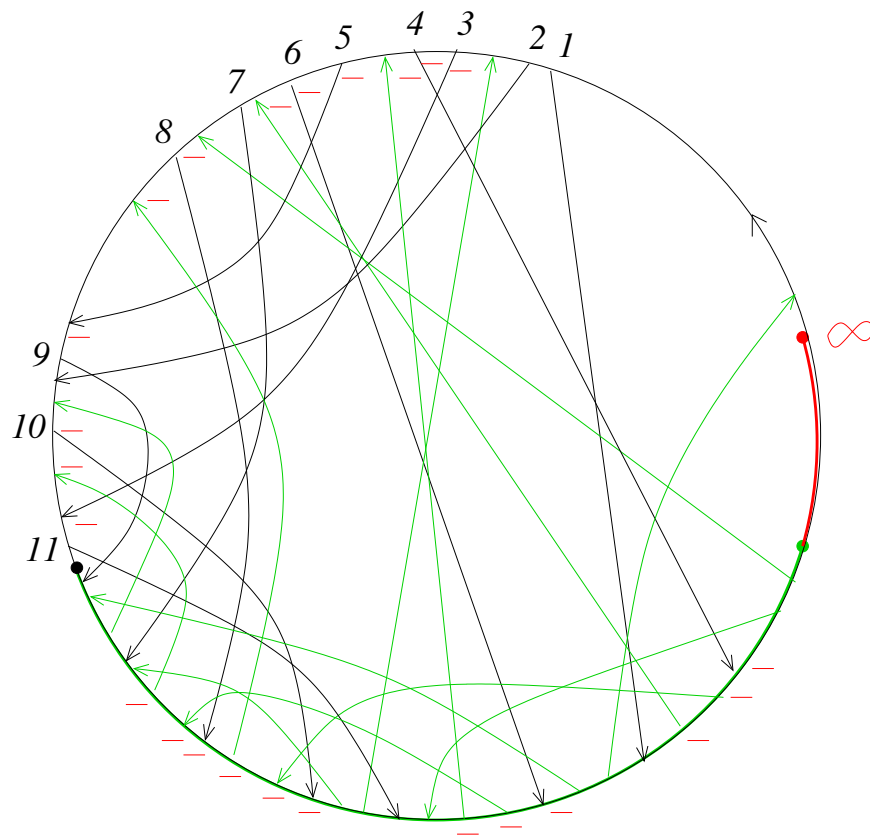


Figure 19: The Gauss diagram of the potential f- and r-crossings for the 3-cable of  $8_{17}$

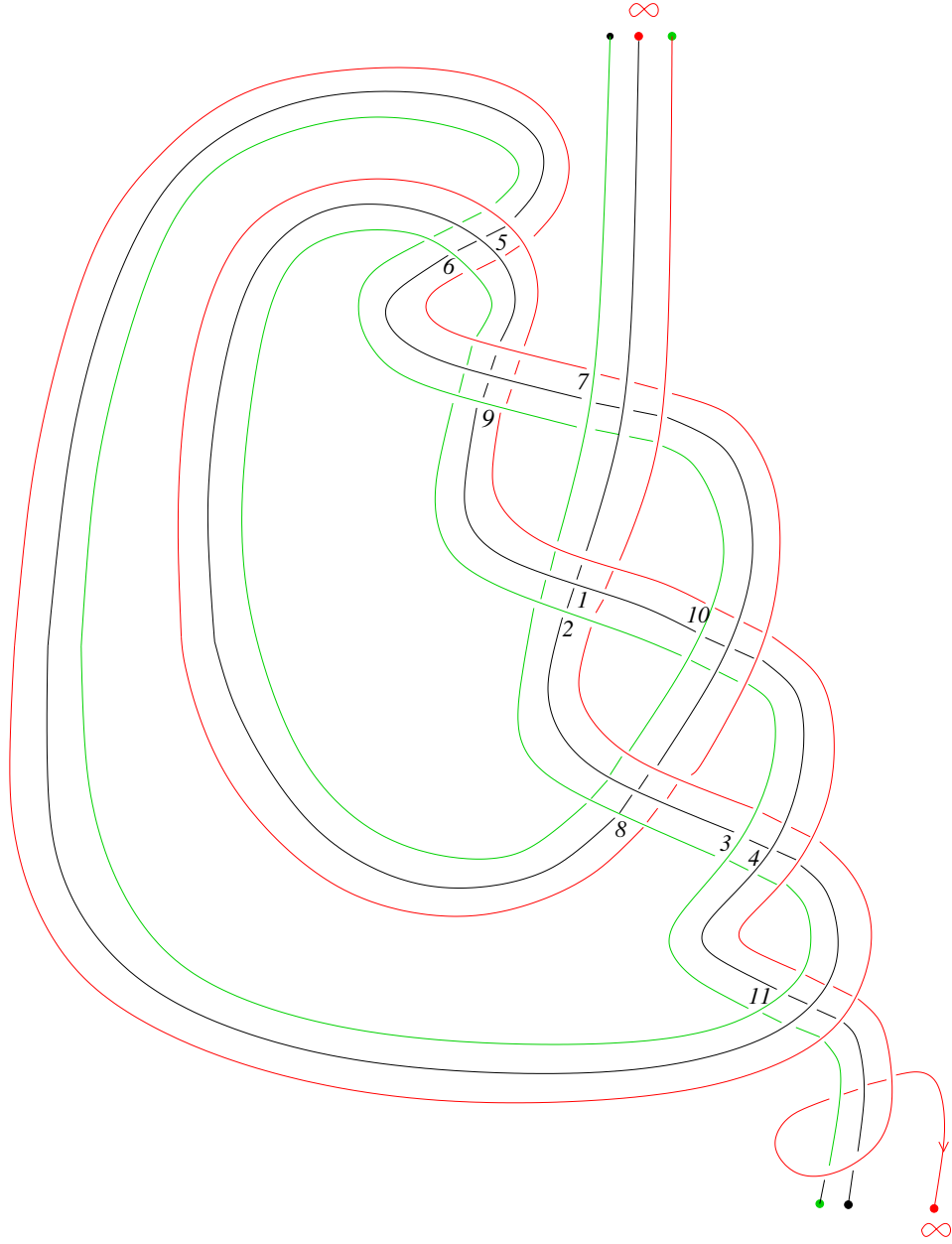


Figure 20: The potential f- and r-crossings for the 3-cable of  $-8_{17}$

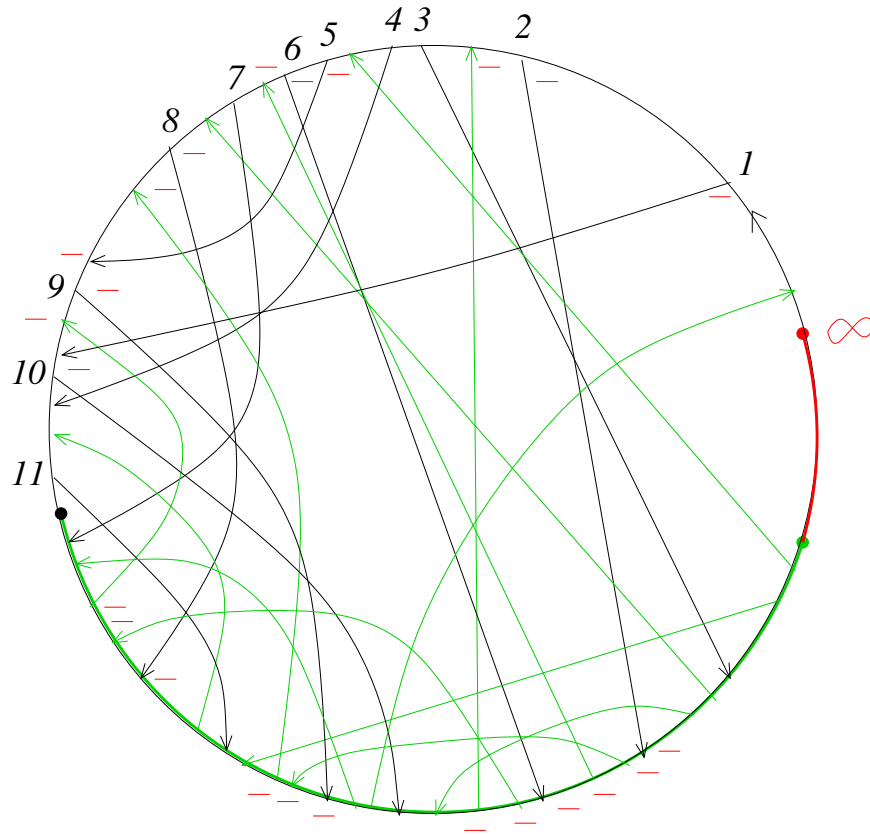


Figure 21: The Gauss diagram of the potential f- and r-crossings for the 3-cable of  $-8_{17}$

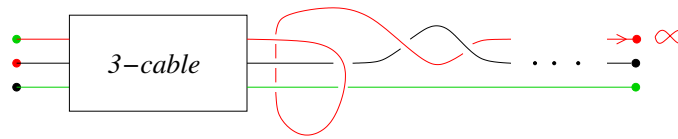


Figure 22: The scan of the 3-cable with  $t/2$  full-twists between the red and the black branch

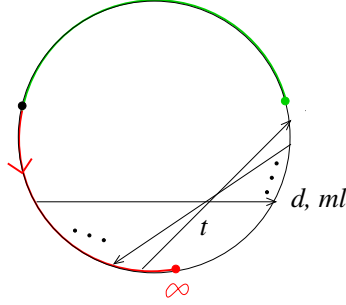


Figure 23: The Gauss diagram of the  $t$  new crossings

**Example 5**  $R_3^1(scan(3 - cable(8_{17}), w = 0, t)) = t^2(\text{terms of degree} \geq -1) + tP_1(x_1) + R_3^1(scan(3 - cable(8_{17}), w))$

$R_3^1(scan(3 - cable(-8_{17}), w = 0, t)) = t^2(x_1^{-2} + \text{terms of higher degree}) + tQ_1(x_1) + R_3^1(scan(3 - cable(-8_{17}), w))$

Indeed, there are no contributions of moves at all with  $x_1^{-2}$  in the case of  $8_{17}$  as was shown in the previous example. Consequently, there is no term with  $x_1^{-2}$  in  $P_2(x_1)$  in this case.

One sees immediately from the sequence of  $W(k)$  in the case of  $-8_{17}$  that only the crossings  $ml$  for  $hm = 2$ ,  $hm = 3$ ,  $hm = 10$  and  $hm = 11$  could contribute to  $t^2x_1^{-2}$ . But  $W_1(hm = 11) = 0$  and hence the R III move with  $hm = 11$  does not contribute. In the remaining three cases  $W_1(hm) \neq 0$  and hence the coefficient of  $x_1^{-2}$  in  $P_2(x_1)$  is odd! This is already sufficient but an easy calculation of the signs gives now that this coefficient is  $+1$ , compare Definitions 7 and 12.

□

It follows from results of Hatcher [24] that  $M_n(K)$  is a contractible space for each  $n$  if  $K$  is the trivial knot. Consequently,  $[R_n] = 0$  in this case.

**Lemma 1** *Let  $(K, w)$  be a long framed non-trivial torus knot. Then the non-trivial classes  $[rot(n - cable(K), w)]$  and  $[fh(n - cable(K), w)]$  are linearly dependent in  $H_1(M_n; \mathbb{Q})$  for each  $n > 0$ .*

*Proof.* Hatcher [24] has proven that for  $n = 1$  the moduli space  $M_K$  deformation retracts onto a circle and more precisely a certain non-trivial integer multiple of the loop  $rot(K)$  is homotopic to some non-trivial integer

multiple of the loop  $fh(K)$ . (The homotopy class of  $rot(K)$  does not depend on the framing and changing the framing adds multiples of  $rot(K)$  to  $fh(K)$ .) We approximate  $rot(K, w)$  and  $fh(K, w)$  by loops in  $M_K^{reg}$  by using Whitney tricks (compare Question 1). We replace now the framed long knot by a  $n$ -cable which we can imagine on a band which projects to the plane by an immersion. The same generic homotopy as for the knot applies still to the band besides that a Reidemeister I move of the knot is now replaced by a Reidemeister I move of the band together with a negative full-twist of the band if the crossing from the cusp is positive and with a positive full-twist of the band if the crossing from the cusp is negative. There can of course occur Reidemeister I moves in the homotopy because a loop can become tangential to  $\Sigma_{cusp}^{(1)}$  or can pass through  $\Sigma_{trans-cusp}^{(2)}$  or  $\Sigma_{cusp-deg}^{(2)}$  (compare Proposition 1). But the homotopy starts and ends with two loops of bands (with a common band as starting point) which all projects to the plane as immersions and which have all the same writhe = framing. It follows that the homotopy adds the same number of positive and negative full-twists to the bands. But full-twists can be moved along the bands (in a unique way up to homotopy because a full-twist can not move over infinity) and moving a full-twist commutes with any regular isotopy of a band. Therefore we can cancel out the positive and the negative full-twists two by two and we obtain a homotopy from a multiple of  $rot(n - cable(K), w)$  to a multiple of  $fh(n - cable(K), w)$  and the conclusion of the lemma follows.

□

Let us call the invariants  $R_n^i(fh(n - cable(K), w))/R_n^i(rot(n - cable(K), w))$  as well as  $R_n(fh(n - cable(K), w))/R_n(rot(n - cable(K), w))$  the *rational knot functions*.

The lemma together with the fact that  $R_n^i$  is a 1-cocycle implies immediately the following corollary.

**Corollary 2** *If  $(K, w)$  is a framed non-trivial torus knot then the rational knot function  $R_n^i(fh(n - cable(K), w))/R_n^i(rot(n - cable(K), w)) \in \mathbb{Q}^*$  for each  $n > 1$ , each choice of a virtual closure to a circle, of a point at infinity and of a admissible coloring  $i$ , whenever  $R_n^i(rot(n - cable(K), w)) \neq 0$ .*

We conjecture that in fact the inverse is true too even in a broader sens.

**Conjecture 2** *(Rational knot functions conjecture)*

*Let  $(K, w)$  be a framed long knot.*

(1)  $K$  is the unknot if and only if  $R_n(fh(n - \text{cable}(K), w)) = R_n(\text{rot}(n - \text{cable}(K), w)) = 0$  for each  $n > 1$ .

(2)  $K$  is a non-trivial torus knot if and only if

$R_n(fh(n - \text{cable}(K), w))/R_n(\text{rot}(n - \text{cable}(K), w)) \in \mathbb{Q}^*$  for each  $n > 1$ , whenever  $R_n(\text{rot}(n - \text{cable}(K), w)) \neq 0$ . Moreover, the values  $R_n(fh(n - \text{cable}(K), w))/R_n(\text{rot}(n - \text{cable}(K), w)) \in \mathbb{Q}^*$  determine the type of the torus knot.

(3) The rational knot functions  $R_n(fh(n - \text{cable}(K), w))/R_n(\text{rot}(n - \text{cable}(K), w))$ , for  $n > 1$ , detect whether or not the simplicial volume of  $S^3 \setminus K$  is 0.

(Compare [28] for the Volume conjecture and [34] for a generalization using the simplicial volume.) Unfortunately, we are missing a computer program in order to calculate lots of examples and to formulate a more precise conjecture for the part (3). (There are simply too many ways to extract 0 from a rational number which is seen as a rational function.) It is likely that for iterated torus knots and for connected sums of torus knots the above rational functions will already no longer be constant (because the two loops are no longer linearly dependent and the calculation of  $R_n^i$  on them has different complexity). However, we have to extract 0 from them. If we extract in the same way a number in the case of a hyperbolic knot (or a satellite which contains a hyperbolic piece in the JSJ-decomposition of its complement in  $S^3$ ) then the result should be different from 0.

G. Kuperberg [31] has observed that if finite type invariants fail to distinguish oriented knots then they fail automatically to distinguish all non-oriented knots as well. Our invariants can sometimes distinguish the orientation of a knot. So at least there is a chance that they perhaps distinguish all knots in 3-space.

We have an enormous amount of new knot invariants: for any knot  $K$  we can choose a framing  $w(K)$ , a natural number  $n > 1$ , a  $n$ -cycle in the symmetric group  $S_n$ , a point at infinity  $\infty \in \{1, \dots, n\}$  and an admissible coloring  $i$  of the corresponding 1-cocycle  $R_1$  and we obtain a rational knot function  $R_n^i(fh(n - \text{cable}(K), w))/R_n^i(\text{rot}(n - \text{cable}(K), w))$ . In fact, for each fixed framing  $w(K)$  there are  $(n-1)!$  different  $n$ -cycles in  $S_n$ , there are  $\{n\}_4 \{3\}_3 3! + \{n\}_3 \{3\}_3 3!$  different non-degenerate admissible colorings  $i$  and there are  $\{n\}_3 \{2\}_2 2! + \{n\}_2 \{2\}_2 2!$  different degenerate admissible colorings  $i$ . Here,  $\{n\}_k$  denotes the *Stirling number of the second kind*. It follows that for each framed knot we have exactly  $n!(4^n - 3^n 2 + 2^n)$  rational knot functions for each

$n > 1$ . Notice that we can order the set of rational knot functions for each  $n$  because the branches of the  $n$ -cable of  $K$  are ordered. A priori the number of our invariants grows exponentially with respect to  $n$ . An important point is of course to find out up to which extend our invariants are related amongst themselves.

As already mentioned, changing the framing  $w(K)$  adds multiples of  $rot(K)$  to  $fh(K)$  for  $n = 1$  and hence  $R_1(fh(K))/R_1(rot(K))$  changes just by an integer. However, this is certainly no longer the case for  $n > 1$ , because changing the framing  $w(K)$  changes the isotopy type of the  $n$ -cable of  $K$ .

If  $K$  is a non-trivial torus knot, then  $R_n^i(fh(n-cable(K), w))/R_n^i(rot(n-cable(K), w)) \in \mathbb{Q}^*$  depends of course only on the type of  $K$  and on the framing  $w(K)$ .

**Question 2** *Are there any relations between the rational knot functions of the same framed knot  $(K, w(K))$ , if  $K$  is not a torus knot? How do the rational knot functions depend on the framing  $w(K)$ ?*

Let us finish this section with some vague questions and speculations about further developments.

Our construction is of combinatorial nature and of complexity of degree at most 4 for each fixed  $n$ . This is an advantage, because each invariant can be really calculated. But it is also a disadvantage, because the physical origin of our results stays completely mysterious and there are no evident connections to other fields in mathematics like e.g. representation theory or differential geometry.

**Question 3** *We can consider our 1-cocycle as an integration of a discrete differential form over a discrete loop. For better understanding it would be very important to transform this into real analysis. Is there a connection with differential or even Riemannian geometry of the infinite-dimensional space  $M_n$  for  $n > 1$ ? More precisely, can the class  $[R_n^i]$  be represented by integrating a closed differential real polynomial valued 1-form over loops in  $M_n$  (in the spirit, but quite different, of the Jones polynomial for links in 3-manifolds by Witten's Feynmann integrals of the Chern-Simons functional over some infinite-dimensional space of  $SU(2)$ -connections, see [43])? But notice that the 1-form should strongly depend on the choice of the abstract closure and of the point at infinity for the points in  $M_n$ . If such a 1-form exists then its "stationary phase approximation", with the critical points of*

the integrand corresponding to the Reidemeister moves, should coincide up to normalization with our combinatorial 1-cocycle  $R_n^i$  of integer polynomials.

Notice also that each  $R_n^i$  is constant on each component of the loop space  $\Omega M_n$  but can have different values on different components.

## 4 Proof

Our main results are based on very complicated combinatorics and the interested reader has certainly a hard time to check all the details. We apologize for this. But we believe that there will be conceptually better proofs in the future (compare Question 3).

### 4.1 Generalities and reductions by using singularity theory

We consider the moduli space  $M$  of all string links in  $\mathbb{C} \times \mathbb{R}$  with a fixed projection  $pr : \mathbb{C} \times \mathbb{R} \rightarrow \mathbb{C}$ . A generic arc  $s$  in  $M$  intersects  $\Sigma_{tri}^{(1)}$ ,  $\Sigma_{tan}^{(1)}$  and  $\Sigma_{cusp}^{(1)}$  transversally in a finite number of points and it does not intersect at all strata of higher codimension. To each intersection point with  $\Sigma_{tri}^{(1)}$  and  $\Sigma_{tan}^{(1)}$  we associate a contribution in  $\mathbb{Z}[x, x^{-1}]$ . We sum up with signs (coming from the co-orientation) the contributions over all intersection points in  $s$  and we obtain  $R_1(s)$ .

We use now the strata from  $\Sigma^{(2)}$  to show the invariance of  $R_1(s)$  under all generic homotopies of  $s$  in  $M$  which fix the endpoints of  $s$ . A homotopy is *generic* if it intersects  $\Sigma^{(1)}$  transversally besides for a finite number of points in  $s$  where  $s$  has an ordinary tangency with  $\Sigma^{(1)}$ , it intersects  $\Sigma^{(2)}$  transversally in a finite number of points and it doesn't intersect at all  $\Sigma^{(i)}$  for  $i > 2$ .

We see immediately that  $R_1(s)$  is invariant by passing through a tangency of  $s$  with  $\Sigma^{(1)}$ . Indeed, the two intersection points have identical contributions but they enter with different signs and cancel out. In order to show the invariance under generic homotopies we have to study now normal 2-discs for the strata in  $\Sigma^{(2)} \subset M$ . For each type of stratum in  $\Sigma^{(2)}$  we have to show that  $R_1(m) = 0$  for the boundary  $m$  of the corresponding normal 2-disc in  $M$ . We call  $m$  a *meridian*.  $\Sigma_{quad}^{(2)}$  is by far the hardest case which leads to the tetrahedron equation. We look at the tetrahedron equation from the



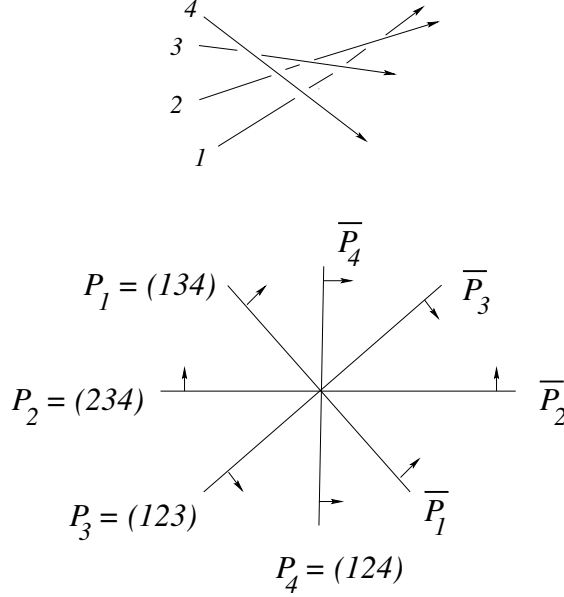


Figure 24: intersection of a normal 2-disc of a positive quadruple crossing with the strata of triple crossings

point of view of singularities of the projection of lines as explained in the Introduction.

Going along the meridian  $m$  of the positive quadruple crossing we see ordinary diagrams of positive 4-braids and exactly eight diagrams with an ordinary positive triple crossing. We show this in Fig. 25. (For simplicity we have drawn the positive triple crossings as triple points, but the branches do never intersect.) However, we have to study  $24 \times 48$  different types of quadruple crossings.

The different local types of triple crossings are shown and numbered in Fig. 26. The sign in the figure indicates the side of the discriminant  $\Sigma^{(1)}$  if the triple crossing is of global type  $r$ . If it is of global type  $l$  then all signs have to be changed to the opposite ones. Triple crossings come together in points of  $\Sigma_{trans-self}^{(2)}$ , but one easily sees that the global type of the triple crossings (i.e. its pointed Gauss diagram without the writhe) is always preserved. We make now a graph  $\Gamma$  for each global type of a triple crossing in the following way: the vertices's correspond to the different local types of triple crossings. We connect two vertices's by an edge if and only if the corresponding strata of triple crossings are adjacent to a stratum of  $\Sigma_{trans-self}^{(2)}$ . One easily sees that

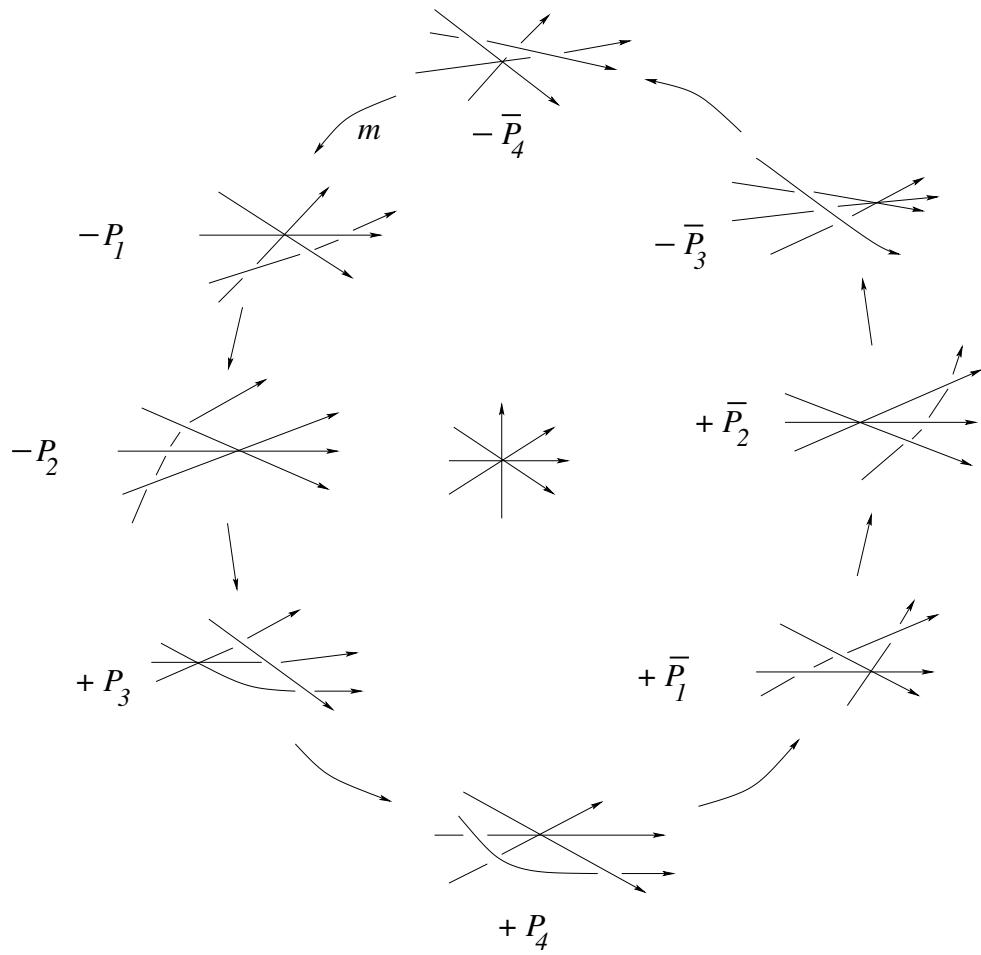


Figure 25: Unfolding of a positive quadruple crossing

the resulting graph is the 1-skeleton of the 3-dimensional cube  $I^3$  (compare Section 4.5). In particular, it is connected. (Studying the normal discs to  $\Sigma_{trans-self}^{(2)}$  in  $M$  one shows that if a 0-cochain is invariant under passing all  $\Sigma_{tan}^{(1)}$  and just one local type of a stratum  $\Sigma_{tri}^{(1)}$  then it is invariant under passing all remaining local types of triple crossings because  $\Gamma$  is connected.) The edges of the graph  $\Gamma = skl_1(I^3)$  correspond to the types of strata in  $\Sigma_{trans-self}^{(2)}$ . The solution of the positive tetrahedron equation tells us what is the contribution to  $R_1$  of a positive triple crossing (i.e. all three involved crossings are positive). The meridians of the strata from  $\Sigma_{trans-self}^{(2)}$  give equations which allow us to determine the contributions of all other types of triple crossings as well as the contributions of self-tangencies. However, a global phenomenon occurs: each loop in  $\Gamma$  could give an additional equation. Evidently, it suffices to consider the loops which are the boundaries of the 2-faces from  $skl_2(I^3)$ . We call all the equations which come from the meridians of  $\Sigma_{trans-self}^{(2)}$  and from the loops in  $\Gamma = skl_1(I^3)$  the *cube equations* (Section 4.5). (Notice that a loop in  $\Gamma$  is more general than a loop in  $M$ . For a loop in  $\Gamma$  we come back to the same local type of a triple crossing but not necessarily to the same whole diagram of  $T$ .)

We need only the following strata from  $\Sigma^{(3)}$  in order to simplify the proof of the invariance of  $R_1$  in generic homotopies which pass through strata from  $\Sigma^{(2)}$ :

- (1) one degenerate quadruple crossing where exactly two branches have an ordinary self-tangency in the quadruple point, denoted by  $\Sigma_{trans-trans-self}^{(3)}$  (see Fig. 27).
- (2) one self-tangency in an ordinary flex with a transverse branch passing through the tangent point, denoted by  $\Sigma_{trans-self-flex}^{(3)}$  (see Fig. 28).
- (3) the transverse intersection of a stratum from  $\Sigma^{(1)}$  with a stratum of  $\Sigma_{trans-self}^{(2)}$

Again, for each fixed global type of a quadruple crossing we form a graph with the local types of quadruple crossings as vertices's and the adjacent strata of  $\Sigma_{trans-trans-self}^{(3)}$  as edges. One easily sees that the resulting graph  $\Gamma$  has exactly 48 vertices's and that it is again connected. Luckily, we don't need to study the unfolding of  $\Sigma_{trans-trans-self}^{(3)}$  in much detail. It is clear that

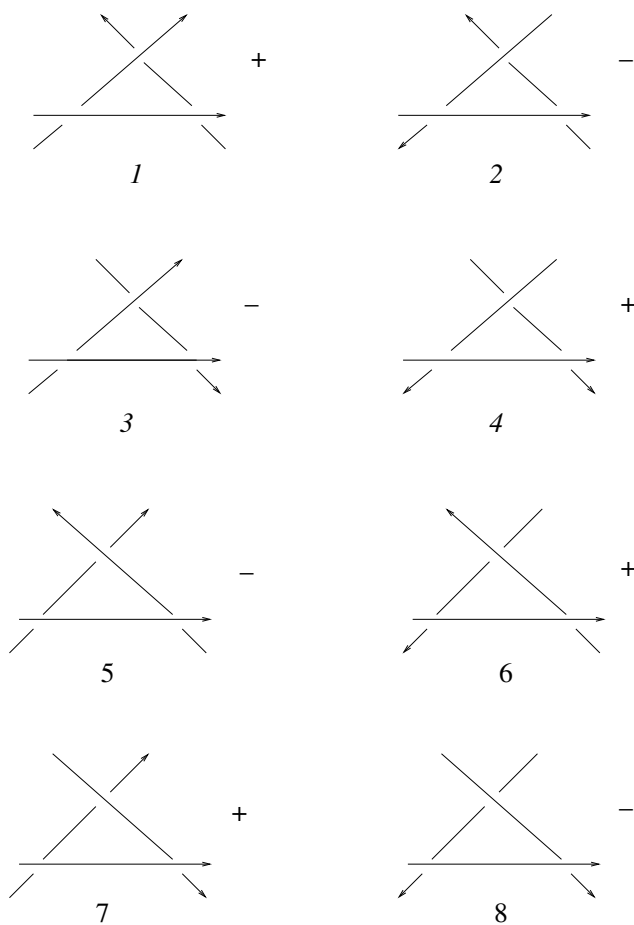


Figure 26: Local types of a triple crossing

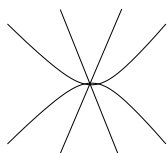


Figure 27: A quadruple crossing with two tangential branches

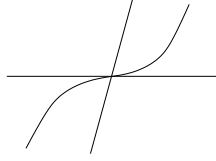


Figure 28: A self-tangency in a flex

each meridional 2-sphere for  $\Sigma_{trans-trans-self}^{(3)}$  intersects  $\Sigma^{(2)}$  transversally in a finite number of points, namely exactly in two strata from  $\Sigma_{quad}^{(2)}$  and in lots of strata from  $\Sigma_{trans-self}^{(2)}$  and from  $\Sigma^{(1)} \cap \Sigma^{(1)}$  and there are no other intersections with strata of codimension 2. If we know now that  $R_1(m) = 0$  for the meridian  $m$  of one of the quadruple crossings, that  $R_1(m) = 0$  for all meridians of  $\Sigma_{trans-self}^{(2)}$  (i.e.  $R_1$  satisfies the cube equations) and for all meridians of  $\Sigma^{(1)} \cap \Sigma^{(1)}$  (i.e.  $R_1$  is invariant under passing simultaneous Reidemeister moves at different places in the diagram) then  $R_1(m) = 0$  for the other quadruple crossing too. It follows that for each of the fixed 24 global types (see Fig. 29, where in each case we have four possibilities for the point at infinity) the 48 tetrahedron equations reduce to a single one, which is called the *positive global tetrahedron equation*. There is no further reduction possible because we are searching for non symmetric solutions and which depend non-trivially from the point at infinity!

In the cube equations there are also two local types of edges, corresponding to the two different local types of a Reidemeister II move with given orientations, compare Fig. 30. We reduce them to a single type of the edge by using the strata from  $\Sigma_{trans-self-flex}^{(3)}$ . The meridional 2-sphere for  $\Sigma_{trans-self-flex}^{(3)}$  intersects  $\Sigma^{(2)}$  transversally in exactly two strata from  $\Sigma_{trans-self}^{(2)}$ , which correspond to the two different types of the edge, and in lots of strata from  $\Sigma_{self-flex}^{(2)}$  and from  $\Sigma^{(1)} \cap \Sigma^{(1)}$ . Hence, again the invariance under passing one of the two local types of strata from  $\Sigma_{trans-self}^{(2)}$  together with the invariance under passing all strata from  $\Sigma_{self-flex}^{(2)}$  and  $\Sigma^{(1)} \cap \Sigma^{(1)}$  guaranties the invariance under passing the other local type of  $\Sigma_{trans-self}^{(2)}$  too.

The unfolding (i.e. the intersection of a normal disc with the stratification of  $M$ ) of e.g. the edge 1 – 5 of  $\Gamma$  is shown in Fig. 31 (compare [19]). The intersection of a meridional 2-sphere for  $\Sigma^{(1)} \cap \Sigma_{trans-self}^{(2)}$  with  $\Sigma^{(2)}$  consists

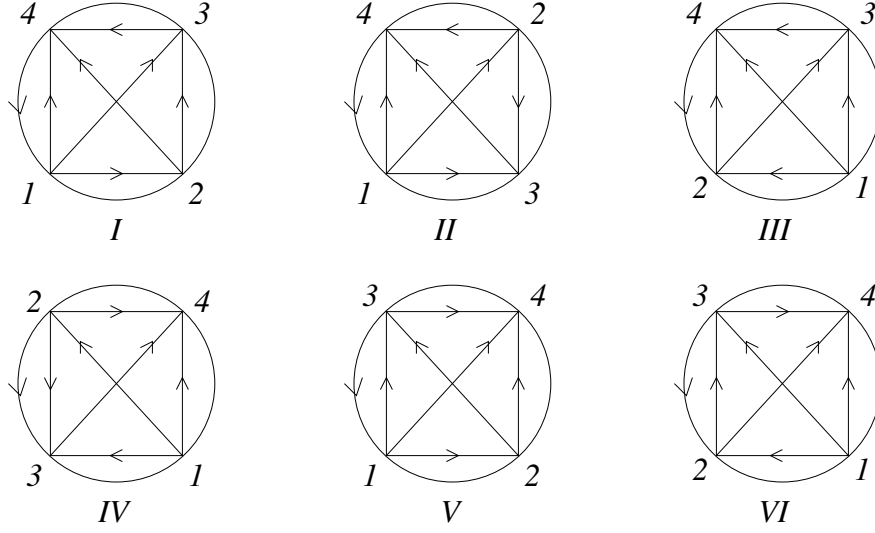


Figure 29: The global types of quadruple crossings

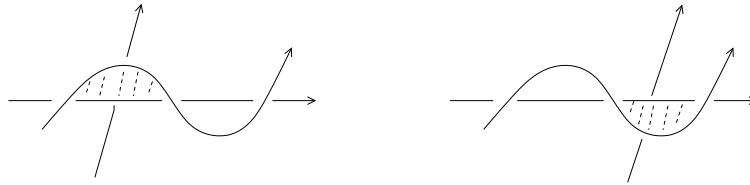


Figure 30: Two different local types of an edge 1-7 in the cube equations and which come together in  $\Sigma_{trans-self-flex}^{(3)}$

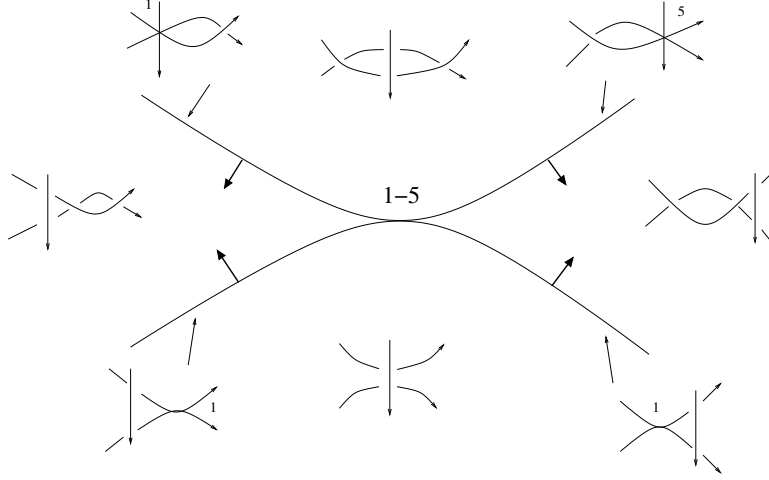


Figure 31: The unfolding of a self-tangency with a transverse branch corresponding to the edge 1 – 5

evidently of the transverse intersections of the stratum  $\Sigma^{(1)}$  with all the strata of codimension 1 in the unfolding of  $\Sigma_{trans-self}^{(2)}$ . It follows again that it is sufficient to prove the invariance under passing  $\Sigma^{(1)} \cap \Sigma^{(1)}$  only for positive triple crossings and only for one of the two local types of self-tangencies with a given orientation.

The remaining part of the paper is now organized as follows: we show the invariance of  $R_1$  under generic homotopies which pass through the strata from Proposition 1 in the following Subsections: 4.2: (3) and (6), 4.3: (4), 4.5: (1), 4.6: (2) and the cube equations, 4.7: (5) besides for  $\Sigma_{trans-cusp, cusp=[ml]=0, [d]=1}^{(2)}$  and the scan property, 4.8: the invariance of  $R_n^i$  for  $n > 1$ .

## 4.2 Reidemeister II moves in a cusp and in a flex

As a warm-up we consider first the less important strata. All weights and contributions were defined in Section 2.1.

Let's start with  $\Sigma_{cusp-deg}^{(2)}$ . A meridian for one type is shown in Fig. 32. There is a single Reidemeister II move  $p$  which could a priori contribute if it has the right global type. It follows easily from the Polyak-Viro formula, see [35], that in this case  $W_2(p) = v_2(K)$ . However, evidently the linking number  $l(d) = 0$  and hence the move does not contribute.

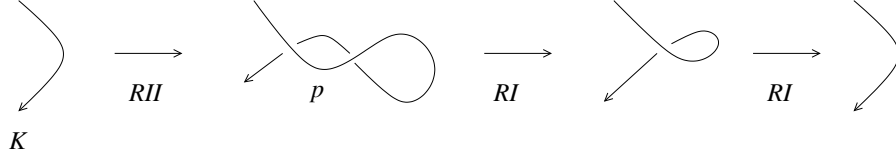


Figure 32: A meridian for a degenerated cusp

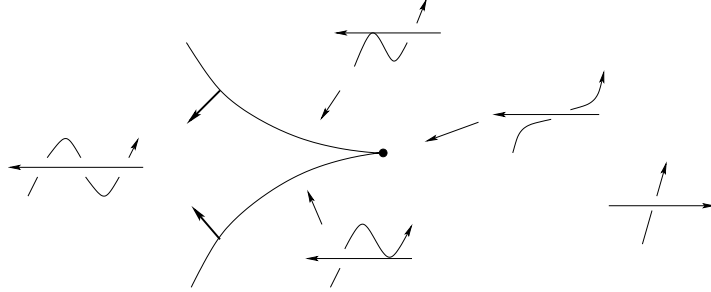


Figure 33: The unfolding for the self-tangency in a flex

The considerations for all other types of  $\Sigma_{cusp-deg}^{(2)}$  are completely analogous.

We show the unfolding and a meridian for one type of  $\Sigma_{self-flex}^{(2)}$  in Fig. 33. There are exactly two Reidemeister II moves,  $p_1$  and  $p_2$ . The third crossings, which are not in the Reidemeister moves, are never f-crossings in the case of long knots. If one is a r-crossing for one of the two moves then the other is a r-crossing for the other move with exactly the same f-crossing. Consequently,  $W_2(p_1) = W_2(p_2)$ . The linking numbers  $l(d)$  are the same for both R II moves but their signs are different and they cancel out. The calculations for all the other types of  $\Sigma_{self-flex}^{(2)}$  are completely analogous.

### 4.3 Simultaneous Reidemeister moves

An example of a meridian of  $\Sigma^{(1)} \cap \Sigma^{(1)}$  is shown in Fig. 34. It is clear that e.g. the f-crossings for  $p_1$  do not change when the meridian  $m$  crosses the discriminant at  $p_2$ .

Let's consider the quadratic weight  $W_2(p)$  (compare Definition 6). Here  $p$  could be the crossing  $d$  or  $ml$ . Evidently  $W_1(hm)$  does not change.

**Lemma 2**  $W_2(p)$  is a relative isotopy invariant for each Reidemeister move of type I, II or III, i.e.  $W_2(p)$  is invariant under any isotopy of the rest of



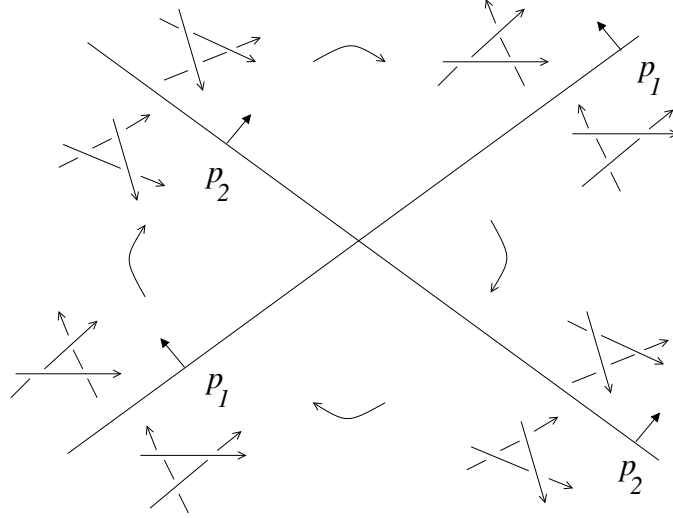


Figure 34: Meridian of two simultaneous Reidemeister III-moves

the diagram outside of  $D_p^2 \times \mathbb{R}$ , where  $D_p^2 \subset \mathbb{C}$  is a small disk around  $p$ .

The lemma implies that  $W_2(p)$  doesn't change under a homotopy of an arc which passes through  $\Sigma^{(1)} \cap \Sigma^{(1)}$ . Evidently, the linking numbers  $l(d)$  and  $l(ml)$  don't change neither and hence the contributions to  $R_1$  cancel out in the meridian  $m$ .

*Proof.* It is obvious that  $W_2(p)$  is invariant under Reidemeister moves of type I and II. The latter comes from the fact that both new crossings are simultaneously crossings of type  $f$  or  $r$  and that they have different writhe. As was explained in Section 4.1 the graph  $\Gamma$  implies now that it is sufficient to prove the invariance of  $W_2(p)$  only under positive Reidemeister moves of type III. There are two global types and for each of them there are three possibilities for the point at infinity. We give names 1, 2, 3 to the crossings and  $a, b, c$  to the points at infinity and we show the six cases in Fig. 35 and Fig. 36. Evidently, we have only to consider the mutual position of the three crossings in the pictures because the contributions with all other crossings do not change. We say that two crossings *intersect* if the corresponding arrows in the Gauss diagram intersect.

$r_a$ : there is only 3 which could be a  $f$ -crossing but it does not contribute with another crossing in the picture to  $W_2(p)$ .

$r_b$ : no  $r$ -crossing at all.

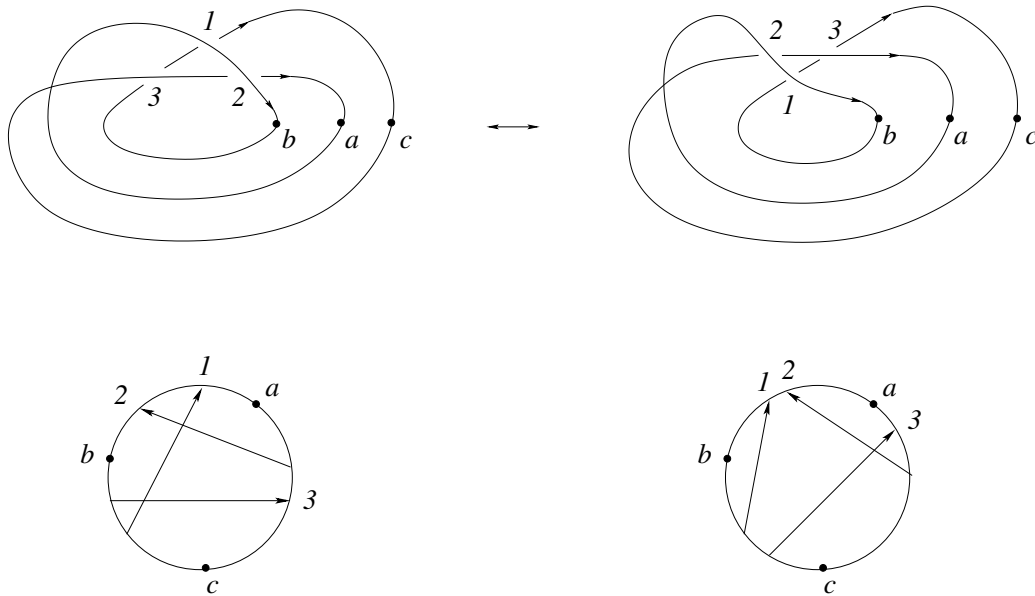


Figure 35:  $RIII$  of type  $r$

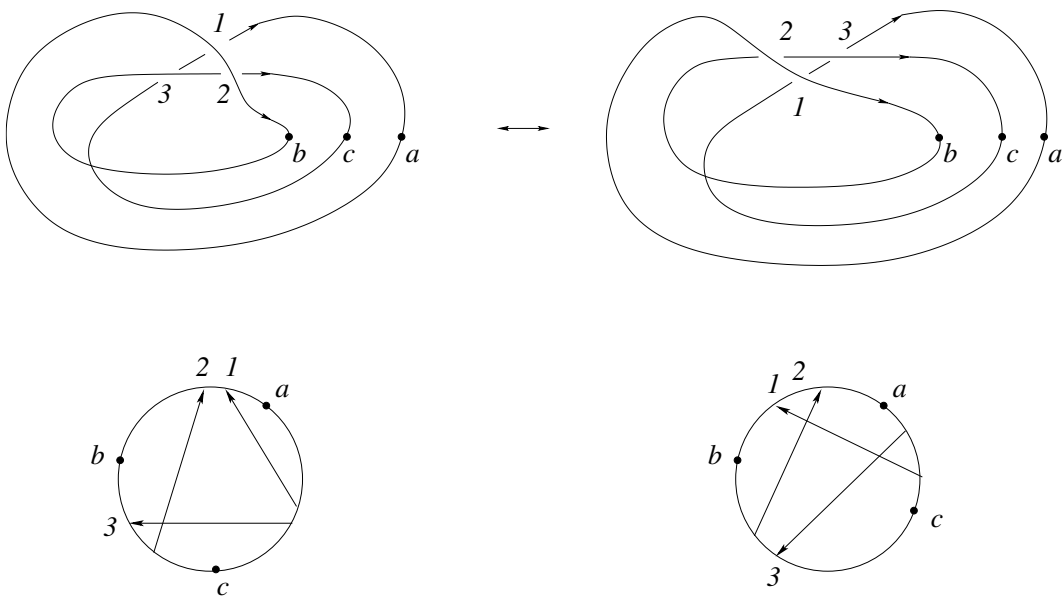


Figure 36:  $RIII$  of type  $l$

$r_c$ : only 2 could be a f-crossing. In that case it contributes on the left side exactly with the r-crossing 1 and on the right side exactly with the r-crossing 3.

$l_a$ : no f-crossing at all.

$l_b$ : 1 and 2 could be f-crossings but non of them contributes with the crossing 3 to  $W_2(p)$ .

$l_c$ : 1 and 3 could be f-crossings. But the foots of 1 and 3 are arbitrary close. Consequently, they can be f-crossings only simultaneously! In that case 3 contributes with 2 on the left side and 1 with 2 on the right side.

Consequently, we have proven that  $W_2(p)$  is invariant.

□

## 4.4 Refined tetrahedron equation for string links

This section contains the heart of this paper.

As explained in Section 4.1 it suffices to consider global positive quadruple crossings with a fixed point at infinity. We naturally identify crossings in an isotopy outside Reidemeister moves of type I and II. The following lemma is of crucial importance.

**Lemma 3** *The f-crossings for  $d$  of the eight adjacent strata of triple crossings (compare Fig. 25) have the following properties:*

- (1) *the f-crossings in  $P_2$  are identical with those in  $\bar{P}_2$*
- (2) *the f-crossings in  $P_1$ ,  $\bar{P}_1$ ,  $P_4$  and  $\bar{P}_4$  are all identical*
- (3) *the f-crossings in  $P_3$  are either identical with those in  $\bar{P}_3$  or there is exactly one new f-crossing in  $\bar{P}_3$  with respect to  $P_3$ . In the latter case the new crossing is always exactly the crossing  $hm = 34$  in  $P_1$  and  $\bar{P}_1$*
- (4) *the new f-crossing in  $\bar{P}_3$  appears if and only if  $P_1$  (and hence also  $\bar{P}_1$ ) is of one of the two global types  $r_a$  or  $l_c$ .*
- (5) *the distinguished crossing  $d$  in  $P_3$  and  $\bar{P}_3$  is always the crossing  $ml$  in  $P_1$  and  $\bar{P}_1$*

*Proof.* We have checked the assertions of the lemma in all twenty four cases (denoted by the global type of the quadruple crossing together with the point at infinity) using Fig. 37-48. These figures are our main instrument. Notice that the crossing  $hm$  in  $P_1$  and  $\bar{P}_1$  is always the crossing 34 and that  $d$  is of type 0 if  $\infty$  is on the right side of it in the figures. The distinguished

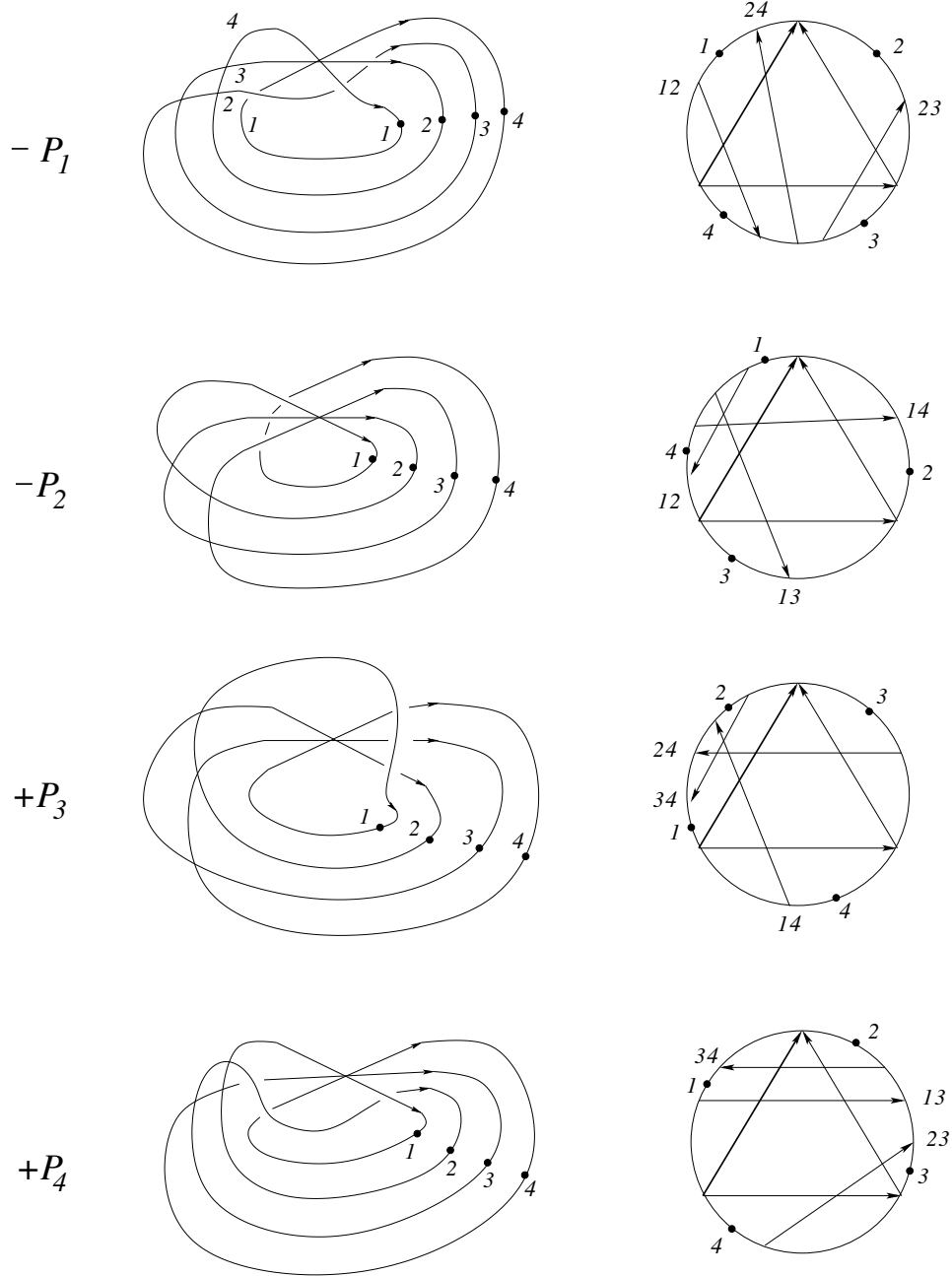


Figure 37: first half of the meridian for global type I

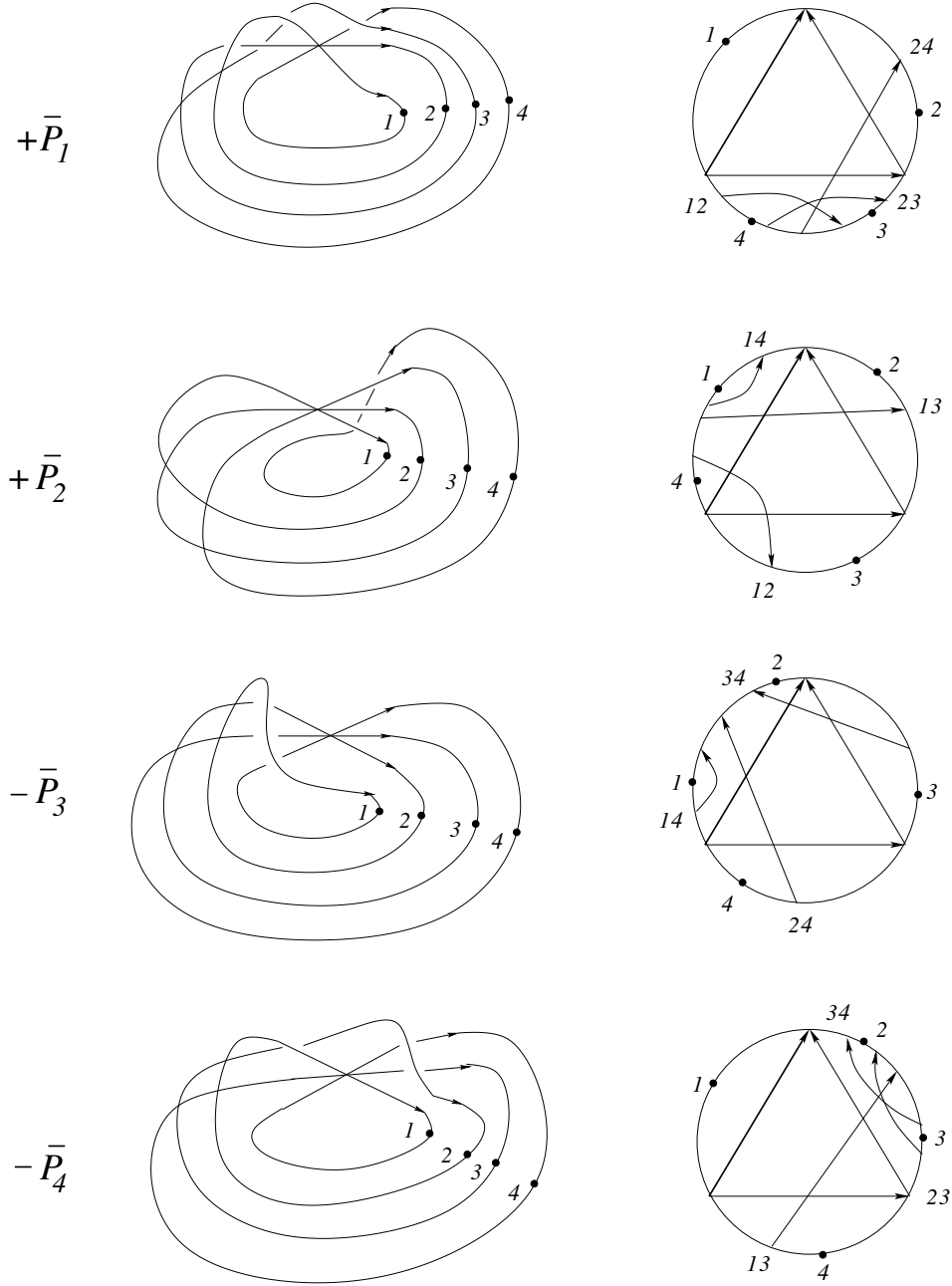


Figure 38: second half of the meridian for global type I

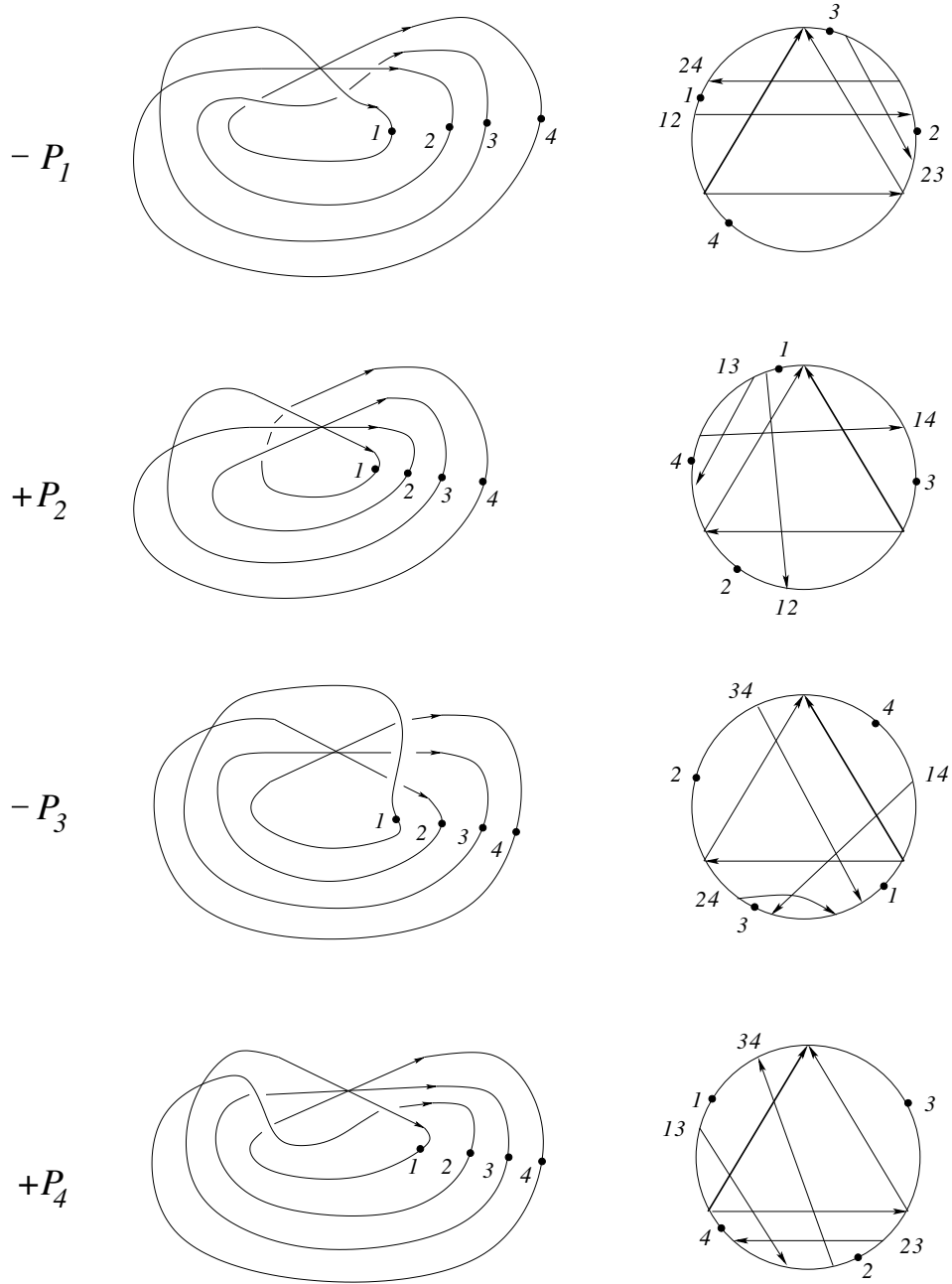


Figure 39: first half of the meridian for global type II

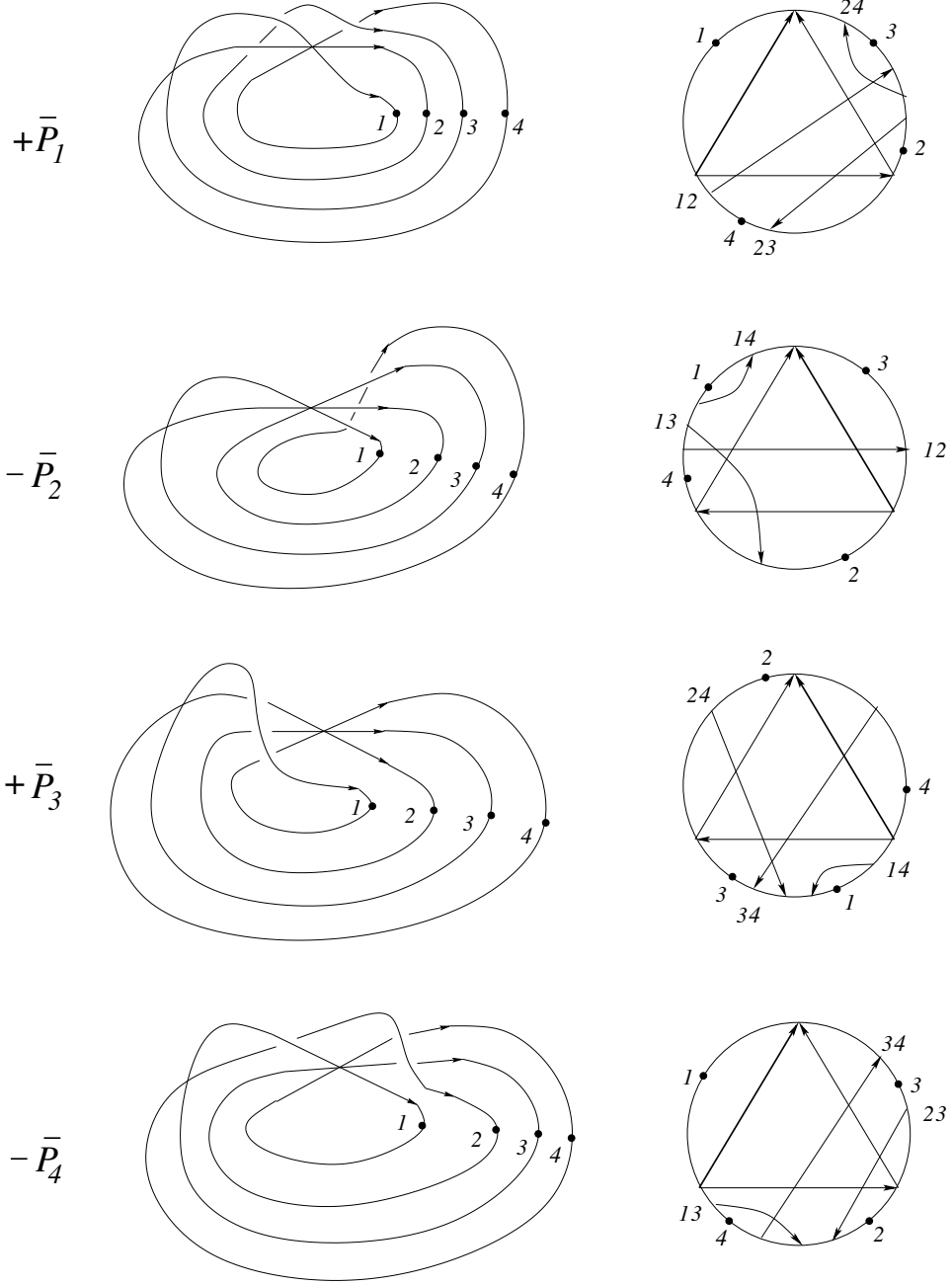


Figure 40: second half of the meridian for global type II

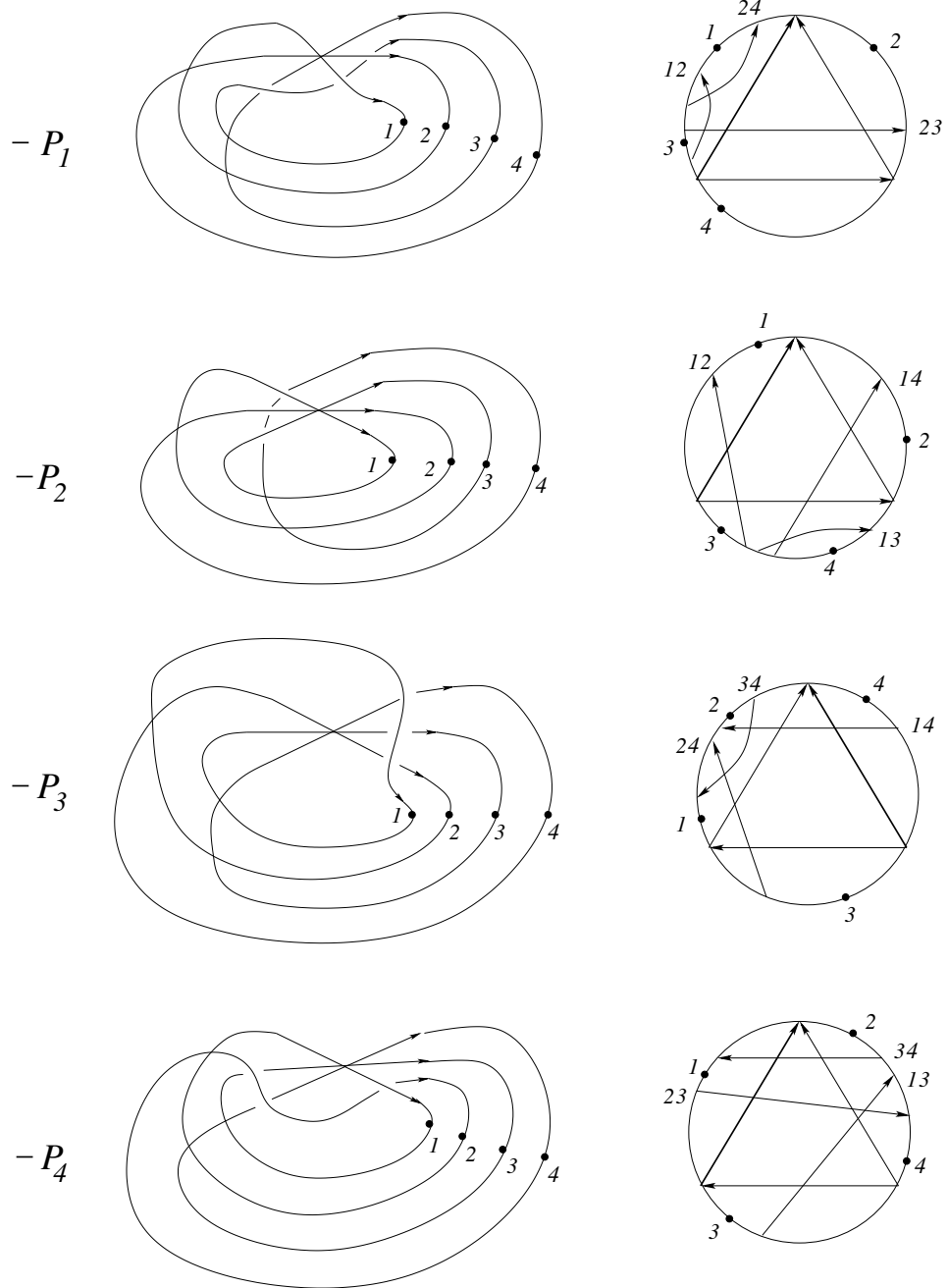


Figure 41: first half of the meridian for global type III



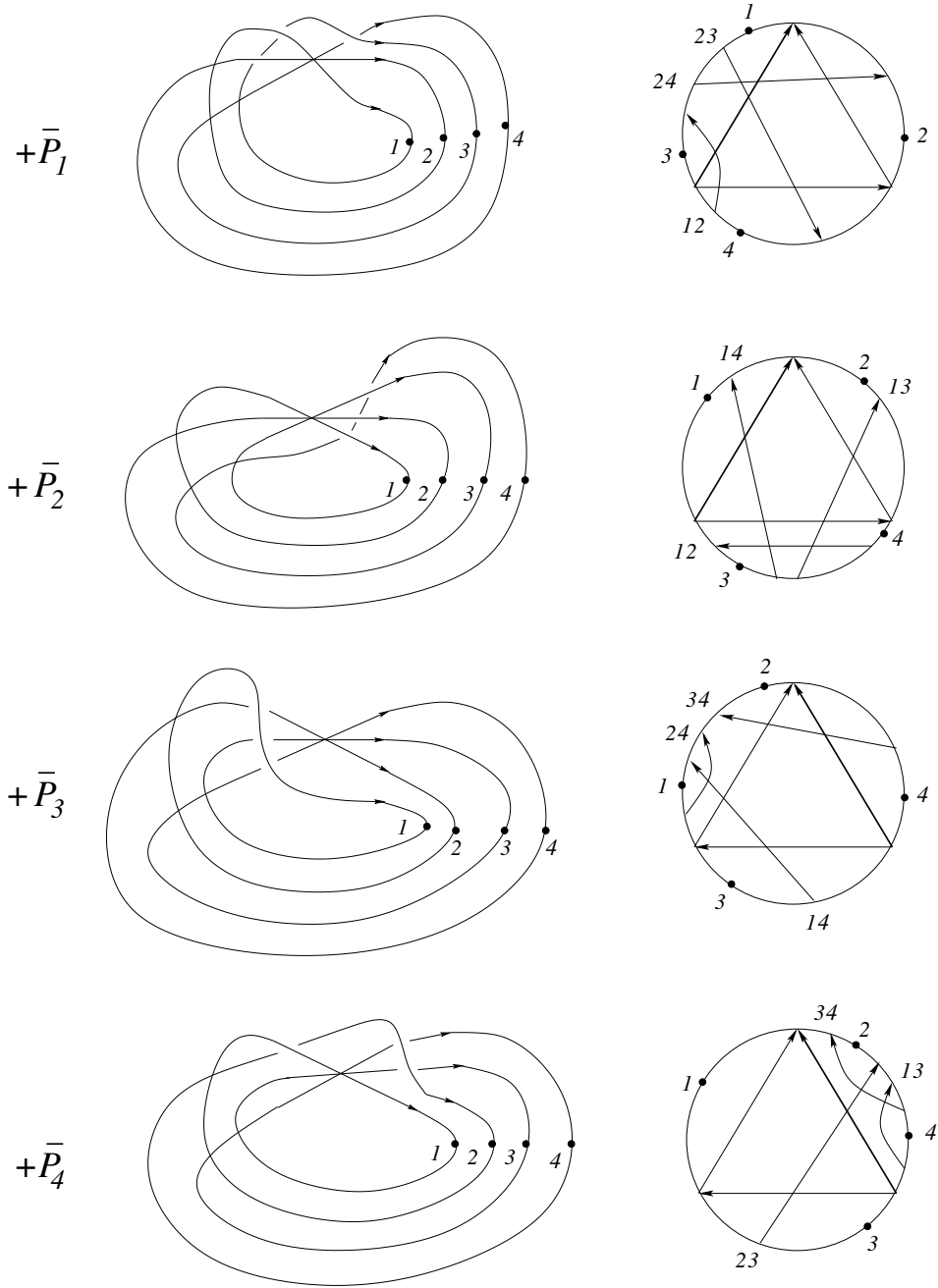


Figure 42: second half of the meridian for global type III

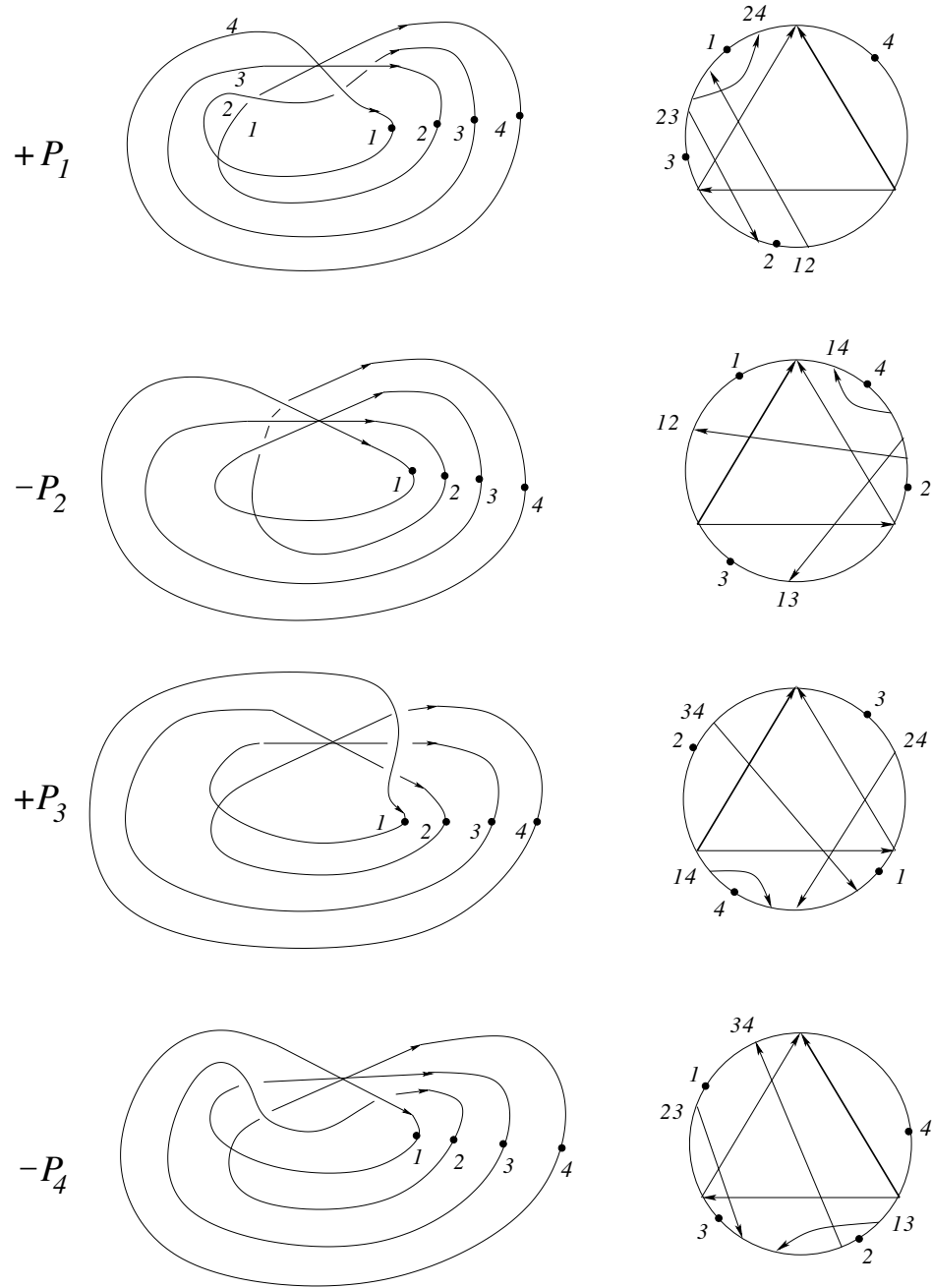


Figure 43: first half of the meridian for global type IV

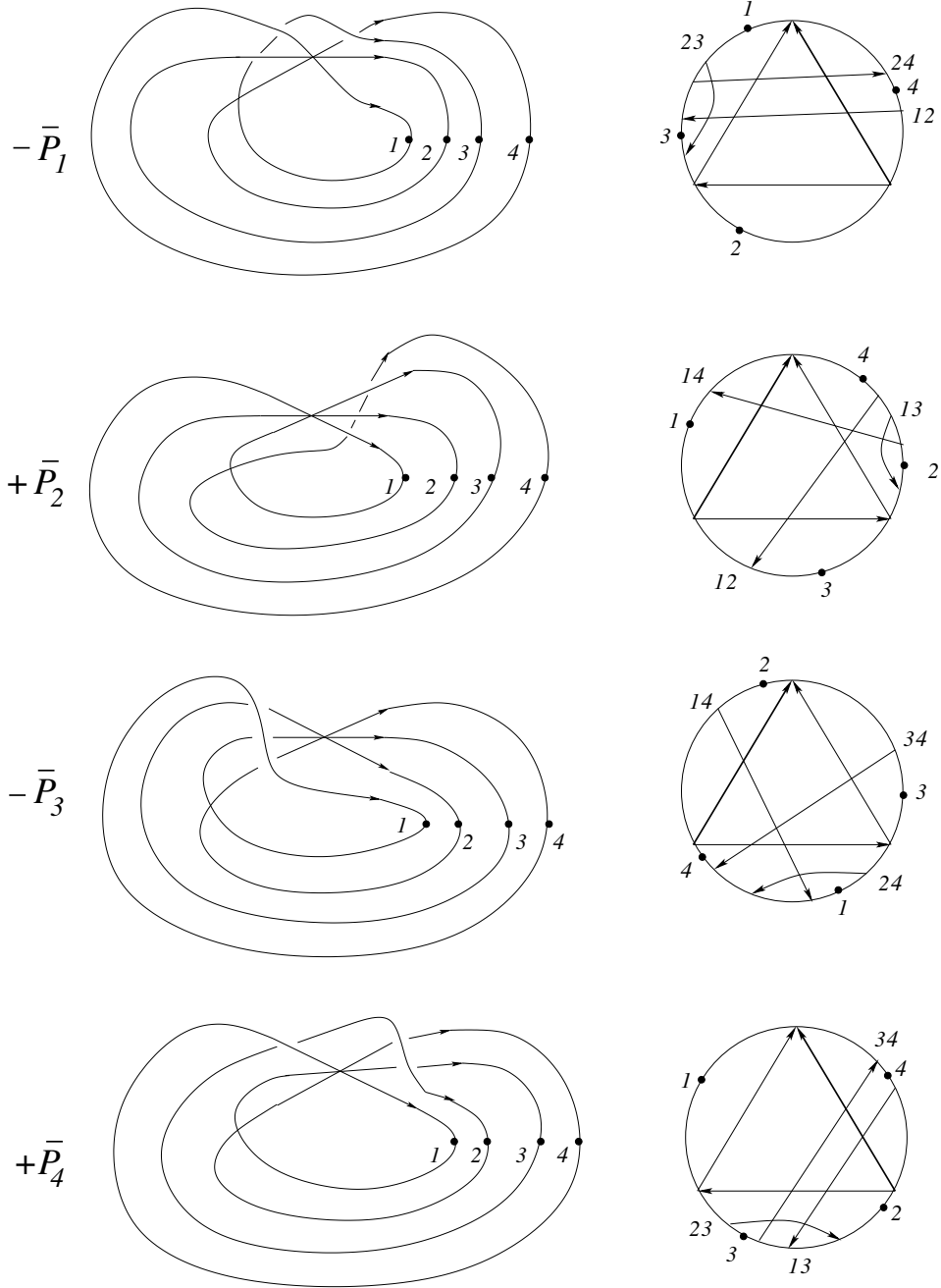


Figure 44: second half of the meridian for global type IV

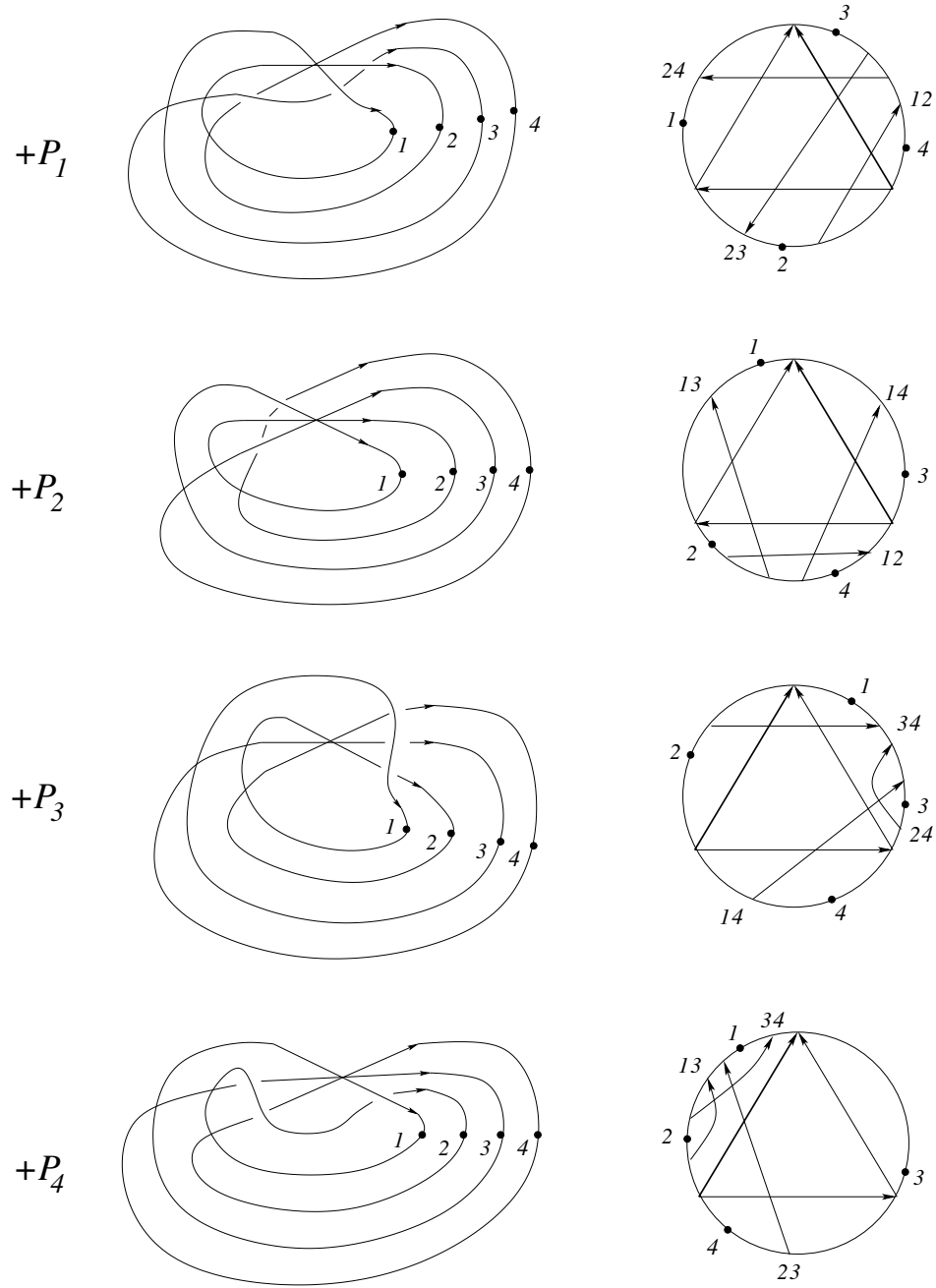


Figure 45: first half of the meridian for global type V

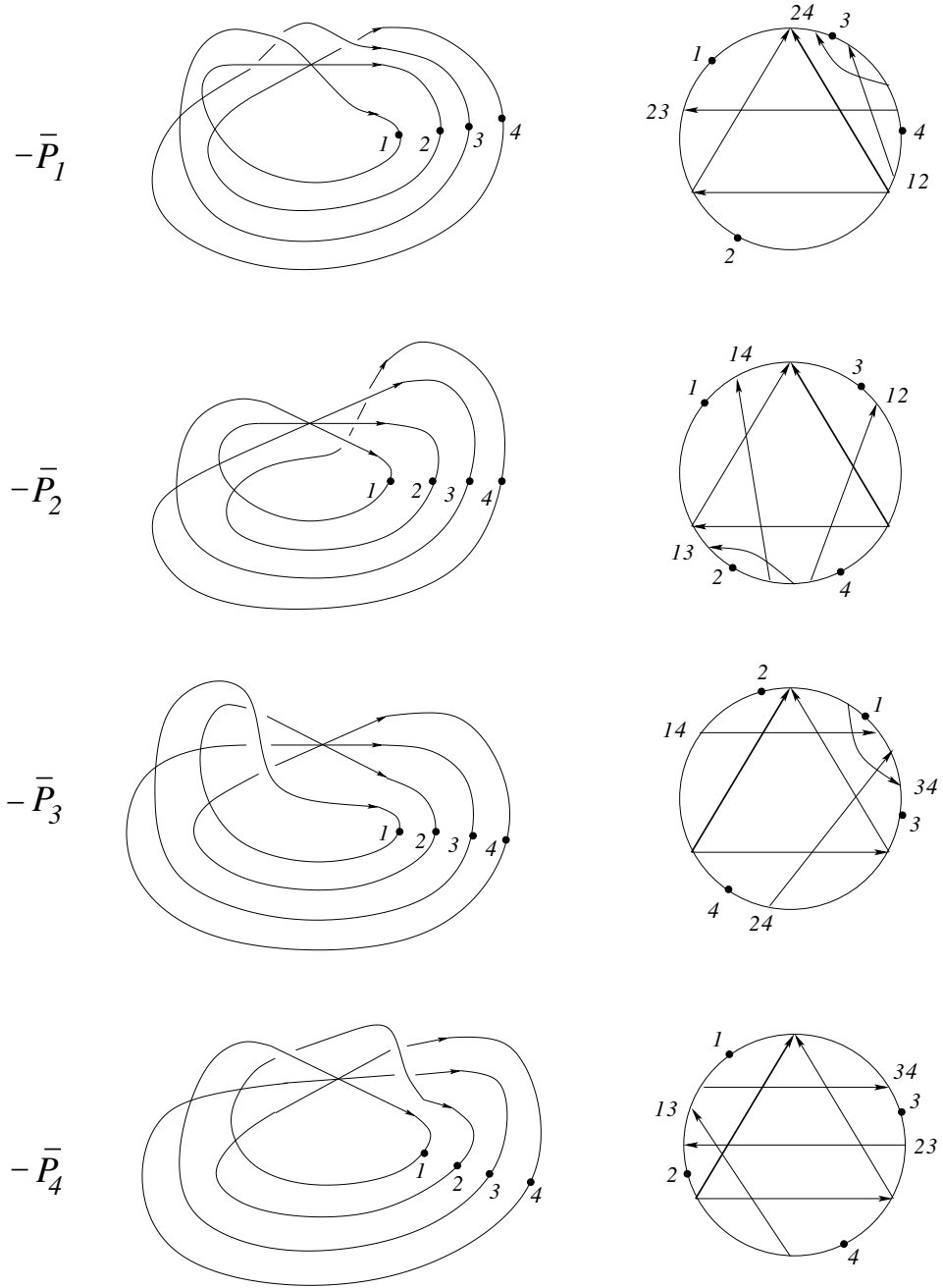


Figure 46: second half of the meridian for global type V

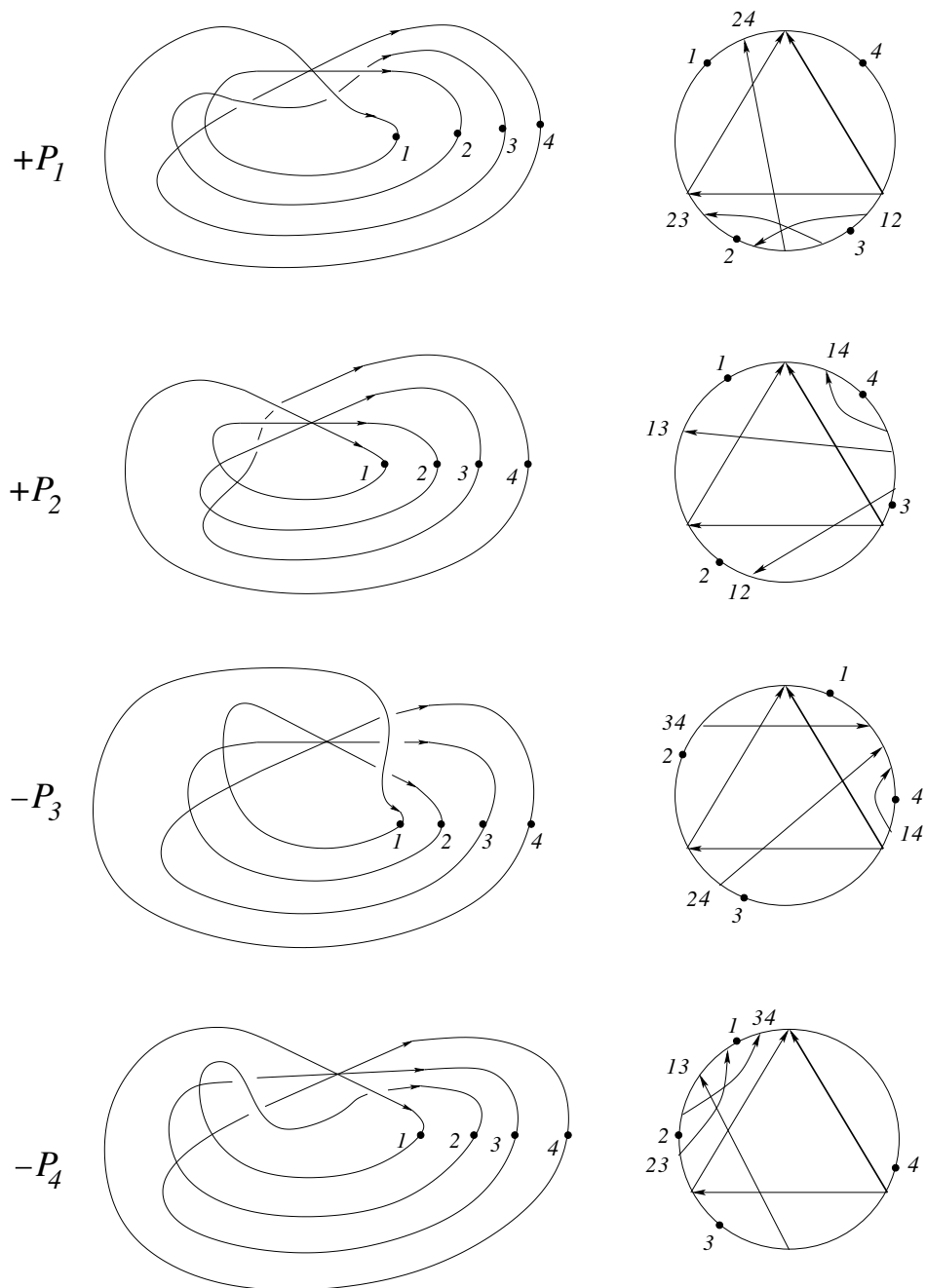


Figure 47: first half of the meridian for global type VI

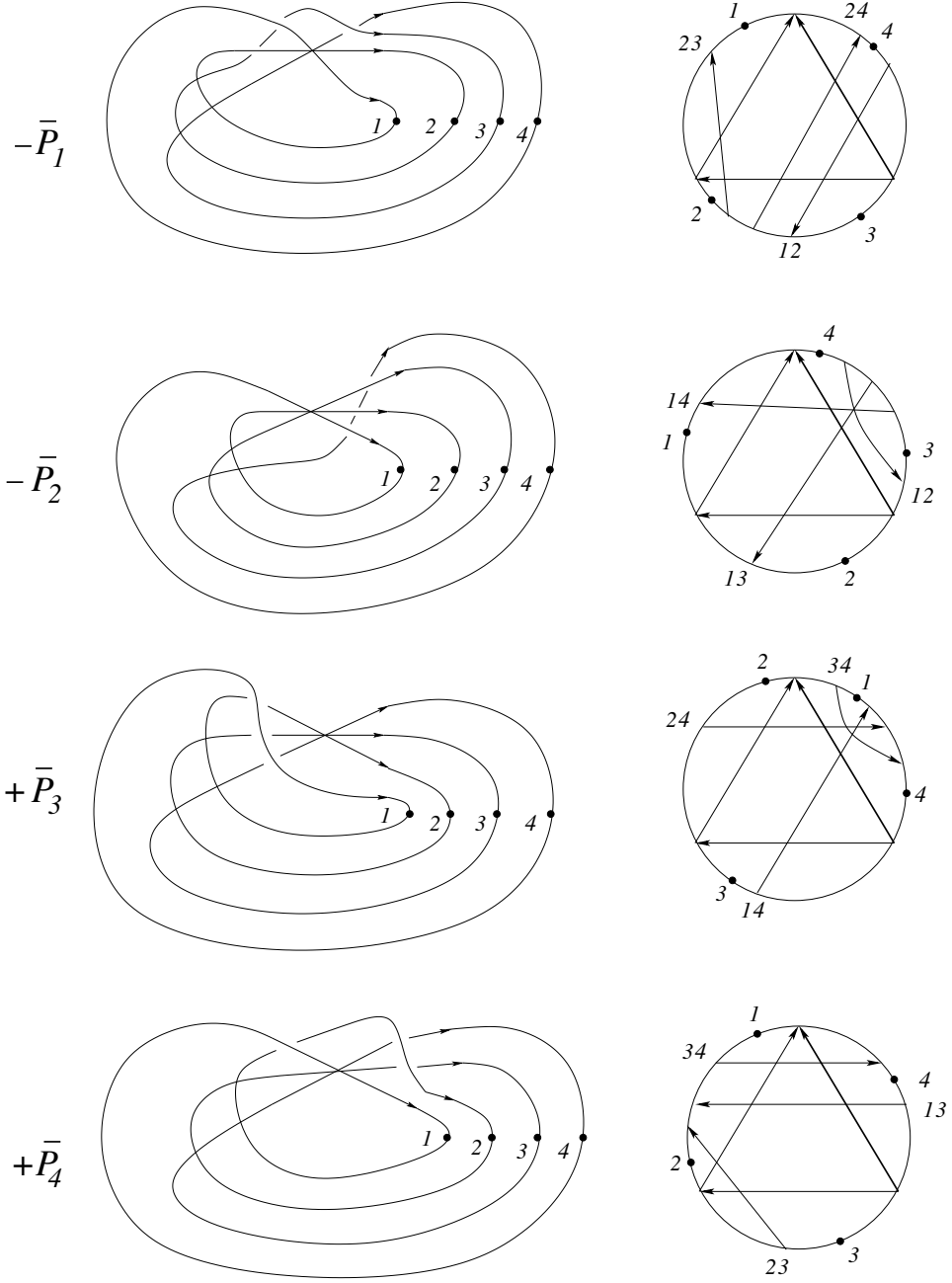


Figure 48: second half of the meridian for global type VI

crossing  $d$  in  $P_3$  is always the crossing 13 which is always the crossing  $ml$  in  $P_1$  too.

We consider just some examples. In particular we show that it is necessary to add the "degenerate" configuration in Fig. 7 and we left the rest of the verification to the reader.

The f-crossings are:

case  $I_1$ . non at all

case  $I_2$ . non at all

case  $I_3$ . In  $P_1, \bar{P}_1$ : 34 (both are the degenerate case). In  $P_4, \bar{P}_4$ : 34 (the third configuration and the first configuration in Fig. 7). In  $P_2, \bar{P}_2$ : 34. In  $P_3$ : non. In  $\bar{P}_3$ : 34.

case  $I_4$ . In  $P_1, \bar{P}_1, P_4, \bar{P}_4$ : 34, 24, 23. In  $P_2, \bar{P}_2$ : non. In  $P_3$ : 23, 24. In  $\bar{P}_3$ : 23, 24, 34.

case  $VI_3$ : In  $P_2$ : 12, 13, 14. In  $\bar{P}_2$ : 12, 13, 14 (12 shows that the fourth configuration in Fig. 7 is necessary too).

case  $VI_1$ : In  $P_3$ : non. In  $\bar{P}_3$ : 34 (shows that the global type  $l_c$  is necessary too).  $\square$

It turns out that Lemma 3 could be used to define already a solution of the global tetrahedron equation. However, this solution is not controllable under moving cusps, compare Section 4.7. This forces us to go one step further and to introduce quadratic weights.

Let us consider now the quadratic weight  $W_2(c)$ . If a f-crossing is one of the six crossings from the positive quadruple crossing than its contribution to  $W_2(c)$  is  $+W_1(f)$ .

*We make the following conventions of notations:*  $W_2(d)$  and  $W_1(hm)$  for  $P_i$  or  $\bar{P}_i$  are shortly denoted by  $W_2(P_i)$  and  $W_1(P_i)$  respectively  $W_2(\bar{P}_i)$  and  $W_1(\bar{P}_i)$ . If a f-crossing is denoted by the names of the two branches  $ij$ , which define the f-crossing, then  $W_1(ij)$  is the sum over all those r-crossings different from the six crossings of the quadruple crossing (i.e. this are the r-crossings which are not drawn in the figures). Consequently,  $W_1(f)$  is the sum of  $W_1(ij)$  and a correction term which comes from the r-crossings amongst the six crossings of the positive quadruple crossing.

In the case that the f-crossings in  $P_3$  and  $\bar{P}_3$  are not the same we get now  $W_2(\bar{P}_3) = W_2(P_3) + W_1(f)$

where  $f$  is the new f-crossing in  $\bar{P}_3$ . But luckily the new f-crossing  $f$  is always just the crossing  $hm = 34$  in  $P_1$  (compare the previous lemma).

The following lemma is a "quadratic refinement" of the previous lemma.



**Lemma 4** (*Weights  $W_2(d)$* )

- (1)  $W_2(P_1) = W_2(\bar{P}_1) = W_2(P_4) = W_2(\bar{P}_4)$
- (2)  $W_2(P_2) = W_2(\bar{P}_2)$
- (3) Let  $P_i$  for some  $i \in \{1, 2\}$  be of one of the global types  $r_a$  or  $l_c$ . Then  $W_1(P_i) = W_1(\bar{P}_i)$ .
- (4) If the  $f$ -crossings in  $P_3$  and  $\bar{P}_3$  coincide then  $W_2(P_3) = W_2(\bar{P}_3)$
- (5) Let  $f$  be the new  $f$ -crossing in  $\bar{P}_3$  with respect to  $P_3$  and let  $f = hm$  be the corresponding crossing in  $P_1$ . Then  $W_2(\bar{P}_3) - W_2(P_3) = W_1(f)$  and  $W_1(f) = W_1(P_1) = W_1(\bar{P}_1)$ .
- (6) Let  $P_i$  for some  $i \in \{3, 4\}$  be of one of the global types  $r_a$  or  $l_c$ . Then either simultaneously  $W_1(P_3) = W_1(\bar{P}_3)$  and  $W_1(P_4) = W_1(\bar{P}_4)$  or simultaneously  $W_1(P_3) = W_1(\bar{P}_3) + 1$  and  $W_1(\bar{P}_4) = W_1(P_4) + 1$ .

*Proof.* The proof is by inspection of all  $f$ -crossings, all  $r$ -crossings and all  $hm$ -crossings in all twenty four cases in the figures. We give it below in details. (Those strata which can never contribute are dropped.) We skip also the  $W_1(ij)$  and  $W_2(ij)$  contributions because they are always determined by  $ij$  and cancel out.

It shows in particular that it is necessary to add the degenerate configurations in Fig. 7 and Fig. 6.

$I_1$ : nothing at all

$I_2$ :  $W_2(P_1) = W_2(\bar{P}_1) = W_2(P_4) = W_2(\bar{P}_4) = 0$ .  $W_2(P_2) = W_2(\bar{P}_2) = 0$ .

$I_3$ :  $W_2(P_1) = W_2(\bar{P}_1) = W_2(P_4) = W_2(\bar{P}_4) = 2$ .  $W_2(P_2) = W_2(\bar{P}_2) = 2$ .  $W_1(P_1) = W_1(\bar{P}_1) = 2$ .  $W_1(P_2) = W_1(\bar{P}_2) = 2$ .  $W_2(P_3) = 0$  and  $W_2(\bar{P}_3) = W_2(\bar{P}_3, f) = 2$ .

$I_4$ :  $W_2(P_1) = W_2(\bar{P}_1) = W_2(P_4) = W_2(\bar{P}_4) = 4$ .  $W_1(P_1) = W_1(\bar{P}_1) = 1$ .  $W_1(P_3) = W_1(\bar{P}_3) = 1$ .  $W_1(P_4) = W_1(\bar{P}_4) = 2$ .  $W_2(\bar{P}_3) - W_2(P_3) = W_2(\bar{P}_3, f) = 1$ .

$II_1$ :  $W_1(P_2) = W_1(\bar{P}_2) = 0$ .

$II_2$ :  $W_2(P_1) = W_2(\bar{P}_1) = W_2(P_4) = W_2(\bar{P}_4) = 2$ .  $W_1(P_3) = 1$  and  $W_1(\bar{P}_3) = 0$ .  $W_1(P_4) = 1$  and  $W_1(\bar{P}_4) = 2$ .

$II_3$ :  $W_2(P_1) = W_2(\bar{P}_1) = W_2(P_4) = W_2(\bar{P}_4) = 0$ .  $W_2(P_2) = W_2(\bar{P}_2) = 0$ .

$II_4$ :  $W_2(P_1) = W_2(\bar{P}_1) = W_2(P_4) = W_2(\bar{P}_4) = 3$ .  $W_1(P_1) = W_1(\bar{P}_1) = 2$ .  $W_1(P_2) = W_1(\bar{P}_2) = 2$ .  $W_2(\bar{P}_3) - W_2(P_3) = W_2(\bar{P}_3, f) = 2$ .  $W_1(P_4) = W_1(\bar{P}_4) = 1$ .

$$III_1: W_1(P_3) = W_1(\bar{P}_3) = W_1(P_4) = W_1(\bar{P}_4) = 0.$$

$$III_2: W_2(P_1) = W_2(\bar{P}_1) = W_2(P_4) = W_2(\bar{P}_4) = 0. W_2(P_2) = W_2(\bar{P}_2) = 0. W_1(P_3) = W_1(\bar{P}_3) = 0.$$

$$III_3: W_2(P_2) = W_2(\bar{P}_2) = 3. W_1(P_2) = W_1(\bar{P}_2) = 1.$$

$$III_4: W_2(P_1) = W_2(\bar{P}_1) = W_2(P_4) = W_2(\bar{P}_4) = 2. W_1(P_1) = W_1(\bar{P}_1) = 2. W_2(P_2) = W_2(\bar{P}_2) = 2. W_1(P_2) = W_1(\bar{P}_2) = 2. W_2(\bar{P}_3) - W_2(P_3) = W_2(\bar{P}_3, f) = 2.$$

$$IV_1: W_1(P_1) = W_1(\bar{P}_1) = 0. W_2(\bar{P}_3) - W_2(P_3) = W_2(\bar{P}_3, f) = 0. W_1(P_3) = W_1(\bar{P}_3) = 1. W_1(P_4) = W_1(\bar{P}_4) = 0.$$

$$IV_2: W_2(P_2) = W_2(\bar{P}_2) = 3.$$

$$IV_3: W_1(P_1) = W_1(\bar{P}_1) = 1. W_1(P_2) = W_1(\bar{P}_2) = 1. W_2(P_2) = W_2(\bar{P}_2) = 2. W_2(\bar{P}_3) - W_2(P_3) = W_2(\bar{P}_3, f) = 1.$$

$$IV_4: W_2(P_1) = W_2(\bar{P}_1) = W_2(P_4) = W_2(\bar{P}_4) = 0. W_2(P_2) = W_2(\bar{P}_2) = 0. W_1(P_3) = W_1(\bar{P}_3) = 1. W_2(P_3) = W_2(\bar{P}_3) = 1.$$

$$V_1: W_1(P_1) = W_1(\bar{P}_1) = 0. W_1(P_2) = W_1(\bar{P}_2) = 0. W_2(\bar{P}_3) - W_2(P_3) = W_2(\bar{P}_3, f) = 0.$$

$V_2$ : nothing at all

$$V_3: W_2(P_1) = W_2(\bar{P}_1) = W_2(P_4) = W_2(\bar{P}_4) = 0. W_2(P_2) = W_2(\bar{P}_2) = 0. W_2(P_3) = W_2(\bar{P}_3) = 0.$$

$$V_4: W_2(P_1) = W_2(\bar{P}_1) = W_2(P_4) = W_2(\bar{P}_4) = 4. W_2(P_3) = W_2(\bar{P}_3) = 4. W_2(P_4) = W_2(\bar{P}_4) = 4. W_1(P_3) = 3. W_1(\bar{P}_3) = 2. W_1(P_4) = 1. W_1(\bar{P}_4) = 2.$$

$$VI_1: W_1(P_1) = W_1(\bar{P}_1) = 0. W_1(P_2) = W_1(\bar{P}_2) = 0. W_1(P_4) = W_1(\bar{P}_4) = 0. W_2(\bar{P}_3) - W_2(P_3) = W_2(\bar{P}_3, f) = 0.$$

$$VI_2: W_1(P_3) = 1. W_1(\bar{P}_3) = 0. W_1(P_4) = 0. W_1(\bar{P}_4) = 1.$$

$$VI_3: W_2(P_2) = W_2(\bar{P}_2) = 4.$$

$$VI_4: W_2(P_1) = W_2(\bar{P}_1) = W_2(P_4) = W_2(\bar{P}_4) = 0. W_2(P_2) = W_2(\bar{P}_2) = 0. W_2(P_3) = W_2(\bar{P}_3) = 0.$$

□

We take now into account also  $W_2(ml)$ .

**Lemma 5** (*Weights with  $W_2(ml)$* )

*We have to consider only the triple crossings of global type  $r_a$  and  $l_c$ .*

- (1)  $ml = 12$  in  $P_3, P_4, \bar{P}_3, \bar{P}_4$ .  
(2)  $13 = d$  in  $P_3, \bar{P}_3$  and  $13 = ml$  in  $P_1, \bar{P}_1$ .  
(3) The  $f$ -crossings for  $ml$  in  $P_2$  and in  $\bar{P}_2$  are the same.  $W_2(ml)$  in  $P_2$  is always equal to  $W_2(ml)$  in  $\bar{P}_2$ .  $W_1(hm)$  in  $P_2$  is always equal to  $W_1(hm)$  in  $\bar{P}_2$ .  
(4) The  $f$ -crossings for  $ml$  in  $P_1$  and in  $\bar{P}_1$  are the same.  $W_2(ml)$  in  $P_1$  is always equal to  $W_2(ml)$  in  $\bar{P}_1$ .  
(5)  $W_2(P_3) = W_2(ml)$  in  $P_1$ .  
(6) the sum of  $x^{W_2(ml)+W_1(hm)} - x^{W_2(ml)}$  over  $+P_3 - \bar{P}_3 + P_4 - \bar{P}_4$  is 0. (Here it can happen that only  $+P_3 - \bar{P}_3$  or  $+P_4 - \bar{P}_4$  are of the right global type  $r_a$  or  $l_c$ .)

*Proof.* (1) and (2) are evident. By inspection of the  $f$ -crossings and the  $r$ -crossings we have

$I_3$ :  $W_2(ml) = 0$  in  $P_1$  and in  $\bar{P}_1$ .  $W_2(ml) = 0$  in  $P_2$  and in  $\bar{P}_2$ .  $W_1(hm) = 2$  in  $P_2$  and in  $\bar{P}_2$ .

$I_4$ :  $W_2(ml) = 3$  in  $P_1$  and in  $\bar{P}_1$ .  $W_2(P_3) = 3 = W_2(ml)$  in  $P_1$ .  $P_3$ :  $x^{W_2(12)+W_1(23)+1} - x^{W_2(12)}$ ,  $\bar{P}_3$ :  $x^{W_2(12)+W_1(23)+1+W_1(24)+2} - x^{W_2(12)+W_1(24)+2}$ ,  $P_4$ :  $x^{W_2(12)+W_1(23)+1+W_1(24)+2} - x^{W_2(12)+W_1(23)+1}$ ,  $\bar{P}_4$ :  $x^{W_2(12)+W_1(24)+2} - x^{W_2(12)}$ .

$II_1$ :  $W_2(ml) = 1$  in  $P_2$  and in  $\bar{P}_2$ .  $W_1(hm) = 0$  in  $P_2$  and in  $\bar{P}_2$ .

$II_2$ :  $P_3$ :  $x^{W_2(12)+W_1(23)+1} - x^{W_2(12)}$ ,  $\bar{P}_3$ :  $x^{W_2(12)+W_1(23)+1+W_1(24)} - x^{W_2(12)+W_1(24)+1}$ ,  $P_4$ :  $x^{W_2(12)+W_1(23)+1+W_1(24)} - x^{W_2(12)+W_1(23)+1}$ ,  $\bar{P}_4$ :  $x^{W_2(12)+W_1(24)+1} - x^{W_2(12)}$ .

$II_4$ :  $W_2(ml) = 0$  in  $P_2$  and in  $\bar{P}_2$ .  $W_1(hm) = 2$  in  $P_2$  and in  $\bar{P}_2$ .  $P_4$ :  $x^{W_2(12)+W_1(34)+2+W_1(24)+1} - x^{W_2(12)+W_1(34)+2}$ ,  $\bar{P}_4$ :  $x^{W_2(12)+W_1(34)+2+W_1(24)+1} - x^{W_2(12)+W_1(34)+2}$ .

$III_1$ :  $P_3$ :  $x^{W_2(12)+W_1(23)} - x^{W_2(12)}$ ,  $\bar{P}_3$ :  $x^{W_2(12)+W_1(23)+W_1(24)} - x^{W_2(12)+W_1(24)}$ ,  $P_4$ :  $x^{W_2(12)+W_1(23)+W_1(24)} - x^{W_2(12)+W_1(23)}$ ,  $\bar{P}_4$ :  $x^{W_2(12)+W_1(24)} - x^{W_2(12)}$ .

$III_2$ :  $P_3$ :  $x^{W_2(12)+W_1(23)} - x^{W_2(12)}$ ,  $\bar{P}_3$ :  $x^{W_2(12)+W_1(23)} - x^{W_2(12)}$ .

$III_3$ :  $W_2(ml) = 3$  in  $P_2$  and in  $\bar{P}_2$ .  $W_1(hm) = 1$  in  $P_2$  and in  $\bar{P}_2$ .

$III_4$ :  $W_2(ml) = 0$  in  $P_1$  and in  $\bar{P}_1$ .  $W_2(P_3) = 0 = W_2(ml)$  in  $P_1$ .  $W_2(ml) = 0$  in  $P_2$  and in  $\bar{P}_2$ .  $W_1(hm) = 2$  in  $P_2$  and in  $\bar{P}_2$ .

$IV_1$ :  $W_2(ml) = 1$  in  $P_1$  and in  $\bar{P}_1$ .  $W_2(P_3) = 1 = W_2(ml)$  in  $P_1$ .  $P_3$ :  $x^{W_2(12)+W_1(23)+1} - x^{W_2(12)}$ ,  $\bar{P}_3$ :  $x^{W_2(12)+W_1(23)+W_1(24)+1} - x^{W_2(12)+W_1(24)}$ ,  $P_4$ :  $x^{W_2(12)+W_1(23)+W_1(24)+1} - x^{W_2(12)+W_1(23)+1}$ ,  $\bar{P}_4$ :  $x^{W_2(12)+W_1(24)} - x^{W_2(12)}$ .

$IV_3$ :  $W_2(ml) = 0$  in  $P_1$  and in  $\bar{P}_1$ .  $W_2(ml) = 0$  in  $P_2$  and in  $\bar{P}_2$ .  $W_1(hm) = 1$  in  $P_2$  and in  $\bar{P}_2$ .

$IV_4$ :  $P_3$ :  $x^{W_2(12)+W_1(23)} - x^{W_2(12)}$ ,  $\bar{P}_3$ :  $x^{W_2(12)+W_1(23)} - x^{W_2(12)}$ .

$V_1$ :  $W_2(ml) = 0$  in  $P_1$  and in  $\bar{P}_1$ .  $W_2(ml) = 0$  in  $P_2$  and in  $\bar{P}_2$ .  $W_1(hm) = 0$  in  $P_2$  and in  $\bar{P}_2$ .

$V_4$ :  $P_3$ :  $x^{W_2(12)+W_1(23)+3} - x^{W_2(12)}$ ,  $\bar{P}_3$ :  $x^{W_2(12)+W_1(23)+2+W_1(24)+2} - x^{W_2(12)+W_1(24)+2}$ ,  
 $P_4$ :  $x^{W_2(12)+W_1(23)+3+W_1(24)+1} - x^{W_2(12)+W_1(23)+3}$ ,  $\bar{P}_4$ :  $x^{W_2(12)+W_1(24)+2} - x^{W_2(12)}$ .

$VI_1$ :  $W_2(ml) = 0$  in  $P_1$  and in  $\bar{P}_1$ .  $W_2(P_3) = 0 = W_2(ml)$  in  $P_1$ .  
 $W_2(ml) = 0$  in  $P_2$  and in  $\bar{P}_2$ .  $W_1(hm) = 0$  in  $P_2$  and in  $\bar{P}_2$ .  $P_4$ :  $x^{W_2(12)+W_1(34)+W_1(24)} - x^{W_2(12)+W_1(34)}$ ,  $\bar{P}_4$ :  $x^{W_2(12)+W_1(34)+W_1(24)} - x^{W_2(12)+W_1(34)}$ .

$VI_2$ :  $P_3$ :  $x^{W_2(12)+W_1(23)+1} - x^{W_2(12)}$ ,  $\bar{P}_3$ :  $x^{W_2(12)+W_1(23)+1+W_1(24)} - x^{W_2(12)+W_1(24)+1}$ ,  
 $P_4$ :  $x^{W_2(12)+W_1(23)+1+W_1(24)} - x^{W_2(12)+W_1(23)+1}$ ,  $\bar{P}_4$ :  $x^{W_2(12)+W_1(24)+1} - x^{W_2(12)}$ .

□

We have to incorporate now the linking numbers  $l(d)$  and  $l(ml)$  in the case of positive triple crossings. First we observe that on the positive side of a positive triple crossing the crossings  $hm$  and  $ml$  do not intersect the crossing  $d$  and that exactly one of the crossings  $d$  or  $hm$  intersects the crossing  $ml$  on either side of the triple crossing, compare Fig. 35 and Fig. 36. It follows that  $l(d)$  and  $(l(ml) - w(ml))$  is exactly the sum of the writhe of those crossings which intersect  $d$  respectively  $ml$  (without counting any degenerations) in the Gauss diagram with the triple crossing. (Remember that  $l(d)$  and  $l(ml)$  do not take into account the homological types of the intersecting crossings.) The correction term  $\epsilon(p)w(hm)(w(ml) - w(d)) = 0$  for positive triple crossings and  $\eta(p) = 1$  for the global type  $l_c$  and  $\eta(p) = -1$  for the global type  $r_a$ . We denote the linking number of a crossing  $ij$  for a stratum  $P_k$  or  $\bar{P}_k$  by  $l(ij)(P_k)$  respectively  $l(ij)(\bar{P}_k)$ .

**Lemma 6** (*Linking numbers*)

(1)  $P_1$  and  $P_4$  share the same  $l(14)$  if and only if they have the same global type  $r$  or  $l$  (this happens exactly for the global types  $I, II, IV, VI$  of the quadruple crossing)

(2)  $\bar{P}_1$  and  $\bar{P}_4$  share the same  $l(14)$  if and only if they have the same global type  $r$  or  $l$

(3)  $P_1$  and  $\bar{P}_4$  share the same  $l(14)$  if and only if they have different global types

(4)  $l(14)(P_1) = l(14)(\bar{P}_1) + 2$  for the global types  $I, II$

- (5)  $l(14)(P_1) = l(14)(\bar{P}_1) - 2$  for the global types IV, VI
- (6)  $l(14)(P_1) = l(14)(P_4) - 2$  for the global type III
- (7)  $l(14)(P_1) = l(14)(P_4) + 2$  for the global type V
- (8)  $12 = ml$  exactly for the strata  $P_3, \bar{P}_3, P_4, \bar{P}_4$  and they share always the same  $l(ml)$
- (9)  $23 = ml$  exactly for the strata  $P_2, \bar{P}_2$  and they share always the same  $l(ml)$
- (10)  $24 = d$  exactly for the strata  $P_2, \bar{P}_2$  and they share always the same  $l(d)$
- (11)  $13 = d$  exactly for the strata  $P_3, \bar{P}_3$  and they share always the same  $l(d)$ .  $13 = ml$  exactly for the strata  $P_1, \bar{P}_1$ :  $l(ml = 13)(P_1) = l(ml = 13)(\bar{P}_1) + 2 = l(d = 13)(P_3) + 1$  if  $P_3$  is of type  $r$  and  $l(ml = 13)(P_1) = l(ml = 13)(\bar{P}_1) - 2 = l(d = 13)(P_3) - 1$  if  $P_3$  is of type  $l$
- (12)  $34$  is never  $d$  or  $ml$ .

*Proof.*

The inspection of Fig. 37-48 proves all assertions immediately.

□

Let  $\gamma$  be an oriented generic arc in  $M$  which intersects  $\Sigma^{(1)}$  only in positive triple crossings. The restriction in Definition 12 to only positive triple crossings leads to the following definition:

**Definition 16** *The evaluation of the 1-cochain  $R_1$  on  $\gamma$  is defined by*

$$\begin{aligned}
R_1(s) = & \sum_{p \in \Sigma_{tri}^{(1)}, [d]=0} sign(p) 4l(d) x^{W_2(d)} \\
& + \sum_{p \in \Sigma_{tri}^{(1)}(l_c)} sign(p) (l(ml) - w(ml))^2 \times \\
& (x^{W_2(ml)+W_1(hm)} - x^{W_2(ml)}) \\
& - \sum_{p \in \Sigma_{tri}^{(1)}(r_a)} sign(p) (l(ml) - w(ml))^2 \times \\
& (x^{W_2(ml)+W_1(hm)} - x^{W_2(ml)})
\end{aligned}$$

**Proposition 4** *Let  $m$  be the meridian for a positive quadruple crossing. Then  $R_1(m) = 0$ .*

*Proof.* The distinguished crossing  $d$  is the same for  $P_1, \bar{P}_1, P_4$  and  $\bar{P}_4$  and which share the same  $W_2(d)$  as follows from (1) in Lemma 4. The contribution of  $P_1$  cancels out with that of  $P_4$  and the contribution of  $\bar{P}_1$  cancels out with that of  $\bar{P}_4$  for the global types  $I, II, IV, VI$  as follows from Lemma 6 parts (1), (2), (4) and (5). The contribution of  $\bar{P}_1$  cancels out with that of  $P_4$  and the contribution of  $P_1$  cancels out with that of  $\bar{P}_4$  for the global types  $III, V$  as follows from Lemma 6 parts (3), (6), and (7). It follows now from (2) in Lemma 4, (3) in Lemma 5 and (9) and (10) in Lemma 6 that the contributions of  $23 = ml$  respectively  $24 = d$  in  $P_2$  and  $\bar{P}_2$  cancel out. The same is true for  $13 = d$  in  $P_3$  and  $\bar{P}_3$  if they share the same f-crossings, as follows from (4) in Lemma 4 and (11) in Lemma 6.

It follows from (4) in Lemma 3 that  $13 = ml$  in  $P_1$  and  $\bar{P}_1$  does not contribute if  $P_3$  and  $\bar{P}_3$  share the same f-crossings, because  $P_1$  and  $\bar{P}_1$  have not the right global type. They contribute only if  $34$  is a f-crossing for  $\bar{P}_3$ . In this case we write shortly  $W_2$  for  $W_2(13 = d) = W_2(13 = ml)$ ,  $W_1$  for  $W_1(34 = hm)$  and  $l$  for  $l(13 = ml)$  but without the crossings involved in the quadruple crossing. We consider the six cases using Lemma 5 and Lemma 6 (compare also Fig. 37-48):

$$I: (l+3)^2(x^{W_2+W_1} - x^{W_2}) - (l+1)^2(x^{W_2+W_1} - x^{W_2}) + 4(l+2)x^{W_2} - 4(l+2)(x^{W_2+W_1} - x^{W_2}) = 0$$

$$II: l^2(x^{W_2+W_1} - x^{W_2}) - (l+2)^2(x^{W_2+W_1} - x^{W_2}) - 4(l+1)x^{W_2} + 4(l+1)(x^{W_2+W_1} - x^{W_2}) = 0$$

$$III: l^2(x^{W_2+W_1} - x^{W_2}) - (l+2)^2(x^{W_2+W_1} - x^{W_2}) - 4(l+1)x^{W_2} + 4(l+1)(x^{W_2+W_1} - x^{W_2}) = 0$$

$$IV: (l+2)^2(x^{W_2+W_1} - x^{W_2}) - l^2(x^{W_2+W_1} - x^{W_2}) + 4(l+1)x^{W_2} - 4(l+1)(x^{W_2+W_1} - x^{W_2}) = 0$$

$$V: (l+2)^2(x^{W_2+W_1} - x^{W_2}) - l^2(x^{W_2+W_1} - x^{W_2}) + 4(l+1)x^{W_2} - 4(l+1)(x^{W_2+W_1} - x^{W_2}) = 0$$

$$VI: (l+1)^2(x^{W_2+W_1} - x^{W_2}) - (l+3)^2(x^{W_2+W_1} - x^{W_2}) - 4(l+2)x^{W_2} + 4(l+2)(x^{W_2+W_1} - x^{W_2}) = 0$$

It follows from (6) in Lemma 4 that we can have only simultaneously  $W_1(P_3) = W_1(\bar{P}_3) + 1$  and  $W_1(\bar{P}_4) = W_1(P_4) + 1$ . It follows now from (6) in Lemma 5 and (8) in Lemma 6 that the contributions of  $12 = ml$  cancel always out together in  $P_3, \bar{P}_3, P_4$  and  $\bar{P}_4$ .

□

**Remark 4** *Let us summarize the combinatorial structure of the tetrahedron equation which leads to  $R_1(m) = 0$  for the meridian  $m$  of a positive quadruple crossing.*

(1) *The strata  $P_1, \bar{P}_1, P_4, \bar{P}_4$  share the same distinguished crossing  $d$  and their contributions with  $d$  cancel out.*

(2) *All contributions of  $P_2$  and  $\bar{P}_2$  cancel out.*

(3) *The strata  $P_3$  and  $\bar{P}_3$  contribute non trivially with  $d$  if and only if  $P_1$  and  $\bar{P}_1$  are of global type  $r_a$  or  $l_c$  and in this case the contributions of  $P_3$  and  $\bar{P}_3$  with  $d$  cancel out with those of  $P_1$  and  $\bar{P}_1$  with  $ml$ . The linking numbers enter here in a non trivial way.*

(4) *The contributions of  $P_3$  and  $\bar{P}_3$  with  $ml$  cancel always out with those from  $P_4$  and  $\bar{P}_4$  with  $ml$  too.*

It follows immediately from this combinatorial structure that we can restrict  $R_1$  to only those crossings  $d$  and  $ml$  with given colors of foots and heads (but of course the same for  $d$  and  $ml$ ).

The lack of symmetry of  $R_1$  is apparent:  $-P_2 + \bar{P}_2$ , where the triple crossing is on the top, does never contribute at all, but  $+P_3 - \bar{P}_3$ , where the triple crossing is on the bottom, can contribute highly non trivially both for  $d$  and for  $ml$ . Its contribution for  $d$  cancels out with the contribution for  $ml$  in  $P_1, \bar{P}_1$  and its contribution with  $ml$  cancels out with the contribution for  $ml$  in  $P_4, \bar{P}_4$ .

**Remark 5** *It seems that the coefficients of  $R_1$  can be generalized to 2-variable polynomials by considering in addition a second type of  $f$ -crossings, called  $h$ -crossings, together with a new variable  $y$ : the head of the  $h$ -crossing of type 1 is in the arc from the foot of the crossing  $c$  to the point at infinity. In order to define the  $r$ -crossings of the  $h$ -crossings we use the second formula of Polyak-Viro for  $v_2(K)$  (compare Fig. 10). Now, also the crossing  $hm$  contributes exactly for the global types  $r_b$  and  $l_a$ . The solution of the tetrahedron equation is still non symmetric because only the global type  $r_c$  does never contribute. The new 1-cocycle doesn't have any longer a scan property. Its specialization for  $y = 1$  coincides with  $R_1$ . But the verifications for the tetrahedron equation and the cube equations become so complicated that we will perhaps come back to them only in a separate paper.*

There are of course also "dual" solutions  $R_1$  by using symmetries as taking mirror images, the orientation change and the rotation by  $\pi$  around the imaginary axes  $i\mathbb{R} \times 0 \subset \mathbb{C} \times \mathbb{R}$  for the definition of the weights  $W_1$  and  $W_2$ . But the linking numbers  $l$  are always defined in the same way.

There is at least one other situation where our approach should work well too.

**Remark 6** *The case of knots which are closed braids in the solid torus is also interesting (i.e. conjugacy classes of braids). We consider the natural projection into the annulus. There are two canonical loops in the moduli space which are induced by the natural rotations of the solid torus. Hatcher has proven that the rational homology classes of these loops are linearly dependent if and only if the braid is periodic. It is well known that the braid is periodic if and only if its closure is a torus knot, see [6]. There is no longer a point at infinity but we have now the homological type of a crossing  $c$  defined by the homology class of  $D_c^+$  in the solid torus, compare Definition 3 and also [15]. The linking numbers  $l$  are defined in exactly the same way as previously, namely as sums of the writhe of crossings. We can still use the same combinatorial structure of the tetrahedron equation as described in Remark 4 because positive quadruple crossings can be represented by braids. The result are polynomial valued 1-cocycles  $R_1$  for closed  $n$ -braids. (There are no moving cusps and no local knots here and we do not need colorings.) We will perhaps come back to this in another paper.*

## 4.5 Cube equations

We have to consider now all other local types of triple crossings together with the self-tangencies. We know already the contributions for the local type 1, the positive triple crossings, from our solution of the tetrahedron equation and we will determine the contributions of all other local types from the cube equations. The local types of triple crossings were shown in Fig. 26. The diagrams which correspond to the edges of the graph  $\Gamma$  (compare Section 4.1) are shown in Fig. 49. The projection of a triple crossing  $p$  into the plan separates the plan near  $p$  into three couples of a region and its dual. The regions correspond exactly to the three edges adjacent to the vertex corresponding to the local type of the triple crossing (we can forget about the three dual regions because of  $\Sigma_{trans-self-flex}^{(3)}$  as was explained in Section 4.1). We show the corresponding graph  $\Gamma$  now in Fig. 50. The unfolding of e.g. the edge 1 – 5 was shown in Fig. 31 (compare [19]).

**Observation 1** *The diagrams corresponding to the two vertices's of an edge differ just by the two crossings of the self-tangency which replace each other*



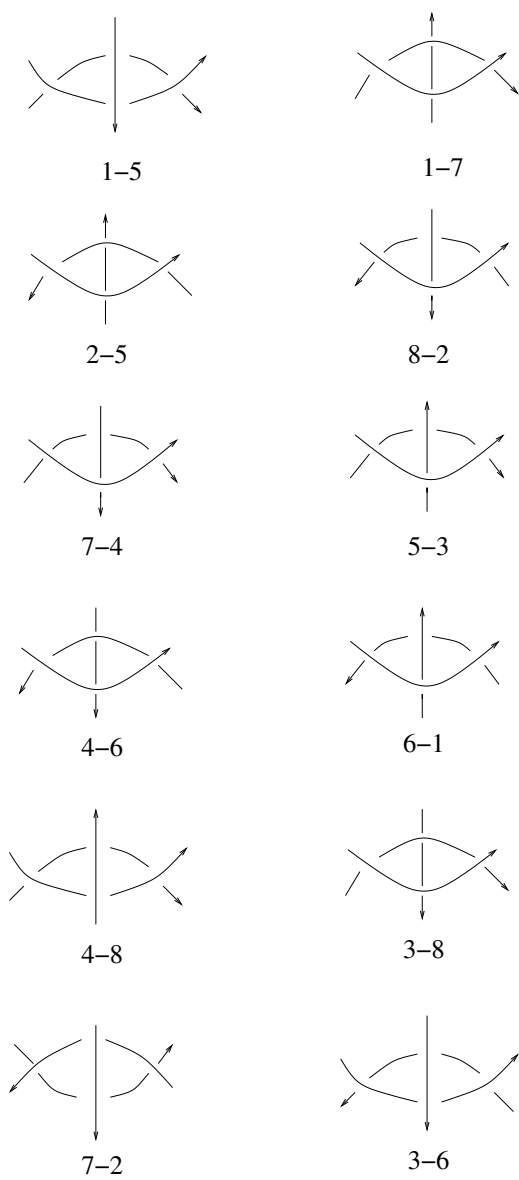


Figure 49: The twelve edges of the graph  $\Gamma$



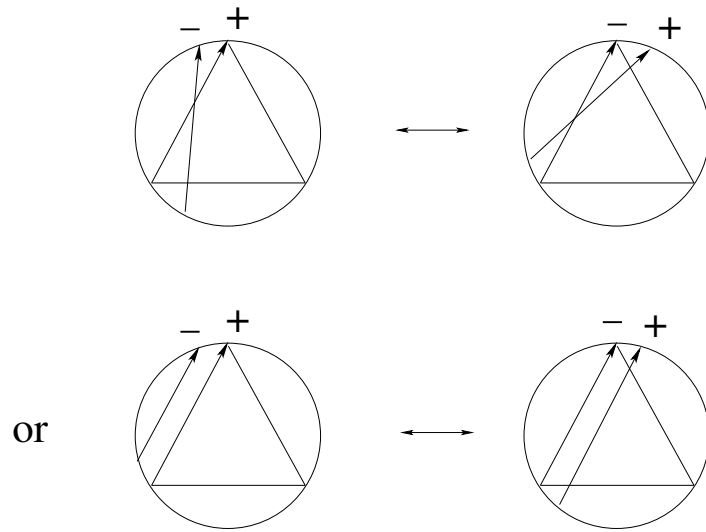


Figure 51: Two crossings replace each other for an edge of  $\Gamma$

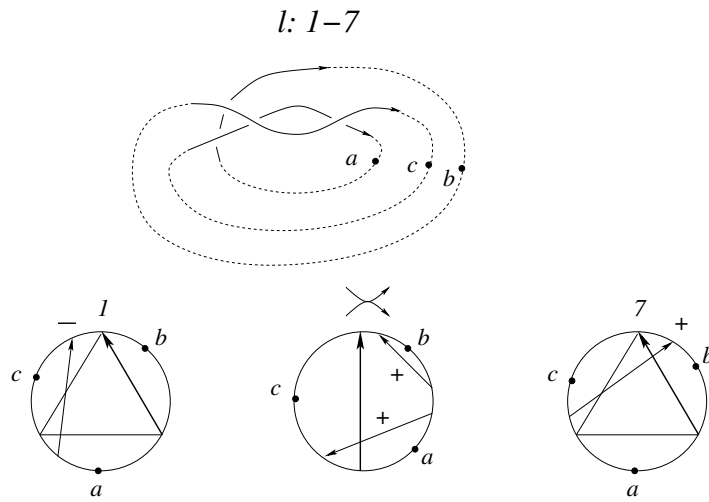


Figure 52:  $l1 - 7$

$l:1-5$

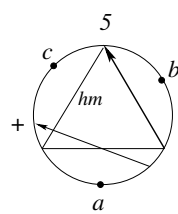
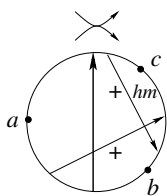
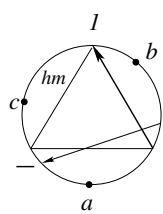
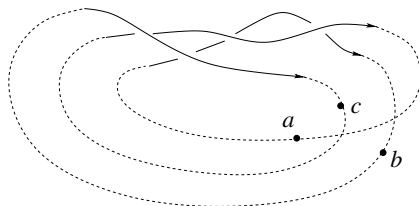


Figure 53:  $l1 - 5$

$l:1-6$

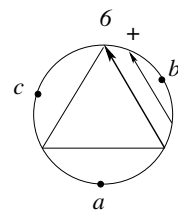
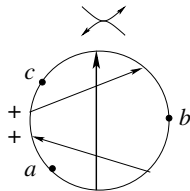
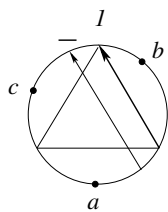
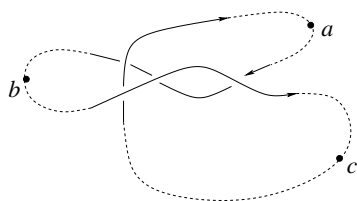


Figure 54:  $l1 - 6$

$l: 7-2$

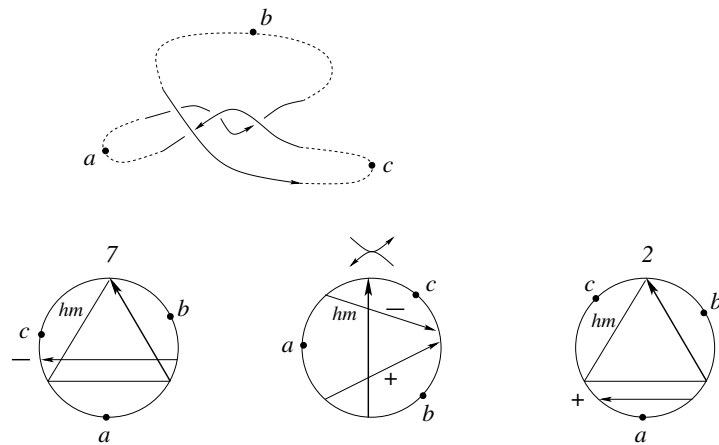


Figure 55:  $l7 - 2$

$l: 7-4$

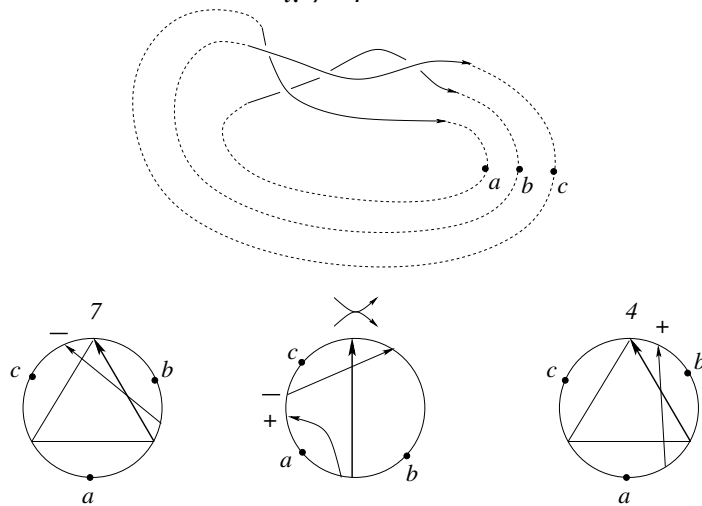


Figure 56:  $l7 - 4$

$r: 1-7$

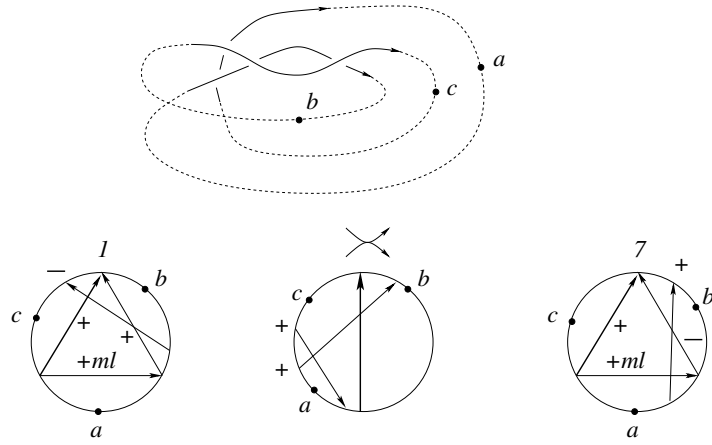


Figure 57:  $r1 - 7$

$r: 1-5$

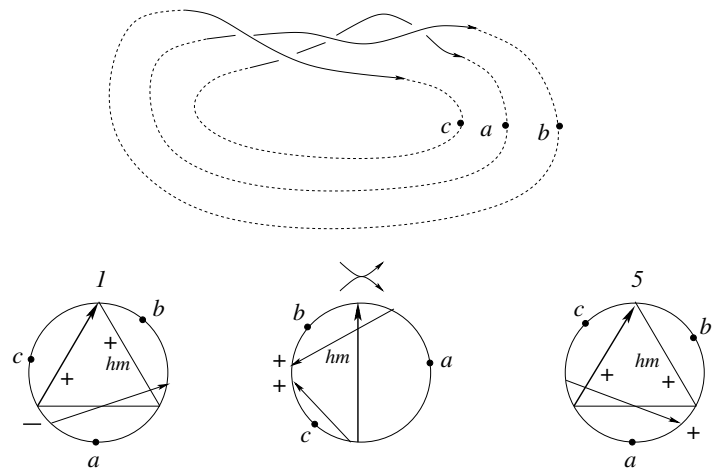


Figure 58:  $r1 - 5$

$r: 1-6$

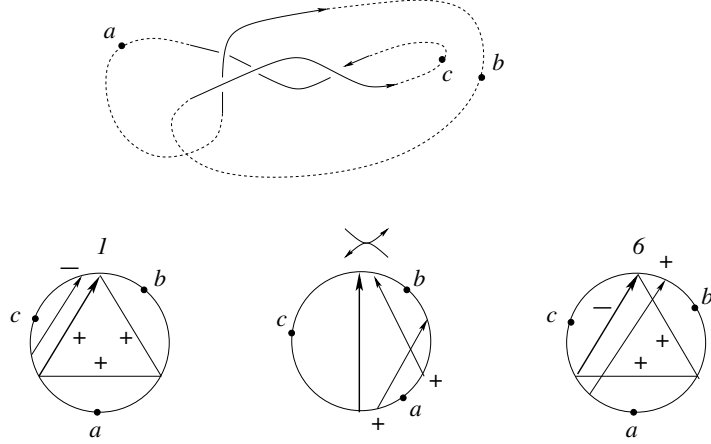


Figure 59:  $r1 - 6$

self-tangency.

**Proposition 5** *Let  $m$  be a meridian of  $\Sigma_{trans-self}^{(2)}$  or a loop in  $\Gamma$ . Then  $R_1(m) = 0$  for the contributions given in Definition 12.*

*Proof.* First of all we observe that the two vertices of an edge (i.e. triple crossings) share the same f-crossings with respect to the crossing  $d$ . The f-crossings could only change if the foot of a f-crossing slides over the head of the crossing  $d$ . But this is not the case as it was shown in Fig. 51. Indeed, the foot of the crossing which changes in the triangle can not coincide with the head of  $d$  because the latter coincides always with the head of another crossing. The f-crossings of the crossings  $ml$  differ just by a crossing  $hm$  and this happens exactly when  $hm$  is a crossing of the self-tangency. The two triple crossings in an edge have always different signs as well as the two self-tangencies.

In the following it suffices of course to consider only the four crossings involved in an edge because the position of the triple crossings and the self-tangencies with respect to all other crossings do not change.

One easily sees that  $\epsilon(p)w(hm)(w(ml) - w(d)) = 0$  in all cases besides for some local types of global type  $r_a$  which will be studied below.

We start with the solutions for triple crossings of global type  $l$ . In the figures we show the Gauss diagrams of the two triple crossings together with

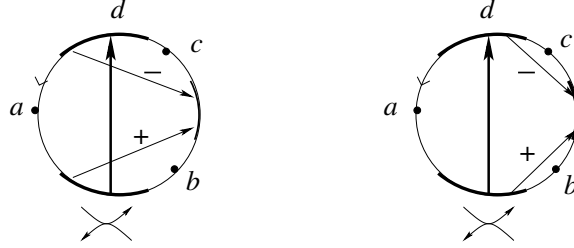


Figure 60: The two self-tangencies for the edge  $l7 - 2$

the points at infinity and the Gauss diagram of just one of the two self-tangencies. The Gauss diagram of the second self-tangency is derived from the first one in the following way: the two arrows slide over the arrow  $d$  but their mutual position does not change. We show an example in Fig. 60. Notice that in the thick part of the circle there aren't any other heads or foots of arrows.

The fourth arrow which is not in the triangle is always almost identical with an arrow of the triangle. Consequently, in the case  $l_c$  it can not be a r-crossing with respect to  $hm$ . In the case  $l_b$  it could be a r-crossing with respect to some f-crossing. But the almost identical arrow in the triangle would be a r-crossing for the same f-crossing too. Their contributions cancel out, because they have different writhe.

It can happen for the type  $l_c$  that the crossing  $hm$  becomes a new f-crossing with respect to  $ml$  for the new triple crossing. This forces us to use the coefficient  $w(hm)$  in Definition 12 for the weights for the new triple crossing.

The type  $l_a$  does never contribute.

The mutual position of the two arrows for a self-tangency does not change. Only the position with respect to the distinguished crossing  $d$  changes. It remains to consider the edges "1-5", "4-8", "2-7" and "3-6" for  $l_c$ , where one of the two self-tangencies has a new f-crossing with respect to the other self-tangency. But one sees immediately from the figures that this new f-crossing is exactly the crossing  $hm$  in the triple crossings. In this case, exactly one of the self-tangencies contributes with the factor  $w(hm)x^{W_2(ml)+w(hm)W_1(hm)}$  and the other contributes with the factor  $w(hm)x^{W_2(ml)}$ .

We consider now some edges in detail.

edge "1-7":  $l_b$ : the contributions of the self-tangencies cancel out together. local types 1 and 7 contribute  $4lx^{W_2(d)}$  and have the same linking number



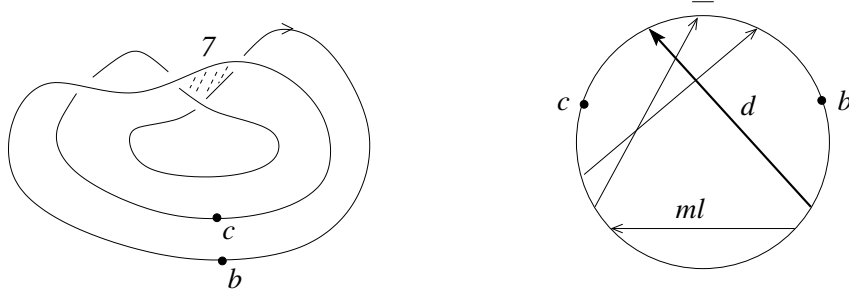


Figure 61: linking numbers for the local type 7 in 11-7

$$l(d) = l.$$

$l_c$ : local type 1 contributes  $-(l-1)^2(x^{W_2(ml)+W_1(hm)} - x^{W_2(ml)})$

local type 7 contributes  $(l-1)^2(-1)(x^{W_2(ml)+W_1(hm)-W_1(hm)} - x^{W_2(ml)+W_1(hm)})$

, compare Fig. 61 for the linking number.

edge "1-5":  $l_b$ : local types 1 and 5 contribute  $4(l-1)x^{W_2(d)}$  and have the same linking number  $l(d)$ , compare Fig. 62 for the linking number.

$l_c$ :  $8(l+1)x^{W_2(ml)+W_1(hm)} + (l-1)^2(x^{W_2(ml)+W_1(hm)} - x^{W_2(ml)}) - (l+2 - (-1))^2(x^{W_2(ml)+W_1(hm)} - x^{W_2(ml)}) - 8(l+1)x^{W_2(ml)} = 0$ , compare Fig. 62 for the linking number.

edge "1-6":  $l_b$ :  $4lx^{W_2(d)} + 4(l+2)x^{W_2(d)} - 4(l+2)x^{W_2(d)} - 4lx^{W_2(d)} = 0$ , compare Fig. 8 for the sign of the local type 6.

$l_c$ :  $l^2x^{W_2(ml)} - l^2x^{W_2(ml)} = 0$ .

edge "7-2":  $l_b$ :  $4lx^{W_2(d)} + 4(l-2)x^{W_2(d)} - 4(l-2)x^{W_2(d)} - 4lx^{W_2(d)} = 0$ .

$l_c$ :  $4lx^{W_2(ml)} + (-1)(l-1)^2(x^{W_2(ml)-W_1(hm)} - x^{W_2(ml)}) - (-1)(l-1)^2(x^{W_2(ml)-W_1(hm)} - x^{W_2(ml)}) - 4lx^{W_2(ml)} = 0$ , compare Fig. 63 for the linking numbers.

edge "7-4":  $l_b$ :  $8(l-1)x^{W_2(d)} - 4(l-2)x^{W_2(d)} + 4(l+2)x^{W_2(d)} - 8(l+1)x^{W_2(d)} = 0$ .

$l_c$ :  $-(-1)(l-1)^2(x^{W_2(ml)-W_1(hm)} - x^{W_2(ml)}) + (-1)(l-1)^2(x^{W_2(ml)-W_1(hm)} - x^{W_2(ml)}) = 0$ , compare Fig. 64 for the linking numbers.

We proceed then in exactly the same way for the global type  $r$ . Exactly the same arguments as previously apply in the case  $r_b$ . In the case  $r_c$  there are no contributions at all. But notice the difference which comes from the fact that we have broken the symmetry: the global type  $r_a$  contributes both with  $ml$  and with  $d$ . Here sometimes the fourth crossing, which is not in the triangle, is a  $r$ -crossing with respect to  $hm$  for exactly one of the two triple crossings. If there could be confusion then we write the local type of the triple crossing in brackets behind the weight (remember that we haven't yet

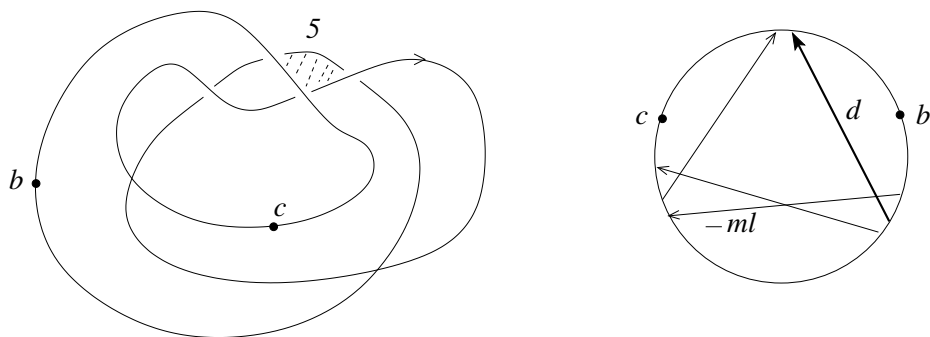


Figure 62: linking numbers for the local type 5 in l1-5

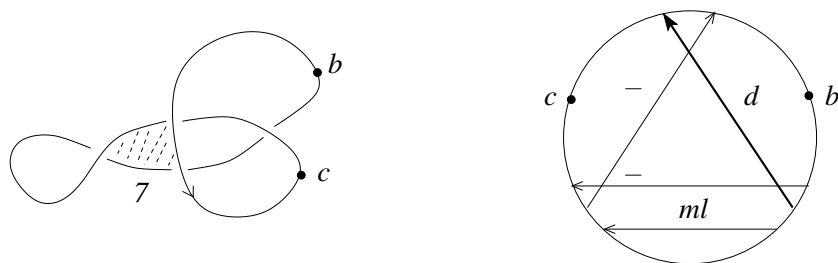


Figure 63: linking numbers for the local type 7 in l7-2

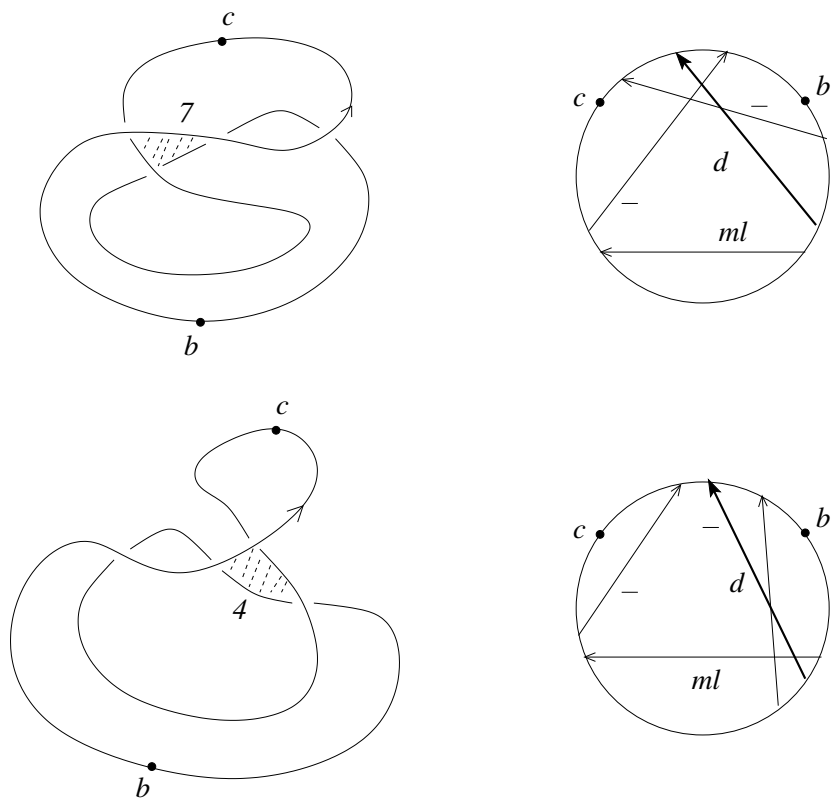


Figure 64: linking numbers for the local types 7 and 4 in l7-4

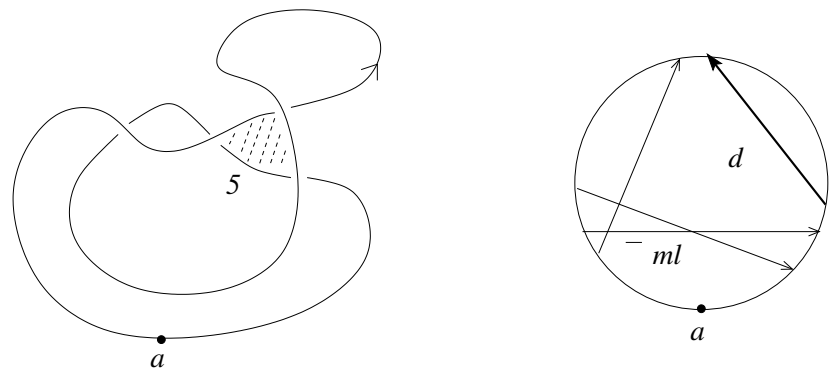


Figure 65: linking numbers for the local type 5 in r1-5

taken into account the correction term for the local type from Definition 12).

We examine now the figures for  $r_a$  (don't forget the degenerate configurations in the definition of the weights):

edge "1-7": type 1 and type 7 share the same  $W_1(hm)$  and  $W_2(d)$ , but  $W_2(ml)(7) = W_2(ml)(1) + W_1(hm)$

edge "1-5":  $W_1(hm)(5) = W_1(hm)(1) + 1$ ,  $W_2(d)(5) = W_2(d)(1) + 1$ , they share the same  $W_2(ml)$

edge "1-6":  $W_1(hm)(6) = W_1(hm)(1) - 1$ ,  $W_2(d)(6) = W_2(d)(1) - 1$ , they share the same  $W_2(ml)$

edge "7-4":  $W_1(hm)(4) = W_1(hm)(7) - 1$ ,  $W_2(d)(4) = W_2(d)(7) + 1$ , they share the same  $W_2(ml)$

edge "7-2":  $W_1(hm)(2) = W_1(hm)(7) + 1$ ,  $W_2(d)(2) = W_2(d)(7) - 1$ , they share the same  $W_2(ml)$

edge "5-2": same  $W_1(hm)$ , but  $W_2(d)(2) = W_2(d)(5) - 2$  and  $W_2(ml)(2) = W_2(ml)(5) + (W_1(hm) - 1)$

edge "5-3":  $W_1(hm)(3) = W_1(hm)(5) - 1$ ,  $W_2(d)(3) = W_2(d)(5) - 1$ , they share the same  $W_2(ml)$

edge "3-8": they share the same  $W_1(hm)$  and  $W_2(d)$ , but  $W_2(ml)(8) = W_2(ml)(3) + W_1(hm)$

edge "3-6":  $W_1(hm)(6) = W_1(hm)(3) - 1$ ,  $W_2(d)(6) = W_2(d)(3) - 1$ , they share the same  $W_2(ml)$

edge "4-8":  $W_1(hm)(8) = W_1(hm)(4) + 1$ ,  $W_2(d)(8) = W_2(d)(4) - 1$ , they share the same  $W_2(ml)$

edge "4-6": same  $W_1(hm)$ , but  $W_2(d)(6) = W_2(d)(4) - 2$  and  $W_2(ml)(6) = W_2(ml)(4) - (W_1(hm) + 1)$

edge "8-2":  $W_1(hm)(8) = W_1(hm)(2) - 1$ ,  $W_2(d)(8) = W_2(d)(2) + 1$ , they share the same  $W_2(ml)$ .

The weights have to be the same for both vertices of an edge. This forces the constant correction term  $\epsilon(p)w(hm)(w(ml) - w(d))$  for the weights given in Definition 12.

For the self-tangencies "8-2" as well as "1-6" both self-tangencies in the unfolding have the same  $W_2(d)$  as the triple crossing in type 8 respectively type 1. In the self-tangencies "7-4" and "5-3" both have the same  $W_2(d)$  as the triple crossing in type 7 respectively type 3. In the remaining cases  $W_2(d)$  is either the same too for the two self-tangencies or they differ exactly by  $W_1(hm)$  of the triple crossing.

We check now some edges of type  $r_a$  (where for shorter writing we do not mention the constant correction term which was already checked).

edge "1-7":  $4(l-1)x^{W_2(d)} - 4(l-1)x^{W_2(d)} = 0$ .  
 $(-1)l^2(x^{W_2(ml)+W_1(hm)} - x^{W_2(ml)}) - (-1)(-1)l^2(x^{W_2(ml)+W_1(hm)-W_1(hm)} - x^{W_2(ml)+W_1(hm)}) = 0$ .  
 edge "1-5":  $4lx^{W_2(d)} - 4lx^{W_2(d)} = 0$ .  
 $8(l+1)x^{W_2(ml)+W_1(hm)} - (-1)(l-1)^2(x^{W_2(ml)+W_1(hm)} - x^{W_2(ml)}) + (-1)(l+2 - (-1))^2(x^{W_2(ml)+W_1(hm)} - x^{W_2(ml)}) - 8(l+1)x^{W_2(ml)} = 0$ , compare Fig. 65 for the linking numbers.  
 edge "1-6":  $4lx^{W_2(d)} - 4lx^{W_2(d)} + 4(l+2)x^{W_2(d)} - 4(l+2)x^{W_2(d)} = 0$ .  
 $-(-1)l^2(x^{W_2(ml)+W_1(hm)} - x^{W_2(ml)}) + (-1)l^2(x^{W_2(ml)+W_1(hm)} - x^{W_2(ml)}) = 0$ .  
 All the remaining cases are quit similar and we leave them to the reader.  
 $\square$

## 4.6 Moving cusps and scan-property

We have to deal now with the irreducible strata of codimension two which contain a diagram with a cusp which moves over or under another branch. We can assume that in the local picture there is exactly one crossing, before the small curl from the cusp appears. Notice that in this case the local types 2 and 6 can evidently not occur as triple crossings. There are exactly sixteen possible local types. We list them in Fig. 66...Fig. 69, where we move the branch from the right to the left. For each local type we have exactly two global types, corresponding to the position of the point at infinity. It is very important that in  $\Sigma_{r_a}^{(2)}$  only the local types 1, 3, 7 and 8 of triple crossings can occur, because these are exactly the local types for which the correction  $\epsilon(p)w(hm)(w(ml) - w(d)) = 0$  (compare the previous subsection).

We give in the figure also the Gauss diagrams of the triple crossing and of one of the self-tangencies. Notice that in each Gauss diagram of a triple crossing one of the three arcs is empty besides just one head or foot of an arrow. Let us denote each stratum of  $\Sigma_{trans-cusp}^{(2)}$  simply by the global type of the corresponding triple crossing.

The following lemma reduces the number of cases which have to be considered.

**Lemma 7** *If  $R_1(m) = 0$  for  $\Sigma_{trans-cusp}^{(2)}$  with one orientation of the moving branch then it is also 0 for the other orientation of the moving branch.*

*Proof.* It suffices to notice that the contributions of the two Reidemeister II moves shown in Fig. 70 obviously cancel out.

$\square$

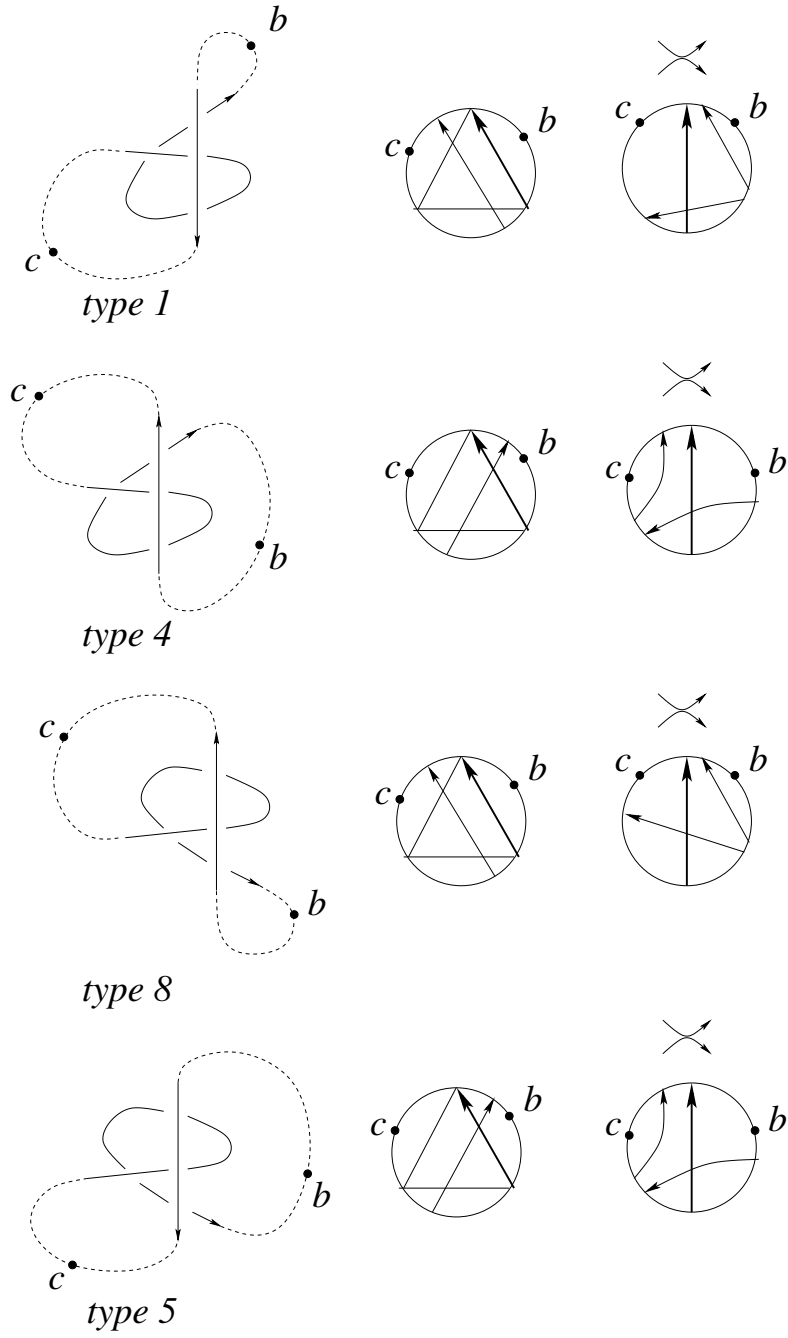


Figure 66: the strata  $\Sigma_{l_c}^{(2)}$  and  $\Sigma_{l_b}^{(2)}$

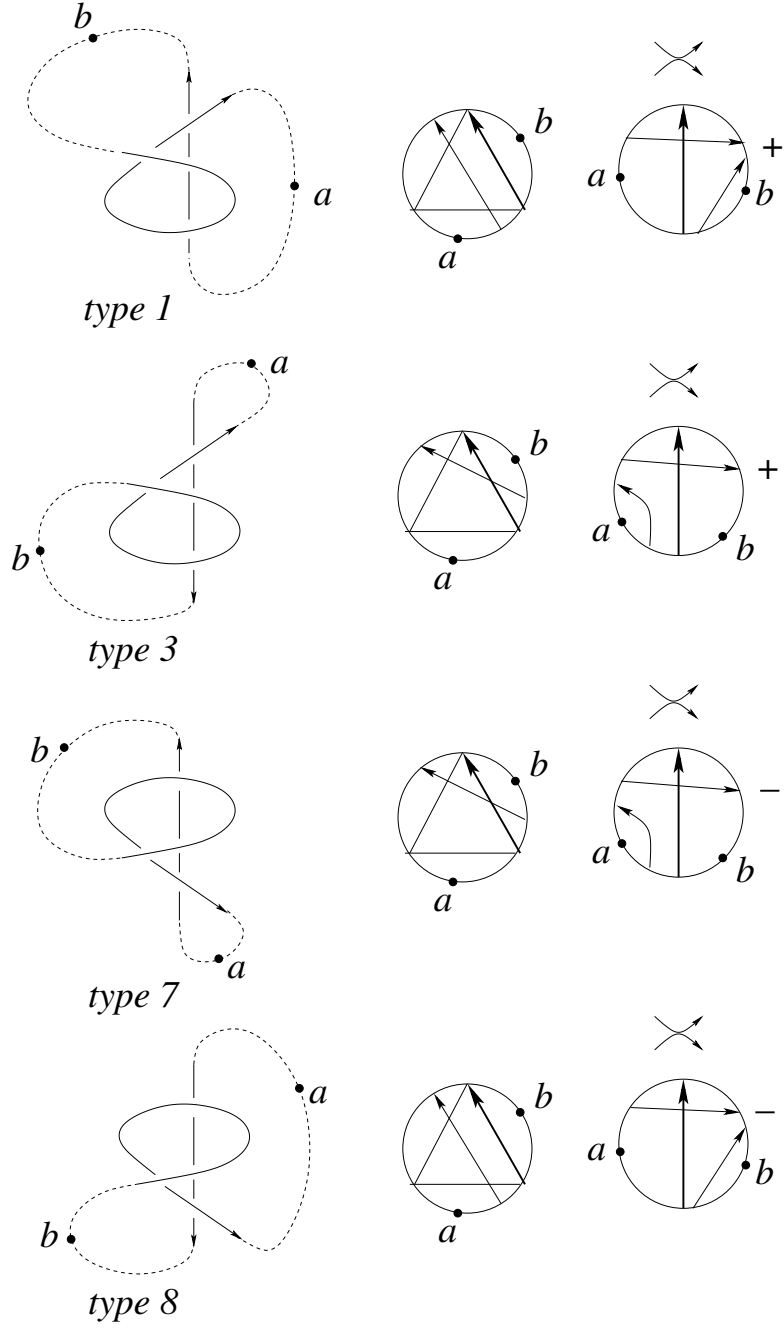


Figure 67: the strata  $\Sigma_{l_a}^{(2)}$  and  $\Sigma_{l_b}^{(2)}$

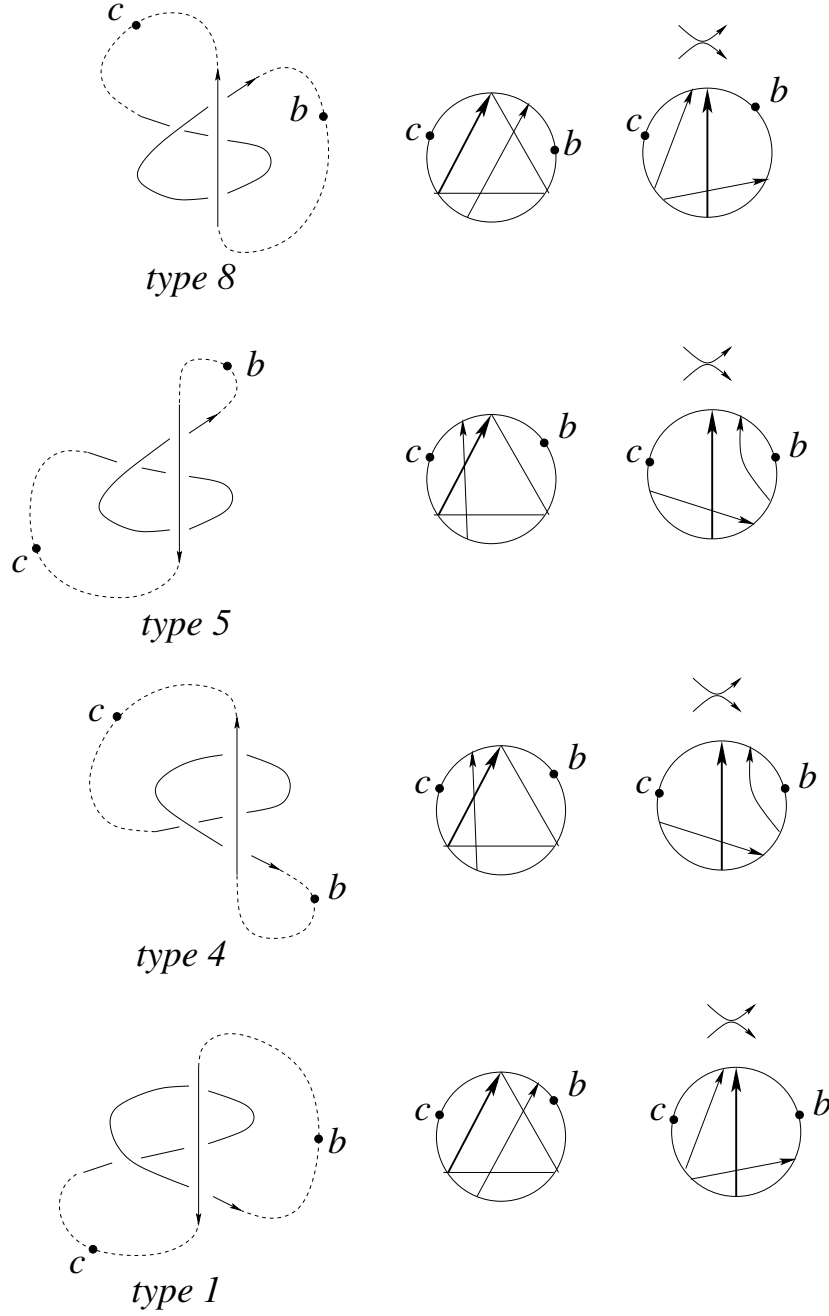


Figure 68: the strata  $\Sigma_{r_b}^{(2)}$  and  $\Sigma_{r_c}^{(2)}$



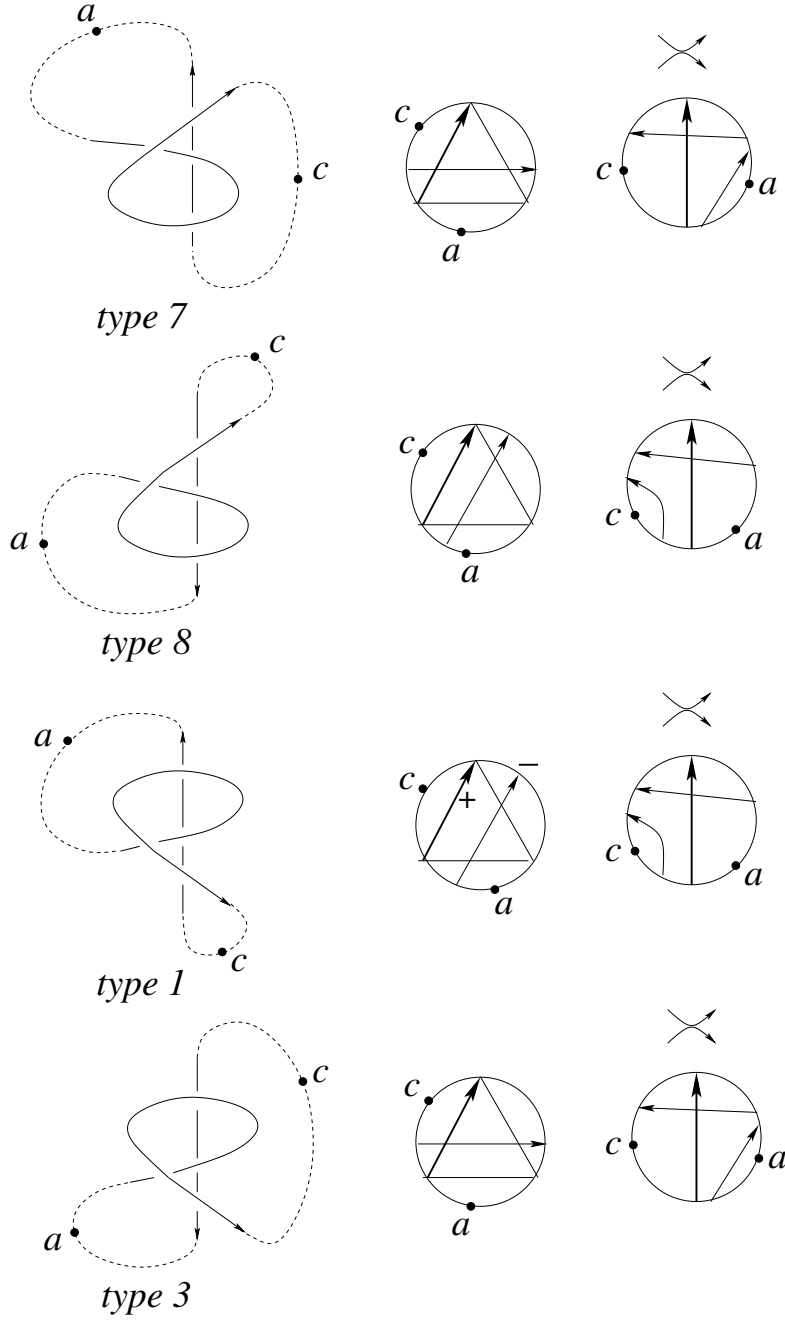


Figure 69: the strata  $\Sigma_{r_a}^{(2)}$  and  $\Sigma_{r_c}^{(2)}$

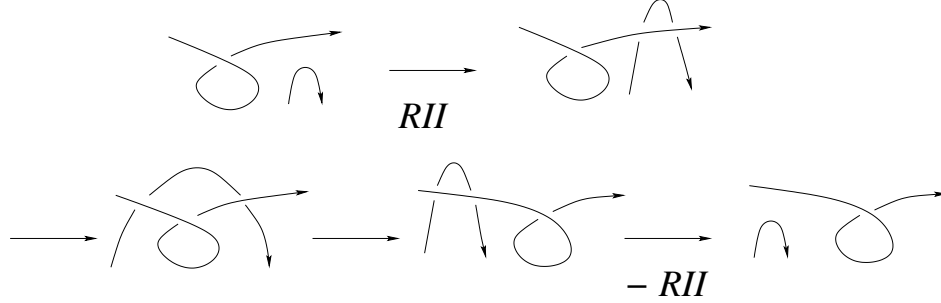


Figure 70: Two Reidemeister  $II$  moves with canceling contributions

**Proposition 6** *Let  $m$  be a meridian of  $\Sigma_{trans-cusp}^{(2)}$ . Then  $R_1(m) = 0$  for all strata of  $\Sigma_{trans-cusp}^{(2)}$  besides for those of the types  $\Sigma_{lc}^{(2)}$ .*

*Proof.* Exactly for the type  $\Sigma_{lc}^{(2)}$  only the triple crossing contributes to  $R_1(m)$ , namely by  $(l(ml) - w(ml))^2(x^{W_2(ml)+W_1(hm)} - x^{W_2(ml)})$ . Notice that  $W_1(hm)$  can be non-trivial as well as  $(l(ml) - w(ml))$ . Consequently,  $R_1$  does not necessarily vanish on this meridian.

Let us show that  $R_1(m) = 0$  for  $\Sigma_{ra}^{(2)}$  of local type 1.

We show the meridian of a stratum  $\Sigma_{ra}^{(2)}$  of local type 1 in Fig. 71 and the Gauss diagram of the triple crossing in Fig. 72.

First of all we observe that  $W_1(hm) = 0$ . Indeed,  $d$  of the triple crossing contributes  $+1$  and the negative crossing from the self-tangency contributes  $-1$  and there are no other crossings at all which contribute to  $W_1(hm)$ . Moreover, as already mentioned  $\epsilon(p)w(hm)(w(ml) - w(d)) = 0$ . Hence  $x^{W_2(ml)+W_1(hm)} - x^{W_2(ml)} = 0$  and the triple crossing does not contribute with  $ml$ . On the other hand,  $W_2(d) = W_2(ml) + W_1(hm) = W_2(ml)$  for the triple crossing because there are no foofs of arrows in the segment from the undercross to the overcross of  $hm$  (this is exactly the small curl). Let  $d'$  be the distinguished crossing of the self-tangencies. One easily sees (compare Fig. 69) that  $W_2(d') = W_2(ml) + W_1(hm) = W_2(ml)$  too. It follows that the weights of degree 2 are all the same and they are simply denoted by  $W_2$ . Moreover, the linking numbers  $l(d)$  and  $l(ml)$  are the same too.

The calculation of  $R_1(m)$  gives now:  $R_1(m) = 8(l+1)x^{W_2} - (-1)(l-1)^2(x^{W_2} - x^{W_2}) - 4(l+2)x^{W_2} - 4(l+2)x^{W_2} = 0$

All the remaining cases are completely analogous and are left to the reader.

□

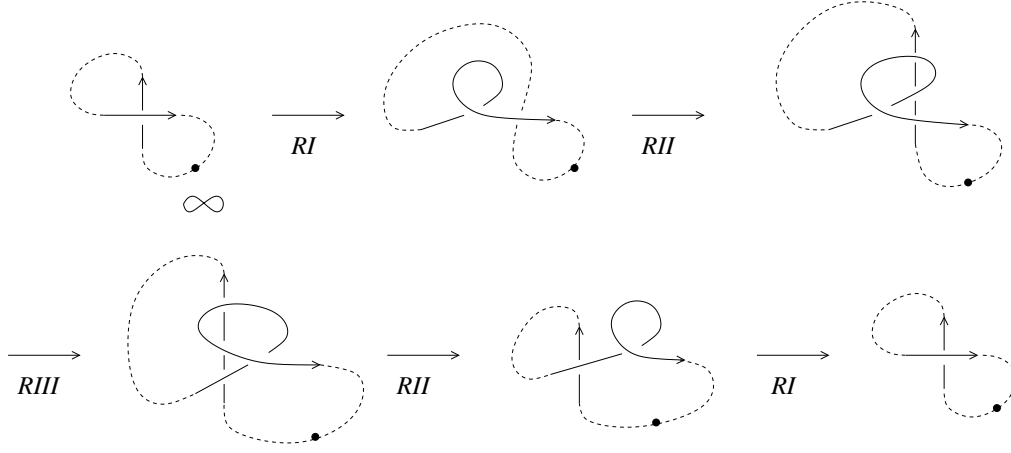


Figure 71: The meridian of a stratum  $\Sigma_{r_a}^{(2)}$  of local type 1

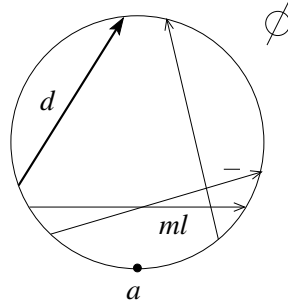


Figure 72: The triple crossing  $\Sigma_{r_a}^{(2)}$  of local type 1

**Remark 7** *It is necessary to use the quadratic weight  $W_2$  for the construction of  $R_1$ . Indeed, assume that we replace  $W_2$  by a linear weight  $W$  (which is just the sum of the writhes of the  $f$ -crossings). This implies that we have to replace  $W_2$  by  $W$  for the self-tangencies too and that we have to replace the linear weight  $W_1$  for the types  $r_a$  and  $l_c$  by the constant weight 1 (forced by the tetrahedron equation). The calculation of  $R_1(m)$  for  $\Sigma_{r_a}^{(2)}$  of local type 1 would give now  $R_1(m) = -(-1)(l-1)^2(x^{W_2+1} - x^{W_2}) \neq 0$ .*

We have proven that  $R_1(\gamma)$  is invariant under all generic homotopies of  $\gamma$  in  $M$  through the six types of strata of Proposition 1 besides  $\Sigma_{l_c}^{(2)}$  and hence  $R_1$  is a 1-cocycle in  $M \setminus \Sigma_{l_c}^{(2)}$ .

**Lemma 8** *Let  $T$  be a diagram of a string link and let  $t$  be a Reidemeister*

*move of type II for  $T$ . Then the contribution of  $t$  to  $R_1$  does not change if a branch of  $T$  is moved under  $t$  from one side of  $t$  to the other.*

*Proof.* Besides  $d$  of  $t$  there are two crossings involved with the branch which goes under  $t$ . Moving the branch under  $t$  from one side to the other slides the heads of the corresponding arrows over  $d$ , see e.g. Fig. 52 and Fig. 57. Consequently, the f-crossings do not change. Notice that the mutual position of the two arrows does not change. Consequently, there are no new r-crossings and  $W_2(d)$  does not change neither. Evidently,  $l(d)$  does not change and the assertion of the lemma follows.

□

We are now ready to prove the *scan-property* which was claimed in Theorem 1.

*Proof.* Let  $T$  be a diagram of a string link and let  $s$  be an isotopy which connects  $T$  with a diagram  $T'$ . We consider the loop

$-s \circ -scan(T') \circ s \circ scan(T)$  in  $M_T$ . This loop is contractible in  $M_T$  because  $s$  and  $scan$  commute. Consequently,  $R_1$  vanishes on this loop, because  $R_1$  is a 1-cocycle. It suffices to prove now that each contribution of a Reidemeister move  $t$  in  $s$  cancels out with the contribution of the same move  $t$  in  $-s$  (the signs of the contributions are of course opposite). The difference for the two Reidemeister moves is in a branch which has moved under  $t$ . It suffices to study the weights and the linking numbers. Evidently, the linking numbers have not changed because the branch has moved under the rest of the diagram. If  $t$  is a positive triple crossing now then the weights are the same just before the branch moves under  $t$  and just after it has moved under  $t$ . Indeed, this follows from the fact that for the positive global tetrahedron equation the contribution from the stratum  $-P_2$  cancels always out with that from the stratum  $\bar{P}_2$  (compare the Section 4.4). If we move the branch further away then the invariance follows from the already proven fact that the values of the 1-cocycles do not change if the loop passes through a stratum of  $\Sigma^{(1)} \cap \Sigma^{(1)}$  (compare Section 4.3). We use now again the graph  $\Gamma$ . The meridian  $m$  which corresponds to an arbitrary edge of  $\Gamma$  is a contractible loop in  $M_T$ , no matter what is the position of the branch which moves under everything. Let's take an edge where one vertex is a triple crossing of local type 1. We know from Lemma 8 that the contributions of the self-tangencies in  $s$  do not depend on the position of the moving branch. Consequently the contribution of the other vertex of the edge doesn't change neither because the contributions from all four Reidemeister moves together sum up to 0.

Using the fact that the graph  $\Gamma$  is connected we obtain the invariance with respect to the position of the moving branch for all Reidemeister moves  $t$  of type III and II. It remains to observe that Reidemeister moves of type I evidently do not change  $R_1(\text{scan}(T))$  and, as already mentioned, strata of type  $\Sigma_{l_c}^{(2)}$  can not occur, because the branch moves under everything else.

□

Notice that  $R_1$  does not have the scan-property for a branch which moves over everything else because the contributions of the strata  $P_3$  and  $-\bar{P}_3$  in the positive tetrahedron equation do not cancel out at all (compare Subsection 4.4). Of course, the "dual" 1-cocycle will have the scan property for a branch which moves over everything (compare Remark 5).

**Question 4** *Does the 1-cocycle  $R_1$  and son "mirror dual", which is obtained by taking in all definitions mirror images, represent always up to normalization the same cohomology class in  $H^1(M^{\text{reg}}; \mathbb{Z}[x, x^{-1}])$ ?*

We have proven that  $R_1$  has the scan-property. It is not always trivial as shows the example in Section 3.1. This finishes the proof of Theorem 1.

#### 4.7 Invariance of $R_n^i$ for $n > 1$

We have to go again through the proof of the invariance of  $R_1$  under generic homotopies of arcs in  $M$  but with taking into account the colorings. Remember that the linking numbers do not depend on the colorings. Therefore we have only to check the weights  $W_2$  and  $W_1$ . We will write shortly  $C_j$  for  $C_{i_j}$ .

*Reidemeister II moves in a cusp and in a flex:* the two respectively three involved crossings have all the same coloring and exactly the same arguments as for  $R_1$  apply.

*Simultaneous Reidemeister moves:* Evidently, a simultaneous R II-move does not change anything because the two new crossings have the same homological and the same colored type. They are only simultaneously potential f-crossings as well as potential r-crossings. In the first case they have the same weight  $W_1$ . But they have different signs and cancel out together.

For the simultaneous R III-moves we reexamine now Fig. 35 and Fig. 36 which were used in the proof of Lemma 2. Only the cases  $r_c$  and  $l_c$  have to be considered as in the proof of Lemma 2.

For  $r_c$  only the crossing 2 could be a potential f-crossing. The crossing 1 is a r-crossing for 2 if and only if its foot is  $C_3$  and its head is  $C_2$  or  $C_3$ . On the other side of the triple crossing the crossing 3 is a r-crossing for 2 if and only if its foot is  $C_3$  and its head is  $C_2$  or  $C_3$ . But the foots of 1 and 2 have always the same color. The head of 1 has the same color as the head of 2 which is  $C_2$  or  $C_3$ . The head of 3 has the same color as the foot of 2 which is  $C_2$ . It follows that 1 and 3 can only be simultaneously r-crossings for 2 and hence the weights of  $R_n^i$  are invariant.

If 1 is a potential f-crossing in  $l_c$  then its foot is  $C_2$ . The foot of 3 is always  $C_2$  too. If 1 is a potential f-crossing then the head of 2 is  $C_2$  or  $C_3$ . Consequently, 2 is a r-crossing for 1 if and only if its foot is  $C_3$ . But the head of 3 has the same color as the foot of 2. Consequently, 2 is a r-crossing for 1 if and only if 3 is a potential f-crossing too. In the latter case 2 is also a r-crossing for 3 and hence the weights of  $R_n^i$  are again invariant. (Notice that we really need here  $C_2$  or  $C_3$  for the heads of both the f-and r-crossings and there is no solution with only  $C_2$  or only  $C_3$ .)

*Refined tetrahedron equation:* We have shown in Lemma 3 that the f-crossings for  $d$  or  $ml$  in the corresponding strata are almost always identical. An exception is the new f-crossing in  $\bar{P}_3$  which is exactly the crossing  $hm = 34$  in  $P_1$  and  $\bar{P}_1$ . The crossing  $d$  in  $P_3$  and  $\bar{P}_3$  contributes only if it is of type  $C_1 \rightarrow C_2$ . In this case the crossing  $ml$  in  $P_1$  and  $\bar{P}_1$  is of the same type and hence  $hm = 34$  has the foot  $C_2$ . Consequently, it is a f-crossing if and only if the head of  $d$  in  $P_1$  and  $\bar{P}_1$  is  $C_2$  or  $C_3$ . The r-crossings of corresponding f-crossings can be different. But the difference comes just from passing adjacent strata of triple crossings in the meridian of the quadruple crossing. But we have already shown above in *Simultaneous Reidemeister moves* that this does not change the weights in  $R_n^i$ . We use here, that in the proof for *Simultaneous Reidemeister moves* we make no use of the mutual position of the two moves. Hence, in particular it applies also to the R III-moves in the meridian of the quadruple crossing, even if these moves can not commute.

*Cube equations:* We use again Fig. 52 up to Fig. 59. For the type  $l_b$  the f-crossings and the r-crossings are always the same for the two triple crossings of an edge. For the type  $l_c$  there can be a new f-crossing for  $ml$  if  $hm$  is one of the crossings of the self-tangencies, compare "11-7". But the remaining two crossings are never r-crossings for  $hm$  and hence the weights of  $R_n^i$  are invariant.

For the type  $r_b$  the f-crossings and the r-crossings are again the same for the two triple crossings of an edge.

Let us consider the edge " $r_a$  1-7":  $d$  contributes if it is of type  $C_1 \rightarrow C_2$ . The crossing  $hm$  and the other crossing from the self-tangencies are now f-crossings if and only if the head of  $ml$  is  $C_2$ . The r-crossings for  $hm$  do not change. For the other crossing of the self-tangencies  $d$  is a r-crossing for the local type 1 and  $ml$  is a r-crossing for the local type 7. But both r-crossings are of type  $C_1 \rightarrow C_2$  and hence the weight of  $R_n^i$  hasn't changed.

The crossing  $ml$  contributes if it is of type  $C_1 \rightarrow C_2$ . The crossing  $hm$  contributes if and only if its head is  $C_2$  or  $C_3$ . But then  $d$  is a r-crossing for the other crossing in the self-tangencies for the local type 1 and  $ml$  is a r-crossing for the other crossing in the self-tangencies for the local type 7 and the weights of  $R_n^i$  are invariant.

Let us consider the edge " $r_a$  1-5":  $d$  contributes if it is of type  $C_1 \rightarrow C_2$ . The crossing  $hm$  is a f-crossing if and only if the head of  $ml$  is  $C_2$ . The crossing  $d$  is a r-crossing for  $hm$  for the local type 1 if and only if it is a r-crossing for  $hm$  for the local type 5 too. The other crossing from the self-tangencies is never a r-crossing for  $hm$  for the local type 5, but it could be a r-crossing for  $hm$  for the local type 1. However, it is of type  $C_1 \rightarrow C_2$ . Consequently, for a non-degenerate admissible coloring ( $C_3 \neq C_1$ ) the weights of  $R_n^i$  are invariant, but for a degenerate admissible coloring we need the same correction term  $\epsilon(p)w(hm)(w(ml) - w(d))$  as for  $R_1$  (compare Definition 12 and the proof of Proposition 4). Exactly the same arguments apply also to the contributions of  $ml$  because  $hm$  is still the only f-crossing.

Let us consider the edge " $r_a$  1-6":  $hm$  is the only potential f-crossing and for the local type 1 only  $d$  can be a r-crossing for  $hm$ . For the local type 6 the crossing  $d$  and the other crossing from the self-tangencies are simultaneously r-crossings. But if  $hm$  is a f-crossing then  $d$  is of type  $C_1 \rightarrow C_2$  or  $C_1 \rightarrow C_3$ . Consequently, for a non-degenerate admissible coloring the weights of  $R_n^i$  are invariant, but for a degenerate admissible coloring we need again the correction term  $\epsilon(p)w(hm)(w(ml) - w(d))$ .

All other cases are completely analogous and are left to the reader.

*Moving cusps and scan-property:* There are evidently at most two colors involved. Only the crossing  $ml$  could contribute in  $\Sigma_{l_c}^{(2)}$ . But its overcross and its undercross have the same color. Consequently, it does not contribute because we would have  $C_1 = C_2$  (compare Remark 3).

Let us consider the stratum  $\Sigma_{r_a}^{(2)}$  of local type 1. The f-and the r-crossings

which contribute to  $W_2$  are all identical in the R III-move and in the two R II-moves. It remains to observe that  $ml$  does not contribute because we have still  $W_1(hm) = 0$ . Indeed, if  $hm$  is a f-crossing for  $ml$  then its foot is  $C_2$  and its head is  $C_2$  or  $C_3$ . The foot of  $d$  is  $C_1$  and hence  $d$  is a r-crossing for  $hm$  if and only if  $C_1 = C_3$  (the degenerate case), compare Fig. 72. But the negative crossing from the self-tangency has also the foot  $C_1$  and it has the head  $C_2$ . Consequently, it is also a r-crossing for  $hm$  and we have still  $W_1(hm) = 0$ .

All other case are completely analogous and are left to the reader.

Notice that we need  $C_2 \neq C_3$  in the definition of an admissible coloring only in order to prevent that adding a local knot on a component of the string link leads to a multiplication of the invariant by some factor, which would imply that the invariant is almost trivial because the position of the local knot on the component does matter (compare Proposition 2 and Remark 3).

The proof of Lemma 8 carries over for  $R_n^i$  without any changes. The corresponding f-crossings and r-crossings are identical in  $-P_2$  and  $\bar{P}_2$  and consequently the corresponding weights in  $R_n^i$  are still the same for the two strata.  $R_n^i$  satisfies the cube equations, as was already shown above. It follows that the proof of the scan-property carries over for  $R_n^i$  without any changes too.

We have proven that  $R_n^i(\gamma)$  is invariant under all generic homotopies of an arc  $\gamma$  in  $M$  through the six types of strata of Proposition 1 and hence  $R_n^i$  is a 1-cocycle in  $M$ . Moreover, it has the scan-property and Examples 4 and 5 show that it can detect the non-invertibility of a knot. Example 3 shows that the cohomology class  $[R_n^i]$  is not always trivial.

This finishes the proof of Theorem 2.

## References

- [1] Bar-Natan D. : On the Vassiliev knot invariants, Topology 34 (1995) 423-472
- [2] Bar-Natan D. : Vassiliev homotopy string link invariants, J. Knot Theory Ramif. 4 (1995) 13-32
- [3] Bar-Natan D. : Some computations related to Vassiliev invariants, <http://www.math.toronto.edu/~drorbn/papers>



- [4] Berger A., Stassen I.: The skein relation for the  $(g_2, V)$ -link invariant, *Comment. Math. Helv.* 75 (2000) 134-155
- [5] Birman J. : Braids , Links and Mapping class groups, *Annals of Mathematics Studies* 82 , Princeton University Press (1974)
- [6] Birman J., Gebhardt V., Gonzáles-Meneses J.: Conjugacy in Garside groups III: Periodic braids, *J. of Algebra* 316 (2007) 746-776
- [7] Budney R., Conant J., Scannell K., Sinha D.: New perspectives on self-linking, *Advances in Math.* 191 (2005) 78-113
- [8] Budney R., Cohen F.: On the homology of the space of knots, *Geometry & Topology* 13 (2009) 99-139
- [9] Budney R. : Topology of spaces of knots in dimension 3, *Proceedings London Math. Soc.* 101 (2010) 477-496
- [10] Budney R. : An operad for splicing, *J. of Topology* 5 (2012) 945-976
- [11] Carter J.S., Saito M.: Reidemeister moves for surface isotopies and their interpretations as moves to movies, *J. Knot Theory Ramif.* 2 (1993) 251-284
- [12] Cooper D., Long D.: Representation theory and the A-polynomial of a knot, *Chaos, Solitons & Fractals* 9 (1998) 748-763
- [13] Duzhin S., Karev M.: Detecting the orientation of string links by finite type invariants, *Functional Analysis and its Appl.* 41 (2007) 208-216
- [14] Fiedler T. : Gauss Diagram Invariants for Knots and Links, *Mathematics and Its Applications* 532 , Kluwer Academic Publishers (2001)
- [15] Fiedler T. : Isotopy invariants for closed braids and almost closed braids via loops in stratified spaces, *arXiv: math.GT/0606443* (48 pp)

- [16] Fiedler T. : Quantum one-cocycles for knots, arXiv: 1304.0970v2 (177 pp)
- [17] Fiedler T. : Singularization of knots and closed braids, arXiv: 1405.5562 v3 (165 pp)
- [18] Fiedler T. : One-cocycle invariants for closed braids, arXiv: 1804.03549 (44 pp)
- [19] Fiedler T., Kurlin V. : A one-parameter approach to knot theory, J. Math. Soc. Japan 62 (2010) 167-211
- [20] Fox R. : Rolling, Bull.Amer. Math. Soc. 72 (1966) 162-164
- [21] Gramain A.: Sur le groupe fondamental de l'espace des noeuds, Ann. Inst. Fourier 27 (1977) 29-44
- [22] Goussarov M., Polyak M., Viro O.: Finite type invariants of classical and virtual knots, Topology 39 (2000) 1045-1068
- [23] Hatcher A. : A proof of the Smale Conjecture, Ann. of Math. 117 (1983) 553-607
- [24] Hatcher A. : Topological moduli spaces of knots, arXiv: math.GT/9909095
- [25] Hatcher A., McCullough D.: Finiteness of classifying spaces of relative diffeomorphism groups of 3-manifolds, Geometry & Topology 1 (1997) 91-109
- [26] Johannson K. : Homotopy equivalences of 3-manifolds with boundary, Lecture Notes in Math. 761, Springer Berlin (1979)
- [27] Jones V.: Hecke algebra representations of braid groups and link polynomials, Ann. of Math. 126 (1987) 335-388
- [28] Kashaev R.: The hyperbolic volume of knots from the quantum dilogarithm, Lett. Math. Phys. 39 (1997) 269-275
- [29] Kashaev R., Korepanov I., Sergeev S.: Functional tetrahedron equation, Theoret. and Math. Phys. 117 (1998) 1402-1413

- [30] Kauffman L. : Knots and Physics, World Scientific, Singapore (1991)
- [31] Kuperberg G.: Detecting knot invertibility, J. Knot Theory Ramifications 5 (1996) 173-181
- [32] Mortier A.: Combinatorial cohomology of the space of long knots, Alg. Geom. Top. 15 (2015) 3435-3465
- [33] Mortier A.: Finite-type 1-cocycles, J. Knot Theory Ramifications 24 (2015) 30 pp.
- [34] Murakami H., Murakami J.: The colored Jones polynomials and the simplicial volume of a knot, Acta Math. 186 (2001) 85-104
- [35] Polyak M., Viro O.: Gauss diagram formulas for Vassiliev invariants, Internat. Math. Res. Notes 11 (1994) 445-453
- [36] Przytycki J.: Skein modules of 3-manifolds, Bull. Polish Acad. Sci. Math. 39 (1991) 91-100
- [37] Sakai K.: An integral expression of the first non-trivial one-cocycle of the space of long knots in  $\mathbb{R}^3$ , Pacific J. Math. 250 (2011) 407-419
- [38] Turaev V.: The Conway and Kauffman modules of a solid torus, J. Soviet. Math. 52 (1990) 2799-2805
- [39] Turchin V. : Computation of the first non-trivial 1-cocycle in the space of long knots, (Russian) Mat. Zametki 80 (2006), no. 1, 105-114; translation in Math. Notes 80 (2006), no. 1-2, 101-108.
- [40] Vassiliev V. : Cohomology of knot spaces // in: Theory of Singularities and its Applications, Advances in Soviet. Math. 1 (1990) 23-69
- [41] Vassiliev V. : Combinatorial formulas of cohomology of knot spaces, Moscow Math. Journal 1 (2001) 91-123
- [42] Waldhausen F. : On irreducible 3-manifolds which are sufficiently large, Ann. of Math. 87 (1968) 56-88

- [43] Witten E.: Quantum field theory and the Jones polynomial,  
Comm. Math. Phys. 121 (1989) 351-399

Institute de Mathématiques de Toulouse, UMR 5219  
Université Paul Sabatier  
118, route de Narbonne  
31062 Toulouse Cedex 09, France  
fiedler@math.univ-toulouse.fr